UNIVERSIDADE FEDERAL DO CEARÁ
CENTRO DE TECNOLOGIA
DEPARTAMENTO DE ENGENHARIA HIDRÁULICA E AMBIENTAL
PROGRAMA DE PÓS-GRADUÇÃO EM ENGENHARIA CIVIL – RECURSOS HÍDRICOS

INDIRA DE MENEZES CASTRO

CONTROLLING THE CYANOBACTERIUM *MICROCYSTIS AERUGINOSA* AND THE CYANOTOXIN MICROCYSTIN BY (ADVANCED) OXIDATION PROCESSES

FORTALEZA
2020

INDIRA DE MENEZES CASTRO

CONTROLLING THE CYANOBACTERIUM *MICROCYSTIS AERUGINOSA* AND THE CYANOTOXIN MICROCYSTIN BY (ADVANCED) OXIDATION PROCESSES

Dissertação apresentada ao Programa de Pós-Graduação em Engenharia Civil – Recursos Hídricos da Universidade Federal do Ceará, como requisito parcial à obtenção do título de Mestre em Engenharia Civil, Área de concentração: Saneamento Ambiental.

Orientador: Prof. Dr. José Capelo Neto.

FORTALEZA

2020

Dados Internacionais de Catalogação na Publicação
Universidade Federal do Ceará
Biblioteca Universitária
Gerada automaticamente pelo módulo Catalog, mediante os dados fornecidos pelo(a) autor(a)

C351c Castro, Indira de Menezes.
CONTROLLING THE CYANOBACTERIUM MICROCYSTIS AERUGINOSA AND THE CYANOTOXIN MICROCYSTIN BY (ADVANCED) OXIDATION PROCESSES / Indira de Menezes Castro. – 2020.
89 f. : il. color.

Dissertação (mestrado) – Universidade Federal do Ceará, Centro de Tecnologia, Programa de Pós-Graduação em Engenharia Civil: Saneamento Ambiental, Fortaleza, 2020.
Orientação: Prof. Dr. José Capelo Neto.

1. Cianobactéria. 2. Peróxido de hidrogênio. 3. Dióxido de titânio. 4. Luz UV. 5. Cianotoxinas. I. Título.
CDD 628

INDIRA DE MENEZES CASTRO

CONTROLLING THE CYANOBACTERIUM *MICROCYSTIS AERUGINOSA* AND THE CYANOTOXIN MICROCYSTIN BY (ADVANCED) OXIDATION PROCESSES

Dissertação apresentada ao Programa de Pós-Graduação em Engenharia Civil da Universidade Federal do Ceará, como requisito parcial à obtenção do título de Mestre em Engenharia Civil. Área de concentração: Saneamento Ambiental.

Orientador: Prof. Dr. José Capelo Neto.

Aprovada em: ___/___/_____.

BANCA EXAMINADORA

_____
Prof. Dr. José Capelo Neto (Supervisor)
Universidade Federal do Ceará (UFC)

_____
Prof. Dr. Sergio Francisco de Aquino
Prof. Dr. Universidade Federal de Ouro Preto (UFOP)

_____
Dr. Carlos João Pestana
Robert Gordon University (RGU)

Aos meus pais, que foram guias para todos os caminhos que trilhei.

RESUMO

Reservatórios são utilizados em grande parte do nordeste brasileiro para o abastecimento humano, porém eles se encontram, comumente, eutrofizados. A eutrofização degrada a qualidade da água *in natura* e corrobora para a floração de cianobactérias potencialmente produtoras de cianotoxinas que e podem ser liberadas a partir de lise celular. Nesse contexto, processos alternativos de tratamento de água que produzem espécies reativas de oxigênio e que podem ser aplicados *in-situ* foram utilizados para avaliar a remoção da cianobactéria *Microcystis aeruginosa* PCC7813 e de quatro variantes de microcistina (MC-LR, MC-LY, MC-LY e MC-LF). Além disso, foi realizada a comparação de diferentes métodos de detecção de estresse em células de cianobactéria. Inicialmente, foi realizada a aplicação de peróxido de hidrogênio para a remoção de *Microcystis aeruginosa* PCC7813 e estudo do estresse celular. Ademais, densidade celular, atividade fotossintética, concentração de clorofila e concentração de microcistina foram utilizadas como diferentes metodologias para detecção de estresse celular. Nesse estudo, além da remoção efetiva de células de *Microcystis aeruginosa* PCC7813 e de microcistinas, a atividade fotossintética indicou o estresse celular das cianobactérias em apenas 6 horas, o que foi consideravelmente mais rápido que os outros métodos. Em um segundo estudo, fotólise e fotocatálise heterogênea foram comparadas utilizando pequenas esferas reutilizáveis feitas de vidro reciclado revestidas com finas camadas de dióxido de titânio e iluminação de diodo emissor de luz (LED) contendo luz UV (365 nm) em um reator de escala piloto para remoção de *Microcystis aeruginosa* PCC7813 e de quatro variantes de microcistina (MC-LR, MC-LY, MC-LY e MC-LF). Durante a fotólise, a densidade celular diminuiu significativamente ao longo de 5 dias até que poucas células permanecessem na amostra a partir de uma concentração inicial de 5,8 x 10^6 células mL^{-1}. Ambas as concentrações de microcistina intra- e extracelular foram significativamente reduzidas em 100 e 92%, respectivamente, no dia 5 do tratamento com UV para todas as variantes de microcistina. Além disso, a fotólise de UV-A mostrou ter efeitos de longo prazo nas células de *M. aeruginosa* PCC7813, inibindo o recrescimento por pelo menos seis dias após tratamento. Durante a fotocatálise heterogênea, houve uma grande variabilidade entre as repetições, dificultando a previsão do comportamento das células e das toxinas.

Palavras-chave: Cianobactéria. Peróxido de hidrogênio. Dióxido de titânio. Luz UV. Cianotoxinas.

ABSTRACT

Reservoirs are used in the northeastern Brazil for human supply. However, most of them are commonly eutrophicated. Eutrophication degrades water quality and corroborates the cyanobacterial blooms which are potentially producers of cyanotoxins that can be released after cell lysis. In this context, alternative water treatment processes that produce reactive oxygen species and that can be applied *in-situ* were used to evaluate the removal of cyanobacterium *Microcystis aeruginosa* PCC7813 and four microcystin variants (MC-LR, MC-LY, MC-LY, MC-LY and MC-LF). In addition, a comparison of different methods for cyanobacterial cells stress detection was performed. Initially, hydrogen peroxide was applied to remove *Microcystis aeruginosa* PCC7813 cells and to evaluate cell stress detection. Cell density, photosynthetic activity, chlorophyll content and microcystin concentration were used as different methodologies for cell stress detection. In this study, the photosynthetic activity indicated cyanobacterial cell stress in just 6 hours which was faster than other methods. Also, there was an effective removal of *Microcystis aeruginosa* PCC7813 cells and of all microcystin analogues. In a second study, photolysis and heterogeneous photocatalysis were compared using small reusable beads made of recycled glass coated with thin layers of titanium dioxide and the illumination of light emitting diodes (LED) using UV light (365 nm) in an experimental scale reactor in order to remove *Microcystis aeruginosa* PCC7813 and four microcystin analogues (MC-LR, MC-LY, MC-LY e MC-LF). During photolysis, cell density significantly decreased over 5 days from an initial concentration of 5.8×10^6 cells mL^{-1} until few cells were left. Both intra- and extracellular microcystin concentration were significantly reduced by 100 and 92%, respectively, by day 5 of the UV treatment for all microcystin analogues. Further, photolysis was shown to have long-term effects on *M. aeruginosa* PCC7813 cells, inhibiting regrowth for at least six days after treatment. During UV/TiO_2 treatment, there was a great variability between replicates, making prediction of cyanobacterial cell and toxin behavior difficult.

Keywords: Cyanobacteria. Hydrogen peroxide. Titanium dioxide. UV light. Cyanotoxins.

LIST OF FIGURES

CHAPTER I

CHAPTER II

LIST OF TABLES

CHAPTER I

CHAPTER II

TABLE OF CONTENTS

1 GENERAL INTRODUCTION

Superficial reservoirs are largely used in the northeast region of Brazil for human supply, however they are, usually, in a eutrophic state (LOPES, 2013) due to the climatic characteristics of the region, the irregularity of rainfall and the properties of the soil, which added to the high rate of evaporation and solar radiation, the exploitation of resources and the lack of sewage systems, affect the quality and quantity of water (ELLIOTT, 2012; PAERL & PAUL, 2012; LOPES, 2013). Eutrophication enhances the phytoplankton blooming process, predominantly dominated by cyanobacteria (BARROS, 2013), which can represent human and animal health hazards, as these organisms may produce toxic compounds (FALCONER *et al*., 1983; JOCHIMSEN *et al*., 1998; PINHO *et al*., 2015). Microcystins (MC) are one of the most commonly reported cyanotoxins found in freshwater (PINHO et al., 2015) and there are at least 247 identified congeners of this toxic compound (SPOOF AND CATHERINE, 2017). Microcystins are normally inside the cells and are mostly released to the water after cell membrane lysis and death (TSAI, 2015).

Conventional water treatment processes such as coagulation, flocculation, sedimentation and filtration can be ineffective in removing dissolved compounds, such as cyanotoxins (FAN *et al*., 2013a). Some oxidants can be used as chemical treatments to help remove cyanobacteria (e.g., ozone, chlorine, potassium permanganate and chlorine dioxide), but they can cause cell lysis and toxins release (CHANG *et al*., 2018; ZAMYADI *et al*., 2011).

As an alternative, treatment processes that produce reactive oxygen species (ROS), such as hydrogen peroxide (H_2O_2) application, UV photolysis and titanium dioxide (TiO_2) photocatalysis illuminated by UV, have been applied to control cyanobacterial blooms and to remove microcystin congeners from water. These treatments are based on the generation of ROS which have a high oxidation power and can promote the degradation of polluting compounds (FIOREZE *et al*., 2014) by partially or totally transforming them into simpler species or less toxic and easily degradable substances (PIGNATELLO *et al*., 2006).

H_2O_2 can be applied in water treatment as an algaecide to promote the degradation of cyanobacterial cells and cyanotoxins (FAN *et al*., 2019; FAN *et al*., 2013b) without producing any toxic residuals, since it decomposes into oxygen and water (BARROIAN AND FEUILLADE, 1986). However, some methods used to evaluate oxidizers effects on cyanobacteria could lead to a misinterpretation of cell damage by late detection of cell inhibition or degradation. Because of this, different methods that point out *Microcystis aeruginosa*

PCC7813 cell stress under H_2O_2 application were compared in this study to identify which method provides the most accurate and rapid response.

TiO_2 is a non-toxic and abundant catalyst with commercial applications (FAGAN *et al*., 2016) that is usually applied as a nanoparticulate which is difficult to separate from suspension after water treatment (PESTANA *et al*., 2015) and can be a hazard for the environment since it can bioaccumulate and damage biota (SCHAUMANN *et al*., 2015; PRAETORIUS *et al*., 2013; ZHU et al., 2010). Because of these problems, materials are developed to be used as immobilization matrix which could be coated with thin layers of TiO_2 and that are also easily removed and reused after treatment. Further, the catalyst activation needs to occur under UV light illumination (< 387 nm) (CHANG *et al*., 2018; HU *et al*., 2017; ZHAO *et al*., 2014), so the use of UV (365 nm) light emitting diodes (LEDs) would be able to overcome the problem associated with high cost of UV irradiation for TiO_2 activation in the use of an *in-situ* UV/TiO_2 photocatalysis treatment. UV photolysis is another alternative water treatment process that has been widely applied for inactivation of pathogenic microbes in water treatment and other applications and can be used as a strategy for removing cyanobacteria and their toxins.

The removal of *Microcystis aeruginosa* PCC7813 cells and four microcystin congeners (MC-LR, -LW, -LY, -LF) by photolysis and photocatalysis using reusable TiO_2 coated recycled foamed glass beads under UV-LED irradiation was evaluated in the current study using a pilot scale reactor as proof-of-principle system that can be applied in drinking water reservoirs.

This present master's thesis is organized on the following five parts:

1 – General introduction

2 – Chapter I which presents the first paper entitled "Oxidative stress in the cyanobacterium *Microcystis aeruginosa* PCC 7813: comparison of different analytical cell stress detection assays"

3 – Chapter II which presents the second paper entitled "Comparison of UV-A photolytic and UV/TiO_2 photocatalytic effects on *Microcystis aeruginosa* PCC7813 and four microcystin analogues: a pilot scale study"

4 – A general conclusion

5 – The references of the General introduction

Each Paper is a complete manuscript published or ready to be sent to an international journal.

CHAPTER I

Oxidative stress in the cyanobacterium *Microcystis aeruginosa* PCC 7813: comparison of different analytical cell stress detection assays

Published at Chemosphere (Qualis Capes A1)

Oxidative stress in the cyanobacterium *Microcystis aeruginosa* PCC 7813: comparison of different analytical cell stress detection assays

Authors: Indira de Menezes Castro; Declan Maxwell-McQueeney; José Capelo Neto; Carlos João Pestana; Christine Edwards; Linda Lawton

ABSTRACT

Cyanobacterial blooms are observed when high cell densities occur and are often dangerous to human and animal health due to the presence of cyanotoxins. Conventional drinking water treatment technology struggles to efficiently remove cyanobacterial cells and their metabolites during blooms, increasing costs and decreasing water quality. Although field applications of hydrogen peroxide have been shown to successfully suppress cyanobacterial growth, a rapid and accurate measure of the effect of oxidative stress on cyanobacterial cells is required. In the current study, H_2O_2 (5 and 20 mg L^{-1}) was used to induce oxidative stress in *Microcystis aeruginosa* PCC 7813. Cell density, quantum yield of photosystem II, minimal fluorescence and microcystin (MC-LR, -LY, -LW, -LF) concentrations were compared when evaluating *M. aeruginosa* cellular stress. Chlorophyll content (determined by minimal fluorescence) decreased by 10% after 48 hours while cell density was reduced by 97% after 24 hours in samples treated with 20 mg L^{-1} H_2O_2. Photosystem II quantum yield (photosynthetic activity) indicated cyanobacteria cell stress within 6 hours, which was considerably faster than the other methods. Intracellular microcystins (MC-LR, -LY, -LW and -LF) were reduced by at least 96% after 24 hours of H_2O_2 treatment. No increase in extracellular microcystin concentration was detected, which suggests that the intracellular microcystins released into the surrounding water were completely removed by the hydrogen peroxide. Thus, photosynthetic activity was deemed the most suitable and rapid method for oxidative cell stress detection in cyanobacteria, however, an approach using combined methods is recommended for efficient water treatment management.

Key words: Cyanobacteria, fluorescence, microcystin, water treatment, hydrogen peroxide.

Highlights:

- Time lag observed between cell stress occurring and its detection by most methods
- Photosynthetic activity analysis was the fastest method for cell stress detection
- Advantages and drawbacks of five different cell stress detection assays elucidated

Graphical Abstract:

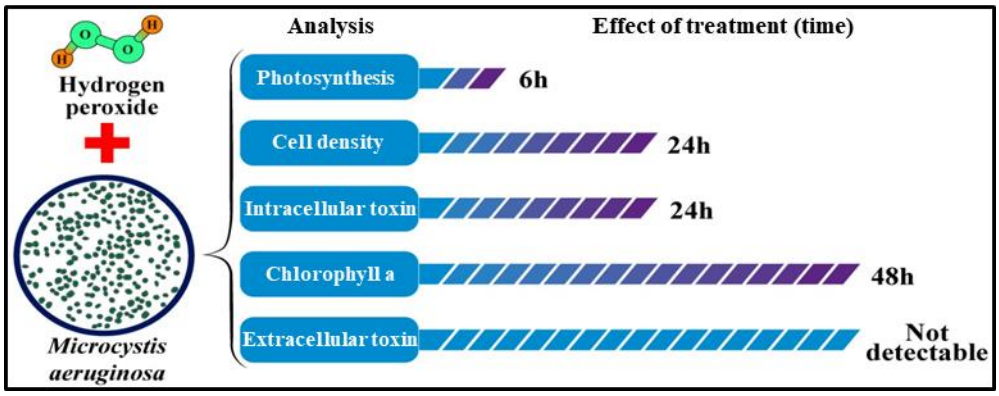

2 INTRODUCTION

Climate change, and eutrophication contribute to cyanobacterial blooms in freshwater reservoirs (WEENINK *et al*., 2015). Cyanobacteria can be a threat to drinking water quality since they are potential producers of a wide variety of toxins. These toxins are a hazard to both human and animal health (FALCONER *et al*., 1983; JOCHIMSEN *et al*., 1998; PINHO *et al*., 2015) and high cell densities may complicate the potable water treatment process by reducing filter run times and increasing the use of chemicals (e.g., coagulants and disinfectants), which raises the cost of water treatment (DE JULIO *et al*., 2010).

Microcystins (MC) are one of the most commonly reported cyanotoxins found in freshwater (PINHO *et al*., 2015). These toxins are cyclic heptapeptides that share a common structure with two amino acid domains which vary in positions 2 and 4 of the structure (RINEHART *et al*., 1994; HARKE *et al*., 2016). Currently, there are at least 247 identified microcystin analogues (SPOOF AND CATHERINE, 2017). Microcystins are normally localized inside the cells and are mostly released to the water after cell membrane lysis and death (TSAI, 2015).

Conventional water treatment processes (coagulation, flocculation, sedimentation and filtration) can be ineffective in removing high quantities of cyanobacteria and their metabolites (FAN *et al*., 2013a; ZHOU *et al*., 2014). Chemical treatments using conventional oxidants may be used to help remove cyanobacteria (e.g., ozone, chlorine, potassium permanganate and chlorine dioxide) but can cause cell damage and the release of cyanotoxins (ZAMYADI *et al*., 2011; CHANG *et al*., 2018). Due to the inefficiency of conventional water treatment for the removal of cyanobacteria and their toxins, it is necessary to evaluate complementary technologies that can be applied in freshwater reservoirs, i.e., eliminating cyanobacteria and their toxins prior to them entering the treatment plant.

Hydrogen peroxide (H_2O_2) has been applied as an algaecide to control cyanobacterial blooms. H_2O_2 can generate reactive oxidative species (ROS) that have high oxidative strength and are capable of compromising the cell wall. Due to this, the detection of cell stress and/or damage is important because it indicates the efficacy of the method and potential toxin release (CHOW *et al*., 1998).

Studies have suggested that H_2O_2 is an effective algaecide for cyanobacterial treatment in-reservoir, however, it is necessary to compare and verify the most suitable and rapid method to analyse the effects of H_2O_2 on cyanobacteria.

Cyanobacteria are particularly susceptible to H_2O_2 due to their physiology. One of the factors promoting the use of hydrogen peroxide is that it can be used directly in freshwater reservoirs as an algaecide to oxidize cyanobacterial cells and their toxins (FAN *et al*., 2013b; FAN *et al*., 2019) without producing oxidant residuals, as it decomposes into water and oxygen (BARROIAN AND FEUILLADE, 1986).

Cell integrity and evaluation of cell numbers can be used to determine the effects of treatment technologies on cyanobacteria. Analytical methods to determine the effect of treatments on cyanobacteria, such as fluorescence detection of photosynthetic activity, can be used as a measure of cell stress providing an indirect measure of photoinhibition in photosynthesis (CAMPBELL *et al*., 1998; YANG *et al*., 2013; SCHUURMANS *et al*., 2015; WEENINK *et al*., 2015; OGAWA *et al*., 2017).

In this study, a range of methods for identifying cell stress in the cyanobacterium *Microcystis aeruginosa* PCC 7813 under the effect of different concentrations of H_2O_2 were compared to identify which analytical method provides the most accurate and rapid response. Further, although several studies have analyzed the effects of H_2O_2 on MC-LR (QIAN *et al*., 2010; MATTHIJS *et al*., 2012; PAPADIMITRIOU *et al*., 2016; KANSOLE AND LIN, 2017; CHANG *et al*., 2018; FAN *et al*., 2019; WANG *et al*., 2015, 2018, 2019), here, for the first time, the degradation of intra- and extracellular concentration of four different microcystin analogues (MC-LR, MC-LF, MC-LY, and MC-LW) was evaluated under different concentrations of H_2O_2.

3 MATERIALS AND METHODS

3.1 Cyanobacteria

The cyanobacterium *M. aeruginosa* PCC 7813 (Pasteur Culture Collection, Paris) was cultured in BG-11 medium (STANIER *et al*., 1971) at 21±1 °C on a 12/12 h light/dark cycle illuminated by cool white fluorescent lights (correlated color temperature 1400K to 5000K) with an average illumination of 10.5 µmol photons m^{-2} s^{-1} without agitation. This particular strain of *M. aeruginosa* produces four main microcystin analogues (MC-LR, MC-LY, MC-LW, and MC-LF).

3.2 *M. aeruginosa* cell enumeration

Cell counting by Multisizer for *M. aeruginosa* numbers and determination of average cell diameter has been previously demonstrated (WOJTASIEWICZ AND STOŃ-EGIERT, 2016; KIM et al., 2020). A Multisizer 3 (Beckman Coulter, USA) was used to enumerate *M. aeruginosa* PCC 7813 cell density, to evaluate biovolume and average cell diameter. A 50 µm aperture was used, which allows particle size detection from 1 to 30 µm. Samples were diluted 100 to 600-fold in Isoton carrier liquid (Beckman Coulter, USA), depending on the sample density.

3.3 Effect of H_2O_2 on cyanobacterium *M. aeruginosa* PCC7813

A 100 mL cell suspension of *M. aeruginosa* PCC7813 (in 250 mL conical flasks) with a final concentration of 5 x 10^6 cells mL^{-1} in BG-11 was prepared and cultured for three days. Hydrogen peroxide (5 and 20 mg L^{-1}) was added to the conical flasks containing *M. aeruginosa* PCC 7813. Aliquots of 3 mL were removed at known intervals (0, 6, 12, 24, 30, 36, 48, 60, 72, 84 and 96 h) over 4 days. Samples were incubated under the same conditions as the strain was initially cultured. Treatments were performed in triplicates. Aliquots were removed for analysis of H_2O_2 concentration (100 µL) and cell enumeration (900 µL), intra/extracellular microcystin determination (1 mL) and photosynthetic activity measurements (1 mL). The aliquots for toxin analysis were centrifuged for 10 minutes at 13000 x g and the supernatant was transferred to a fresh microcentrifuge tube (1.5 mL) and stored at -20 °C, with the cell pellet also stored at -20 °C. The aliquots for all other analyses were used immediately. A negative control (no H_2O_2 addition) was also prepared in triplicate.

3.4 Analysis

3.4.1 H_2O_2 analysis

To determine the H_2O_2 concentration, a method by Drábková *et al*. (2007a) with modifications by Fan *et al*. (2013b) was used. A phosphate buffer solution was prepared with 0.5 M sodium phosphate dibasic (Na_2HPO_4) solution and 0.5 M sodium phosphate monobasic (NaH_2PO_4) solution with a final pH of 6 (all Sigma-Aldrich, UK). A solution with 0.1 g of N,N-

diethyl-1,4-phenylendiammoniumsulphate (Sigma-Aldrich, UK) in 10 mL of 0.1 N sulfuric acid (H_2SO_4, Fisher, UK) was prepared (DPD solution). Further, a horseradish peroxidase (HRP) (Sigma-Aldrich, UK) solution 1 mg L^{-1} in ultrapure water was prepared.

For analysis, 900 µL of ultrapure water and 100 µL of phosphate buffer solution were transferred into a 1 mL cuvette. Aliquots of the cell suspension were centrifuged and 40 µL of the supernatant were added to the cuvette, followed by 40 µL of DPD solution and 10 µL of HRP solution. A blank was prepared by adding 900 µL of ultrapure water followed by 100 µL of buffer solution, 40 µL of the supernatant from the control and 40 µL of DPD solution into a cuvette. All the samples were measured using a UV/VIS spectrophotometer (WPA Lightwave II, UK) at a wavelength of 551 nm. H_2O_2 (30%, Fisher, UK) was used for the H_2O_2 degradation assay. Sodium Thiosulfate ($Na_2S_2O_3.5H_2O$, Fisher, UK) was added to excess into the supernatant after the H_2O_2 determination to quench the sample.

3.4.2 High performance liquid chromatography (HPLC) analysis of extra- and intra cellular microcystin concentrations

The supernatant was removed and freeze-dried. Aliquots were resuspended in methanol (1 mL), vortexed and centrifuged for 10 minutes at 13000 G. Following this, 950 µL were transferred to a fresh microcentrifuge tube (1.5 mL) and dried in a Genevac (EZ-II evaporator, UK), resuspended in 80% methanol (100 µL) and analyzed. To the cell pellet, 80% aqueous methanol (250 µL) was added and sample tubes placed in a dispersive extractor for 5 minutes at 2500 rpm followed by centrifugation for 5 minutes at 13000 G and if not analyzed immediately, samples were stored at -20 °C until analysis.

The concentrations of four microcystin analogues (MC-LR, MC-LY, MC-LW and MC-LF) were quantified using a 2965 separation module and a 2996 photodiode array (PDA) detector (Waters, United States). Separation of analytes was achieved on a Symmetry C18 column (5 µm, 2.1 mm x 150 mm) (Waters, United States). The mobile phases used for analysis were A: ultrapure water (18.2 MΩ) and B: acetonitrile each with 0.05% trifluoroacetic acid at a flow rate of 0.3 mL min^{-1}, an injection volume of 35 µL, column temperature of 40 ºC. Initial condition was set to 80% A and 20% B, increasing to 70% B over 25 minutes followed by an organic wash and a return to the initial conditions. All chromatograms were analyzed at 238 nm and quantified using standards (as per Enzo Life Sciences) for calibration between 0.05 and 25 µg mL^{-1} in the Empower software (V3). The limit of quantification was 0.05 µg mL^{-1}.

3.4.3 Determination of photosynthetic activity

A Mini-PAM system (Walz, Germany) was used at room temperature to determine the effect of H_2O_2 on the photosynthetic activity. This instrument evaluates the photosynthetic activity by measuring the maximal values of quantum yield of photosystem II (PSII) (F_V/F_M), where F_V is the difference between the true maximal fluorescence (F_M) and the minimal fluorescence (F_0).

F_0 is determined by emitting a low intensity measuring light for 20 seconds, followed by a saturating pulse, which yields the maximal fluorescence (F_M). After 40 seconds, actinic light is activated (actinic light intensity at specified level 3), which allows the determination of the steady-state fluorescence (F_S) (OGAWA *et al*., 2017). This is true for higher plants and green algae, however the photosynthetic complex in cyanobacteria functions differently due to an effect called state transition. This means that there is a change in energy allocation between the two photosystems (PSI and PSII) in the cells, resulting in more energy in PSI (SCHUURMANS *et al*., 2015; OGAWA *et al*., 2017). Due to this, it is necessary to add diuron (Sigma-Aldrich, UK), an algaecide capable of inhibiting photosynthesis, under actinic light to detect the true maximal fluorescence in cyanobacteria (F_M') by a saturating pulse (OGAWA *et al*., 2017).

A sample of cells (400 µL) was added into a cuvette containing a small stirrer bar for agitation. After measuring F_0 and F_M readings, Diuron (0.5 M) was added to photoquench the sample and measure F_M' (CAMPBELL *et al*., 1998).

3.5 Statistical analyses

The values shown are the results of the mean of triplicates and all results were analyzed using One-way ANOVA. A significance level of $p<0.05$ was used to identify significant differences between the results.

4 RESULTS AND DISCUSSION

4.1. Cell numeration and characterization

When analyzing *M. aeruginosa* PCC 7813 cell density, the distribution was observed for the particle diameter range of 2.8 to 6.9 µm (Figure 1A and 1B) for all the samples at time

T_0 which were considered cells. Particles in the range of 1.3 to 2.7 µm were considered cell fragments. The decision to consider particles in the range of 2.8 and 6.9 µm cells, was based on the size distribution of the initial sample (Figure 1) and published data. For example, Komárek *et al*. (2002) report average cell sizes from 4 to 6 µm for *M. aeruginosa* and Harke *et al*. (2016) report cell sizes from 1 to 9 µm for the genus *Microcystis*. A decrease in the average particle diameter and an increase in the distribution maxima caused by a rise in cell density were observed in the control (Figure 1A) and the 5 mg L^{-1} (Figure 1B) samples from 0 to 96 hours. The particle diameter decrease is likely due to cyanobacterial reproduction by binary fission, which leads to a decrease in individual cell diameter due to cell division (CASSIER-CHAUVAT, CHAUVAT, 2014).

The 20 mg L^{-1} of H_2O_2 caused extensive cell damage to *M. aeruginosa* PCC 7813, increasing the number of fragments (particles in the range of 1.3 to 2.8 µm) (Figure 1C).
The effect of 20 mg L^{-1} H_2O_2 was immediate with cells rapidly fragmenting by 97%. Over the next 24 hours the cell density increased slightly again from about 45 hours onwards (Figure 2), which could represent post-treatment recovery. Although cells did not show immediate removal in the 5 mg L^{-1} H_2O_2 samples, there is evidence of growth inhibition with cell density significantly lower (p=1 x 10^{-4}) than that of the control (Figure 2).

Figure 1 – *Microcystis aeruginosa* PCC7 813 cell density (A) control, (B) 5 and (C) 20 mg L^{-1} hydrogen peroxide over 96 hours under cool white fluorescent lights of 10.5 µmol photons m^{-2} s^{-1}.

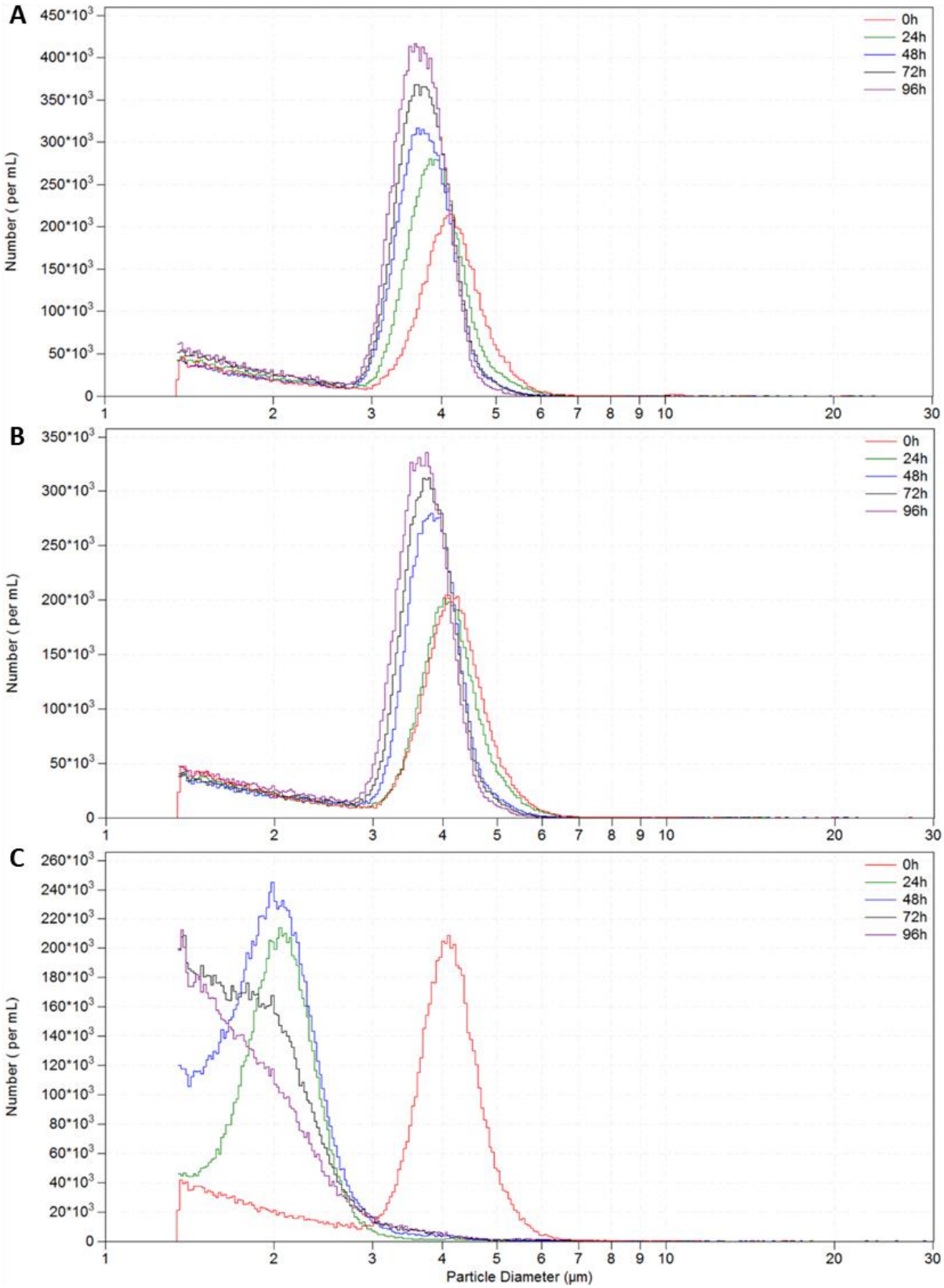

Figure 2 – *Microcystis aeruginosa* cell density for particle size range 2.8 to 6.9 µm after exposure to 0 (●), 5 (■) and 20 (▲) mg L^{-1} H_2O_2 over 96 hours under cool white fluorescent lights of 10.5 µmol photons m^{-2} s^{-1}. Grey sections on the graph denote dark time a, aa, aaa = significantly different from time T_0; b = significantly different from 96 hours 5 mg L^{-1}. (*n = 3,* error bars = $\boldsymbol{\sigma}^{-1}$).

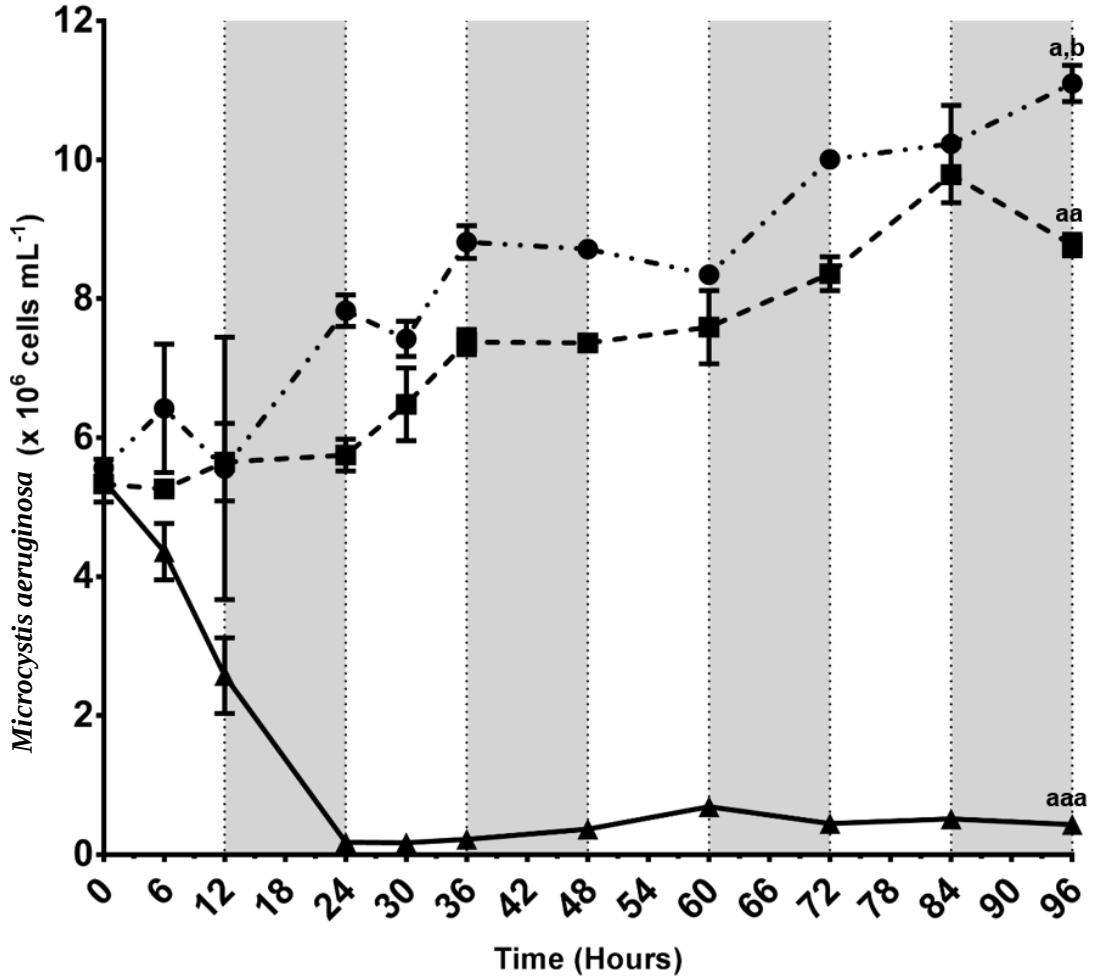

Particles in the range from 1.3 to 2.8 µm were classified as cell debris (Figure 3), which included damaged cells and cell fragments. No significant change (p=9 x 10^{-2}) was observed between 0 mg L^{-1} and 5 mg L^{-1} H_2O_2. However, the amount of cell debris in the 20 mg L^{-1} sample significantly increased (p=9.2 x 10^{-6}) over 60 hours of exposure as cells continued to fragment. There was an increase of cell fragment density over the first 60 hours which then decreased as the cell debris continued to break down into smaller fragments to the point where fragments had decreased in size to below 1.3 µm and were undetectable (Figure 1C). A similar observation was made by Fan *et al*. (2013b) where the effects of hydrogen peroxide doses (10.2, 51 and 102 mg L^{-1}) on *M. aeruginosa* (strain 338) membrane integrity were evaluated over 7 days. There were no significant differences in cyanobacterial cell density after 7 days of exposure to H_2O_2, although it was possible to observe a decrease in cell density in the present

study when using 20 mg L^{-1}. However, despite the differences in cell density results between the two studies, in Fan *et al*. (2013b), the cells decreased in size and fragmented under all the H_2O_2 concentrations which suggests a similar response as indicated by the cell debris observed in the current study.

The cyanobacterial degradation processes by H_2O_2 occur by the production of ROS that attack and destroy the cyanobacterial cell membrane. After that, ROS enter the cell resulting in photoinhibition while the cyanobacterial intracellular material is released into the extracellular matrix. Finally, ROS facilitate the oxidation of pigments (e.g. chlorophyll *a*) (WANG, XIN, WANG *et al.*, 2017).

Comparing the current study with the study of Fan *et al*. (2013b), there were differences in the study design that could explain the differences in the results observed: the growth light intensity and the light intensity used during the current experiment were almost five times lower compared to the Fan *et al*. (2013b) study. Further, the growth media used in the current study (BG-11) had a higher iron content than the one used (ASM-1) in the study by Fan *et al*. (2013b). This higher iron content may lead to photo-fenton reactions, intensifying cell disruption in the present study. The toxicity of H_2O_2 on cyanobacteria depends on several factors such as light intensity, pre-adaptation to growth at a higher light intensity and the generation of hydroxyl radicals by the photo-fenton reaction of H_2O_2 with Fe^{2+} ions present in the medium (DRÁBKOVÁ *et al.*, 2007a; CHEN *et al*., 2016). Further, a different strain of *M. aeruginosa* was used in the current investigation which might cause further differences in the results.

Figure 3 – *Microcystis aeruginosa* PCC7813 particle density for particle size range 1.3 to 2.8 µm after exposure to 0 (●), 5 (■) and 20 (▲) mg L^{-1} H_2O_2 over 96 hours under cool white fluorescent lights of 10.5 µmol photons m^{-2} s^{-1}. Grey sections on the graph denote dark time a = significantly different from time T_0. (*n = 3,* error bars = $\boldsymbol{\sigma}^{-1}$).

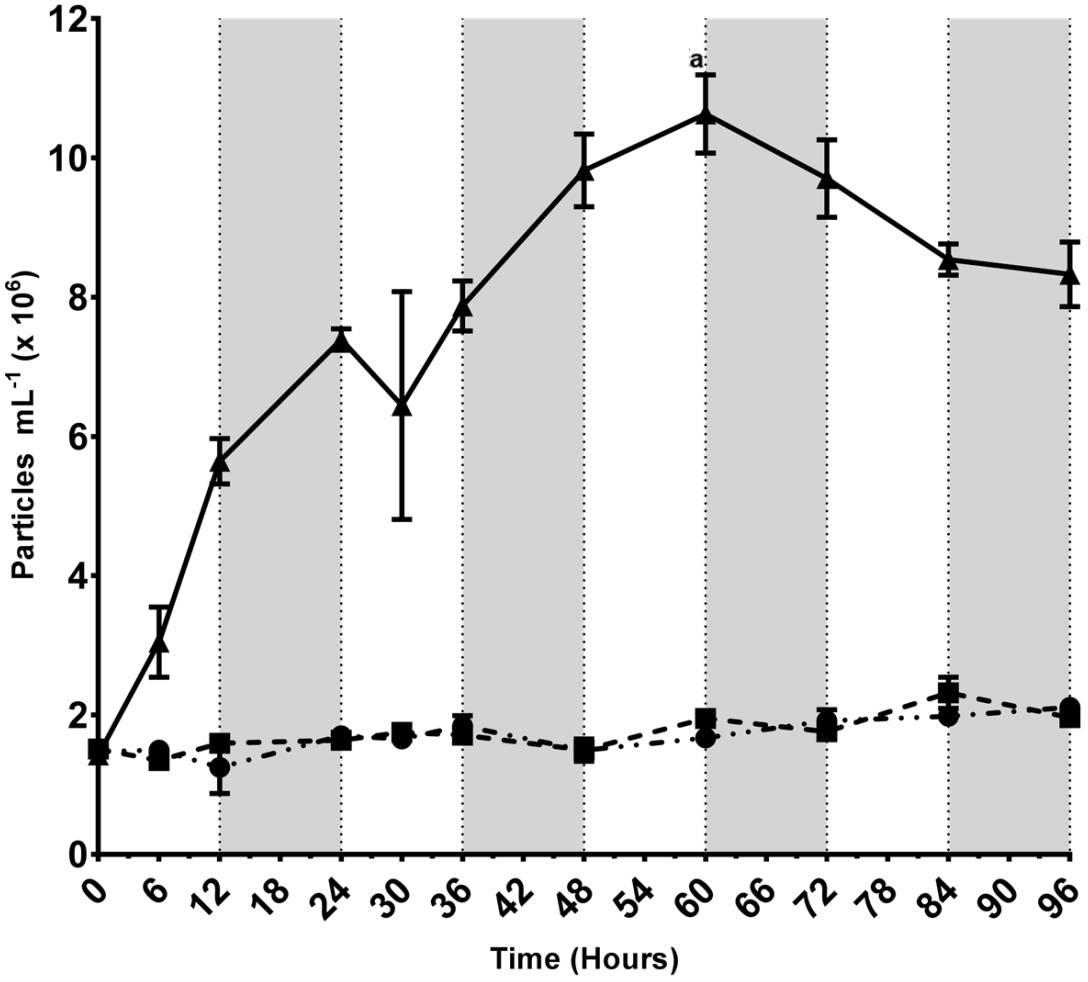

4.2 *M. aeruginosa* photosynthetic activity assay

A factor that can represent the level of stress in a cyanobacterial cell is photosynthetic activity as expressed as the F_V/F_M ratio (YANG *et al.*, 2013). Photosynthesis is the primary production in cyanobacteria/algae. Energy, in the form of light, is captured and drives the synthesis of sugar while consuming carbon dioxide and generating oxygen. The addition of H_2O_2 can generate the production of intracellular ROS that are mainly created in cyanobacteria when the absorption of light energy by chlorophyll *α* is higher than the amount of energy that can be used by the photosynthetic apparatus of the cell. These ROS cause damage in cyanobacteria by blocking the electron transport of PSII thus decreasing the photosynthetic activity, this process is known as photoinhibition (LUPÍNKOVÁ AND KOMENDA, 2004,

WANG *et al.*, 2019). Photoinhibition in cyanobacteria causes a decrease in F_V/F_M and, when F_V/F_M is close to or zero, the cells are so damaged or stressed that photosynthetic activity is completely absent. F_V/F_M was not significantly different for the control and the 5 mg L^{-1} samples of the experiment (for all samples $p>0.05$) (Figure 4). F_V/F_M decreased in the 20 mg L^{-1} samples and the photosynthetic activity was inhibited from 6 to 48 hours indicating that the photosynthetic system of *M. aeruginosa* cells was inhibited from at least 6 hours onwards (Figure 4). It must be noted that the observed increase in F_V/F_M after 48 hours is likely to be an artifact as one of the triplicate samples started showing signs of recovery.

The immediate decrease of F_V/F_M was detected after 6 hours of exposure in the 20 mg L^{-1} samples. It is possible that F_V/F_M was affected before 6 hours of treatment but was not detected earlier because the first sampling was only performed after six hours of exposure to H_2O_2.

Figure 4 – *Microcystis aeruginosa* PCC7813 maximal quantum yield results after being treated with 0 (●), 5 (■) and 20 (▲) mg L^{-1} H_2O_2 over 96 hours under cool white fluorescent lights of 10.5 µmol photons m^{-2} s^{-1}. Each point represents the individual replicates.

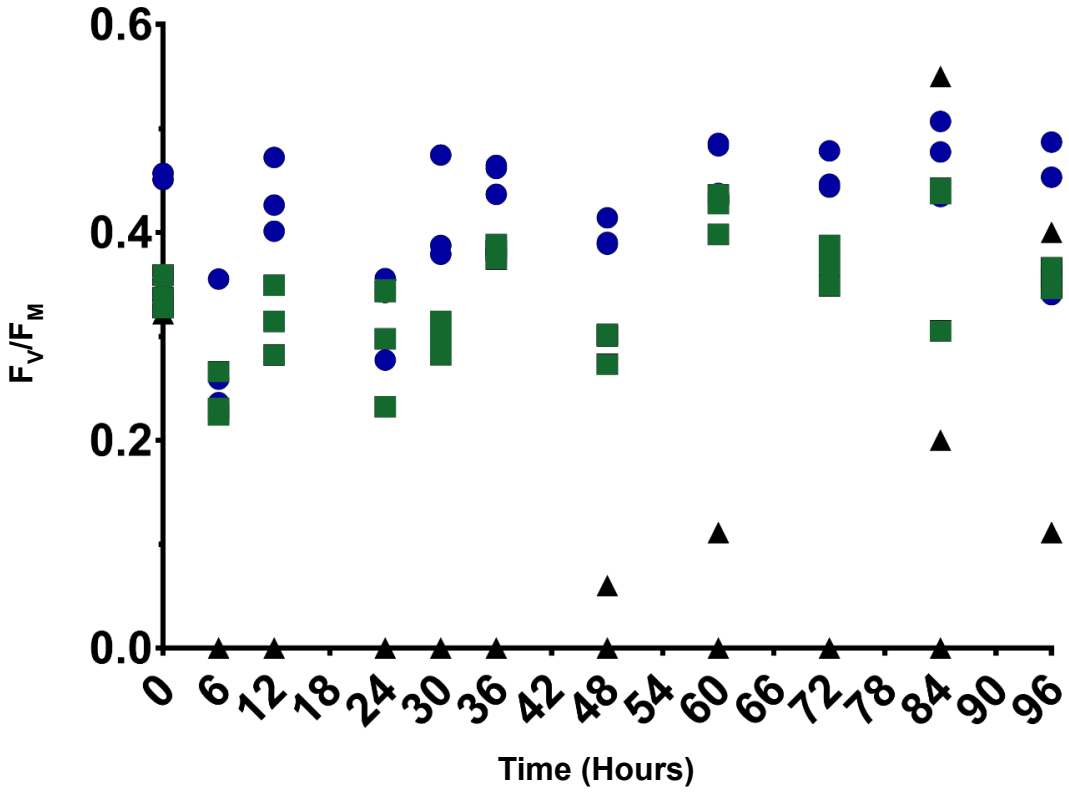

The difference between replicates in the 20 mg L^{-1} dose from 60 hours onwards can be

explained by the fact that the differences after the photoinhibition were very small (Figure 4), therefore even small variance can cause large error. The F_0 varied between 7 and 15 and the F_M varied between 7 and 24. Further, one of the samples showed signs of recovery with a F_V/F_M increasing from 0.06 to 0.44 between 48 and 60 hours.

The H_2O_2 concentration was analyzed over the 96 hours of treatment. After 30 hours, the H_2O_2 was completely consumed in the 5 and 20 mg L^{-1} samples (Figure 5). The fast decrease of the H_2O_2 concentration in the 20 mg L^{-1} samples could have made recovery possible for the *M. aeruginosa* PCC 7813 cells, which, in turn, would have prevented longer-term suppression.

Figure 5 – Decrease in hydrogen peroxide concentration of different dosages 0 (●), 5 (■) and 20 (▲) mg L^{-1} over 96 hours in the presence of *Microcystis aeruginosa* PCC7813 under cool white fluorescent lights of 10.5 µmol photons m^{-2} s^{-1} (n = 3, error bars = $\boldsymbol{\sigma}^{-1}$).

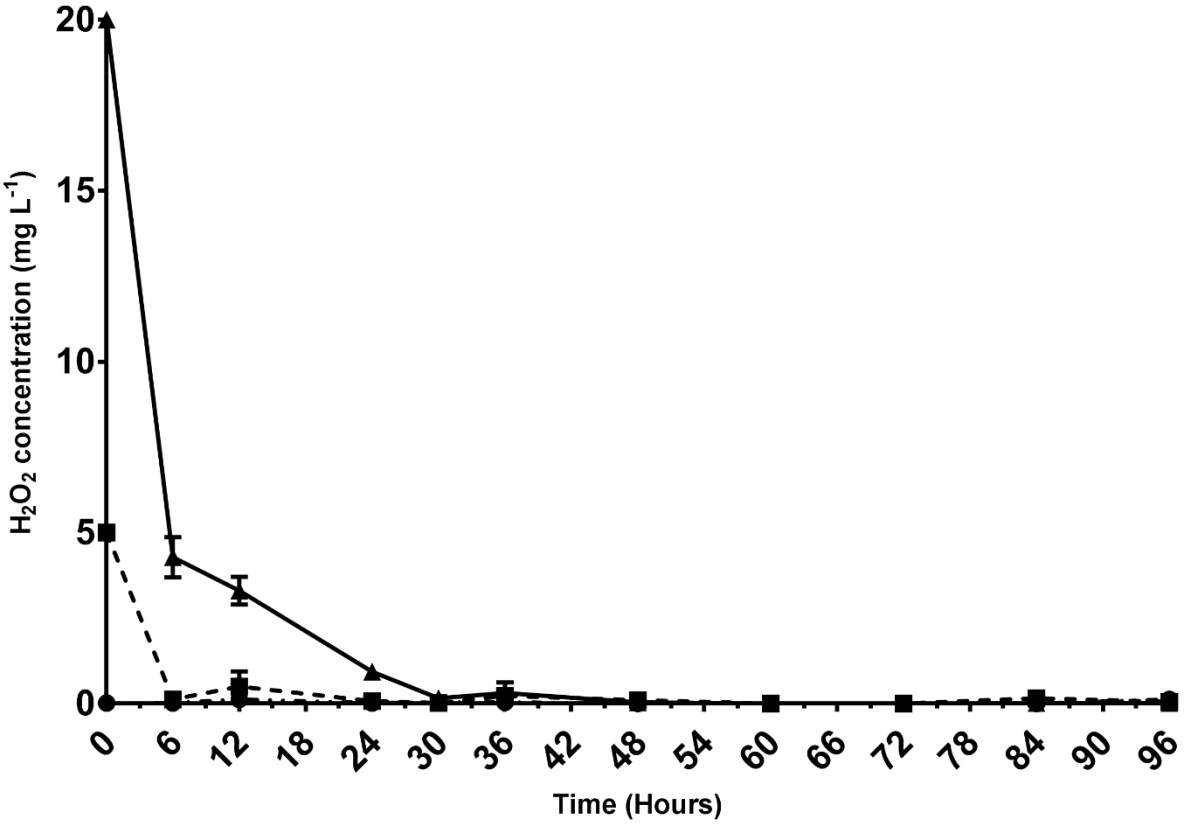

Several investigations described the behavior of *M. aeruginosa* maximal photosynthetic yield when treated with different H_2O_2 concentrations. In a study by Wang *et al*., (2019), *M. aeruginosa* FACHB-905 was treated with different concentrations of H_2O_2 (0, 2, 5, 8 and 10 mg L^{-1}) for 2 hours. A decrease in the F_V/F_M was observed for every dosage used by *Wang et al*. (2019), even for lower dosages than the H_2O_2 concentration used in the present study (20 mg L^{-1}). This decrease could be because the photosystem II of the cells was not completely quenched, so part of the energy was allocated to photosystem I. This reallocation of light energy from one photosystem to another in cyanobacteria is called state transition (OGAWA *et al.*, 2017). To suppress state transition, diuron was added in the current study, allowing a determination of the true maximal fluorescence F_M value in cyanobacteria. Further, in the Wang *et al*. (2019) study the cells were centrifuged before analysis, which could have further affected the cell stress response.

Wang *et al*. (2018) demonstrated the effects of H_2O_2 at different dosages (0, 2, 5 and 10 mg L^{-1}) on *M. aeruginosa* FACHB-905 cells using the same initial cell density analyzed in the

present study. In the Wang *et al*. (2018) study, a significant decrease in the F_V/F_M ratio after 72 hours was observed even when using lower dosages of H_2O_2 (5 mg L^{-1}) compared to the present study (20 mg L^{-1}). Again, this could have happened due to the reallocation of energy to PSI, decreasing F_V/F_M value as no addition of state transition suppressing chemicals was reported. The higher illumination and temperature used by Wang *et al*. (2018), 40 µmol m^{-2} s^{-1} at 25 °C compared to 10.5 µmol m^{-2} s^{-1} and 21°C, could be another factor that influenced the results.

Other studies evaluated different cyanobacterial species. Weenink *et al*. (2015) studied the effects of different concentrations of H_2O_2 (2.5, 5, 10, 20 and 50 mg L^{-1}) treating *Planktothrix*-dominated lake samples containing three phytoplankton groups (cyanobacteria, green algae, and diatoms). In the concentrated sample, the fluorescence value increased after 4 days of treatment in all H_2O_2 concentrations, showing similar signs of recovery from the ones found in the current study. In another large-scale study using different cyanobacterial species, Matthijs *et al*. (2012) verified a similar decrease in the photosynthetic viability when analyzing *Planktothrix agardhii*-dominated lake samples under the effects of lower dosages of H_2O_2 (0, 0.5, 1, 2 and 4 mg L^{-1}).

In the present study, the F_0 was used as an indirect indicator of chlorophyll *α* concentration which plays a central role in cyanobacterial photosynthesis (QIAN *et al.*, 2010). After 6 hours, the impact on photosynthetic activity (decrease in F_V/F_M) was already obvious in the 20 mg L^{-1} samples (Figure 4) but a decrease in F_0 (i.e. chlorophyll *α*) was only noticed after 48 hours of H_2O_2 exposure (Figure 6).

The increase in the fluorescence in 20 mg L^{-1} samples when compared to the control between 6 and 36 hours (Figure 6) was also observed by Chen *et al*. (2016). When analyzing the effects of 0, 1, 5, and 20 mg L^{-1} on lake samples dominated by *Microcystis* sp. And *Anabaena* sp. over 72 hours, they also found a chlorophyll *α* increase between 12 and 24 hours for 5 and 20 mg L^{-1} H_2O_2 samples. An increase in F_0 values is connected to cell damage after stress (DRÁBKOVÁ *et al*., 2007b) so it is possible that the increase in F_0 is a fast chemical response due to an increase in measurable chlorophyll *α* as a cell protection mechanism or a physical change in the cells which allow more chlorophyll *α* to be detected.

Figure 6 – *Microcystis aeruginosa* PCC7813 minimal fluorescence (indicative of chlorophyll α) results (percentage of the control) after being treated for 96 hours with different H_2O_2 dosages 5 ( ) and 20 ( ) mg

L^{-1} under cool white fluorescent lights of 10.5 µmol photons m^{-2} s^{-1} (*n = 3,* error bars = σ^{-1}).

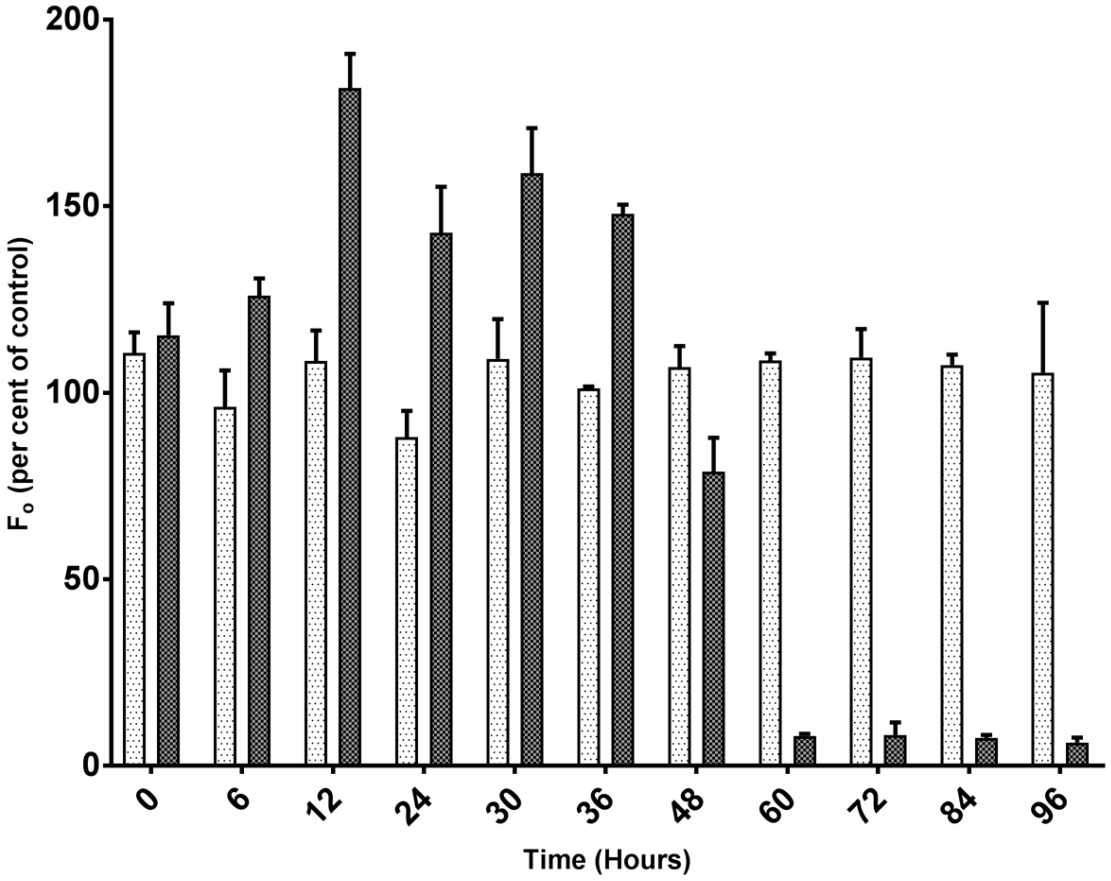

4.3 Effect of H_2O_2 on intracellular and extracellular microcystin analogues

The removal efficiency of microcystins by H_2O_2 depended on the dosage of H_2O_2 (Figure 7). All four intracellular microcystin analogues were completely degraded after 24 hours of treatment when using 20 mg L^{-1} H_2O_2, i.e., as cells were lysed and microcystins released, toxin was rapidly degraded. However, a significant increase of intracellular MC-LW and -LF after 60 hours, and in MC-LY after 72 hours (for all the samples tested $p<0.05$) was observed. There was an increase ($p<0.05$) of intracellular MC-LR, -LY, -LW and -LF after 96 hours of exposure when using 0 and 5 mg L^{-1} of H_2O_2 which corresponds to the increase in *M. aeruginosa* PCC 7813 cell density (Figure 2) for the same dosages due to cell growth. The increase for MC-LR was more marked than for the other microcystin analogues produced by *M. aeruginosa* PCC 7813 which can be explained by the fact that MC-LR is the main microcystin produced by this organism and has been observed previously (PESTANA *et al*.,

2020).

Figure 7 – Removal of intracellular MC-LR, -LY, -LW and -LF after exposure to 0 (●), 5 (■) and 20 (▲) mg L^{-1} H_2O_2 over 96 hours under cool white fluorescent lights of 10.5 µmol photons m^{-2} s^{-1}. a, aa = significantly different from time 0; b = significantly different from 48 hours; c = significantly different from 60 hours. (*n = 3,* error bars = $\boldsymbol{\sigma}^{-1}$).

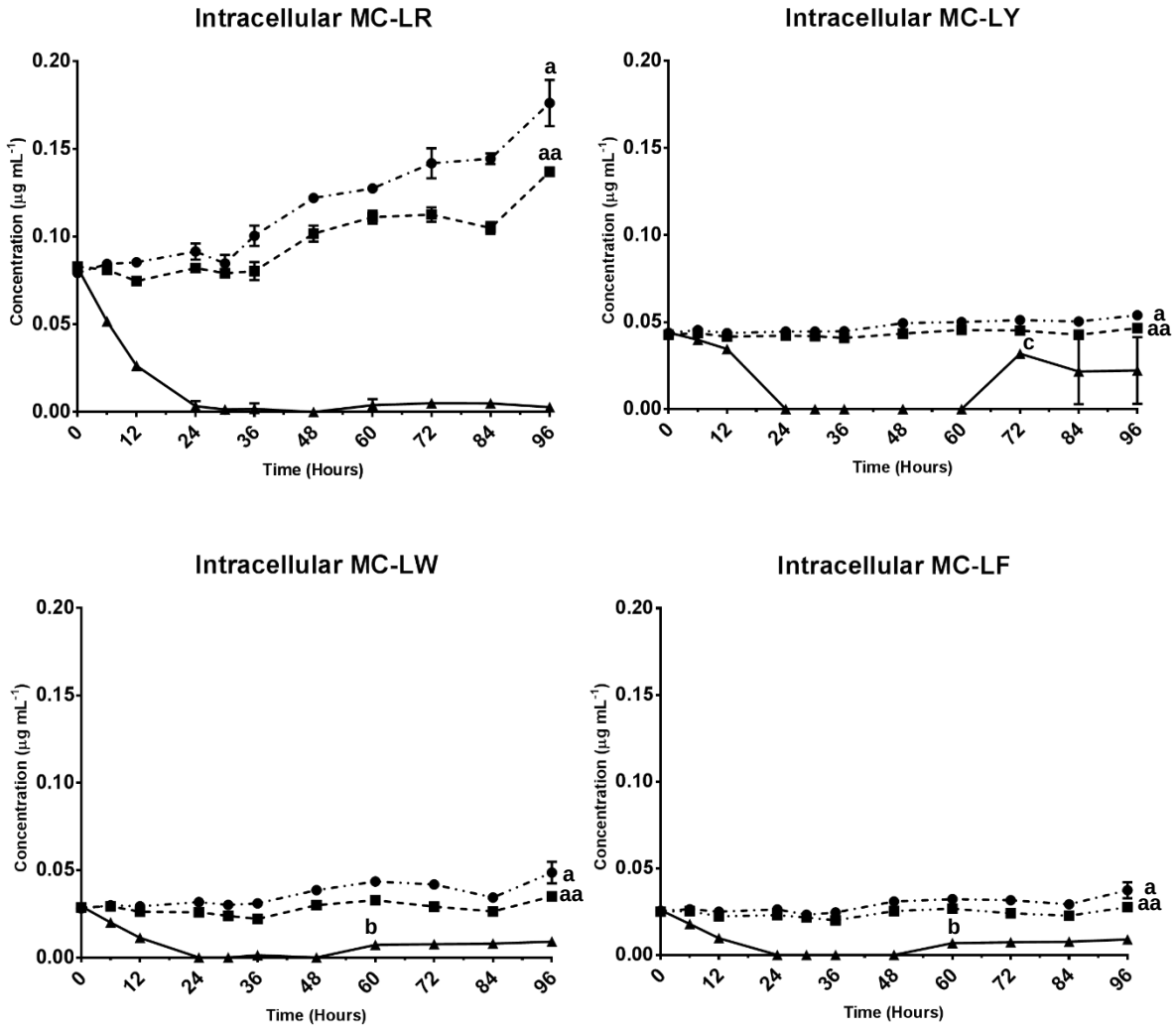

Microcystins are normally contained within the cells and are released into the surrounding water along with other intracellular contents when cell integrity is compromised. H_2O_2 is capable of lysing cells and releasing the microcystins. After the liberation of intracellular microcystins in all the 20 mg L^{-1} samples (Figure 7), no extracellular microcystins were detected. This suggests that the intracellular microcystins that were released into the surrounding water were also removed by H_2O_2.

A few studies have investigated the removal of MC-LR by H_2O_2, but this is the first time that the effect of H_2O_2 on the concentration of four analogues for both intra- and extracellular

microcystin were evaluated (MC-LR, -LY, -LW and -LF). Papadimitriou *et al*. (2016) showed that both intra- and extracellular MC-LR decreased over 4 hours in a study with naturally occurring MC-LR and 4 mg L^{-1} H_2O_2. The study by Papadimitriou *et al*. (2016) observed that the use of H_2O_2 caused cyanobacterial cell lysis followed by a release of intracellular MC which became extracellular MC and then was removed by H_2O_2. The successful removal of MC-LR even at lower H_2O_2 dosages was most likely due to a lower initial concentration of dissolved toxins used by Papadimitriou *et al*. (2016), intracellular and extracellular microcystins were below 2.5 µg L^{-1} and 0.5 µg L^{-1}, respectively.

Kansole and Lin (2017), showed similar results to the present study when evaluating cyanobacterium *M. aeruginosa* PCC 7820 with a similar initial cell density (2 x 10^6 cells mL^{-1}) and under the effects of several H_2O_2 dosages (0, 1, 2, 3, 5, 10 and 20 mg L^{-1}). The highest dosage of H_2O_2 used was able to remove both MC-LR and *M. aeruginosa* PCC 7820 cells by 40% and 95%, respectively. It should be noted that *M. aeruginosa* PCC 7813 is almost identical to *M. aeruginosa* PCC 7820 (isolated from the same original bloom), producing the same microcystins, with the exception that the PCC 7813 strain does not contain gas vesicles. As would be expected, the presence of gas vesicles does not affect cell inhibition by H_2O_2.

4.4 Comparison of cell stress detection methods

While there are more sophisticated methods that can be used for cell stress determination, such as flow cytometer with nucleioid acid dyes or cellular ROS determination, the methods used in the current study to analyse cyanobacterial cell stress were selected considering operation and availability in a water treatment company laboratory. Each method presented advantages and disadvantages for the determination of H_2O_2 induced oxidative stress in *M. aeruginosa* PCC 7813. It is possible to notice an early stress response from the cells when analyzing the inhibition of photosynthetic activity in cyanobacterial cells compared to other methods (Table 1), such as cell density analysis, chlorophyll α and toxin determination. While F_0 (the indicator of chlorophyll *α*) decreased after 48 hours (Figure 6) and cell density indicated complete removal after 24 hours (Figure 2), F_V/F_M provided a more accurate and rapid response demonstrating cyanobacteria cell stress detectable at 6 hours after exposure to H_2O_2 (Figure 4). Chlorophyll *α* concentration is a poor indicator of cellular stress, as it is initially intracellular and its concentration is only affected a considerable time after cell lysis and intracellular matter leakage into the surrounding water. Detection of chlorophyll α only indicates that this pigment

is present in the samples. It is not a measure of cell viability, as demonstrated by the fact that a decrease in F_0 was detected only after 48 hours but decline cell density was clearly seen after 24 hours.

Similar limitations are true for microcystins as an indicator cell lysis and death. After the degradation of the cell membrane, intracellular microcystin is released into the surrounding water which was observable after 24 hours, thus, while a reliable proxy measurement for cell integrity, the effects on the intracellular microcystins are less rapid than measurement of the photosynthetic activity. Since it is not possible to detect any differences in extracellular microcystin concentration over 96 hours, this method is not suitable to identify cyanobacterial cellular stress responses during oxidation. The measurement of extracellular levels of microcystin as an indicator of cell lysis is confounded by the on-going destruction of the toxins by the oxidant. As the microcystins increase in concentration in the surrounding media due to leakage from cells they will rapidly be chemically degraded by the H_2O_2. Hence, the detected concentration is a result of the total excreted microcystin minus the toxin which has been oxidized.

A further consideration when selecting a suitable cell stress detection method is the applicability of the required equipment. The time from sampling to results with the Mini-PAM fluorescence detection system is less than 10 minutes and it can be used as a portable instrument. Furthermore, the Mini-PAM can be operated on a boat during in-reservoir treatment, compared to laboratory analysis taking at least one hour for sample preparation and HPLC analysis of microcystins. While results by a particle counter can be acquired in a similar time frame to the Mini-PAM, the Multisizer can only be used in laboratory, however, both methods using the Mini-PAM (indication of photosynthesis and chlorophyll α) are non-specific, which means that in a natural water sample these would also measure the photosynthesis and chlorophyll α from other organisms, such as diatoms and green algae.

Table 1 – Comparison of different analytical methods for cell stress determination.

Method	Response time	Advantages	Disadvantages
F_v/F_M photosynthetic activity (photosynthesis)	6 hours	• Fastest response of cell stress • Applicable for *in-situ* and laboratory • Rapid analysis (< 10 minutes)	• Requires diuron which is hazardous • Non-specific (no differentiation between phytoplankton species)
Cell density (by particle counter)	24 hours	• Detects changes in particle distribution • Rapid analysis (< 10 minutes)	• Laboratory analysis • Does not differentiate viable from non-viable cells • Less suitable for filamentous organisms
Minimal fluorescence F_0 (chlorophyl *α*)	48 hours	• Applicable for *in- situ* and laboratory • Rapid analysis (< 10 minutes)	• Slowest detection of cellular stress • Non-specific (no differentiation between phytoplankton species) • Detection of chlorophyll, but not viability
Intracellular toxin	24 hours	• Good proxy for cell integrity	• Laboratory analysis • Requires long time for sample preparation and analysis (> 1 hour)
Extracellular toxin	Not detectable	• Can indicate cell lysis if toxins are not oxidized	• Laboratory analysis • Requires long time for sample preparation and analysis (> 3 hours) • Unsuitable cell stress detector due to inability to measure dissolved toxins after oxidation

5 CONCLUSION

Many studies evaluate the effects of H_2O_2 on cyanobacteria, but a reliable and rapid detection method for cell stress caused by oxidative processes is needed to allow inter-study comparison. Several approaches are suitable as a measure of cell stress in cyanobacteria with the present study was able to compare different cell stress assessment methods which could be available to most water treatment laboratories.

The current study clearly demonstrates efficacy of hydrogen peroxide in reducing cyanobacterial cell numbers, viability and microcystin contents. From the five methods investigated, the Mini-PAM fluorometer which measured photosynthetic activity (F_V/F_M) provided the most rapid analysis (< 10 minutes) and presented the fastest response time (i.e., was the method which detected stress first), and is therefore the most suitable method for cyanobacterial cell stress detection. To have a complete understanding of algaecide treatment it is desirable to combine photosynthesis, cell number and intracellular toxin detection methods. Therefore, an approach using combined methods is advisable for successful water management and to determine the efficacy of cyanobacterial removal methods.

REFERENCES

ARMOZA-ZVULONI, R., SCHNEIDER, A., SHAKED, Y. "Rapid hydrogen peroxide release during coral-bacteria interactions", **Frontiers in Marine Science**, v. 3, n. JUL, p. 1–10, 2016. DOI: 10.3389/fmars.2016.00124.

BARROIN, G., FEUILLADE, M., 1986. "Hydrogen peroxide as a potential algicide for *Oscillatoria Rubescens* D.C.", **Water Res.**, v. 20, n. 5, p. 619–623, 1986.

CAMPBELL, D., HURRY, V., CLARKE, A. K., *et al.* "Chlorophyll fluorescence analysis of cyanobacterial photosynthesis and acclimation.", **Microbiology and molecular biology reviews : MMBR**, v. 62, n. 3, p. 667–83, 1998.

CASSIER-CHAUVAT, C., CHAUVAT, F., 2014. "Cell division in cyanobacteria.", **The cell biology of cyanobacteria**. [S.l: s.n.]., 2014

CHANG, C. W., HUO, X., LIN, T. F. "Exposure of *Microcystis aeruginosa* to hydrogen peroxide and titanium dioxide under visible light conditions: Modeling the impact of hydrogen peroxide and hydroxyl radical on cell rupture and microcystin degradation", **Water Research**, v. 141, p. 217–226, 2018. DOI: 10.1016/j.watres.2018.05.023.

CHEN, C., YANG, Z., KONG, F., *et al.* "Growth, physiochemical and antioxidant responses of overwintering benthic cyanobacteria to hydrogen peroxide", **Environmental Pollution**, v. 219, p. 649–655, 2016. DOI: 10.1016/j.envpol.2016.06.043.

CHOW, C. W. K., HOUSE, J., VELZEBOER, R. M. A., *et al.* "The effect of ferric chloride flocculation on cyanobacterial cells", **Water Research**, v. 32, n. 3, p. 808–814, 1998. DOI: 10.1016/S0043-1354(97)00276-5.

DE JULIO, M., FIORAVANTE, D. A., DE JULIO, T. S., *et al.* "A methodology for optimising the removal of cyanobacteria cells from a brazilian eutrophic water", **Brazilian Journal of Chemical Engineering**, v. 27, n. 1, p. 113–126, 2010. DOI: 10.1590/S0104-66322010000100010.

DRÁBKOVÁ, M., MATTHIJS, H. C. P., ADMIRAAL, W., *et al.* "Selective effects of H_2O_2 on cyanobacterial photosynthesis", **Photosynthetica**, v. 45, n. 3, p. 363–369, 2007. DOI: 10.1007/s11099-007-0062-9.

DRÁBKOVÁ, Michaela, ADMIRAAL, W., MARŠÁLEK, B. "Combined exposure to hydrogen peroxide and light-selective effects on cyanobacteria, green algae, and diatoms", **Environmental Science and Technology**, v. 41, n. 1, p. 309–314, 2007. DOI: 10.1021/es060746i.

FALCONER, I. R., BERESFORD, A. M., RUNNEGAR, M. T. C. "Evidence of liver damage by toxin from a bloom of the blue-green alga, *Microcystis aeruginosa*", **Medical Journal of Australia**, v. 1, n. 11, p. 511–514, 1983. DOI: 10.5694/j.1326-5377.1983.tb136192.x.

FAN, F., SHI, X., ZHANG, M., *et al.* "Comparison of algal harvest and hydrogen peroxide treatment in mitigating cyanobacterial blooms via an in situ mesocosm experiment", **Science**

of The Total Environment, v. 694, p. 133721, 2019. DOI: 10.1016/j.scitotenv.2019.133721.

FAN, J., DALY, R., HOBSON, P., *et al.* "Impact of potassium permanganate on cyanobacterial cell integrity and toxin release and degradation", **Chemosphere**, v. 92, n. 5, p. 529–534, 2013. DOI: 10.1016/j.chemosphere.2013.03.022.

FAN, J., HO, L., HOBSON, P., *et al.* "Evaluating the effectiveness of copper sulphate, chlorine, potassium permanganate, hydrogen peroxide and ozone on cyanobacterial cell integrity", **Water Research**, v. 47, n. 14, p. 5153–5164, 2013. DOI: 10.1016/j.watres.2013.05.057.

HARKE, M. J., STEFFEN, M. M., GOBLER, C. J., *et al.* "A review of the global ecology, genomics, and biogeography of the toxic cyanobacterium, *Microcystis* spp.", **Harmful Algae**, v. 54, p. 4–20, 2016. DOI: 10.1016/j.hal.2015.12.007.

JOCHIMSEN, E. ., CARMICHAEL, W. W., AN, J., *et al.* "Liver failure and death after exposure to microcystins", **The New England Journal of Medicine**, v. 338, n. 13, p. 873–878, 1998. DOI: 10.1080/13504509.2013.856048 M4 - Citavi. .

KANSOLE, M. M. R., LIN, T. F. "Impacts of hydrogen peroxide and copper sulfate on the control of *Microcystis aeruginosa* and MC-LR and the inhibition of MC-LR degrading bacterium *Bacillus* sp", **Water (Switzerland)**, v. 9, n. 4, p. 1–18, 2017. DOI: 10.3390/w9040255.

KIM, M., MOON, J., LEE, Y. "Biomass and Bioenergy Loading effects of low doses of magnesium aminoclay on microalgal *Microcystis* sp. KW growth , macromolecule productions, and cell harvesting", **Biomass and Bioenergy**, v. 139, n. May, p. 105619, 2020. DOI: 10.1016/j.biombioe.2020.105619.

KOMÁREK, J., KOMÁRKOVÁ-LEGNEROVÁ, J., SANT'ANNA, C. L., *et al.* "Review of the European *Microcystis*-morphospecies (*Cyanoprokaryotes*) from nature Two common *Microcystis* species (*Chroococcales*, Cyanobacteria) from tropical America, including *M. panniformis* sp . nov .", **Cryptogamie, Algol.**, v. 23, n. 2, p. 159–177, 2002.

LUPÍNKOVÁ, L., KOMENDA, J. "Oxidative Modifications of the Photosystem II D1 Protein by Reactive Oxygen Species: From Isolated Protein to Cyanobacterial Cells", **Photochemistry and Photobiology**, v. 79, n. 2, p. 152, 2004. DOI: 10.1562/0031-8655(2004)079<0152:omotpi>2.0.co;2.

MATTHIJS, H. C. P., VISSER, P. M., REEZE, B., *et al.* "Selective suppression of harmful cyanobacteria in an entire lake with hydrogen peroxide", **Water Research**, v. 46, n. 5, p. 1460–1472, 2012. DOI: 10.1016/j.watres.2011.11.016.

OGAWA, T., MISUMI, M., SONOIKE, K. "Estimation of photosynthesis in cyanobacteria by pulse-amplitude modulation chlorophyll fluorescence: problems and solutions", **Photosynthesis Research**, v. 133, n. 1–3, p. 63–73, 2017. DOI: 10.1007/s11120-017-0367-x.

PAPADIMITRIOU, T., KORMAS, K., DIONYSIOU, D. D., *et al.* "Using H_2O_2 treatments for the degradation of cyanobacteria and microcystins in a shallow hypertrophic reservoir",

Environmental Science and Pollution Research, v. 23, n. 21, p. 21523–21535, 2016. DOI: 10.1007/s11356-016-7418-2.

PINHO, L. X., AZEVEDO, J., MIRANDA, S. M., *et al.* "Oxidation of microcystin-LR and cylindrospermopsin by heterogeneous photocatalysis using a tubular photoreactor packed with different TiO_2 coated supports", **Chemical Engineering Journal**, v. 266, p. 100–111, 2015. DOI: 10.1016/j.cej.2014.12.023.

QIAN, H., YU, S., SUN, Z., *et al.* "Effects of copper sulfate, hydrogen peroxide and N-phenyl-2-naphthylamine on oxidative stress and the expression of genes involved photosynthesis and microcystin disposition in *Microcystis aeruginosa*", **Aquatic Toxicology**, v. 99, n. 3, p. 405–412, 2010. DOI: 10.1016/j.aquatox.2010.05.018. Disponível em: http://dx.doi.org/10.1016/j.aquatox.2010.05.018.

RINEHART, K.L., NAMIKOSHI, M., CHOI, B.W. "Structure and biosynthesis of toxins from blue-green algae (cyanobacteria)", **Journal of Applied Phycology**, v. 6, n. 2, p. 159-176, 1994. DOI: 10.1007/BF02186070.

SCHUURMANS, R. M., VAN ALPHEN, P., SCHUURMANS, J. M., *et al.* "Comparison of the photosynthetic yield of cyanobacteria and green algae: Different methods give different answers", **PLoS ONE**, v. 10, n. 9, p. 1–17, 2015. DOI: 10.1371/journal.pone.0139061.

SPOOF, L., CATHERINE, A., "Cyanobacteria samples: preservation, abundance and biovolume measurements". In: MERILUOTO, J., SPOOF, L., A. CODD, G. (Org.), **Handbook of Cyanobacterial Monitoring and Cyanotoxin Analysis**, Chichester, UK, John Wiley & Sons, 2017. p. 526–537. DOI: 10.1002/9781119068761.

STANIER, R. Y., KUNISAWA, R., MANDEL, M., *et al.* "Purification and properties of unicellular blue-green algae (order *Chroococcales*).", **Bacteriological reviews**, v. 35, n. 2, p. 171–205, 1971. DOI: 10.1128/mmbr.35.2.171-205.1971.

TSAI, K. "Ecotoxicology and Environmental Safety Effects of two copper compounds on *Microcystis aeruginosa* cell density, membrane integrity, and microcystin release", **Ecotoxicology and Environmental Safety**, v. 120, p. 428–435, 2015. DOI: 10.1016/j.ecoenv.2015.06.024.

WANG, B., SONG, Q., LONG, J., *et al.* "Optimization method for *Microcystis* bloom mitigation by hydrogen peroxide and its stimulative effects on growth of chlorophytes", **Chemosphere**, v. 228, p. 503–512, 2019. DOI: 10.1016/j.chemosphere.2019.04.138. Disponível em: https://doi.org/10.1016/j.chemosphere.2019.04.138.

WANG, B., WANG, X., HU, Y., *et al.* "The combined effects of UV-C radiation and H_2O_2 on *Microcystis aeruginosa*, a bloom-forming cyanobacterium", **Chemosphere**, v. 141, p. 34–43, 2015. DOI: 10.1016/j.chemosphere.2015.06.020.

WANG, J., CHEN, Z., CHEN, H., *et al.* "Effect of hydrogen peroxide on *Microcystic aeruginosa*: Role of cytochromes P450", **Science of the Total Environment**, v. 626, p. 211–218, 2018. DOI: 10.1016/j.scitotenv.2018.01.067.

WANG, X., WANG, X., ZHAO, J., *et al.* "Solar light-driven photocatalytic destruction of cyanobacteria by F-Ce-TiO_2/expanded perlite floating composites", **Chemical Engineering Journal**, v. 320, p. 253–263, 2017. DOI: 10.1016/j.cej.2017.03.062. DOI: 10.1016/j.cej.2017.03.062.

WEENINK, E. F. J., LUIMSTRA, V. M., SCHUURMANS, J. M., *et al.* "Combatting cyanobacteria with hydrogen peroxide: A laboratory study on the consequences for phytoplankton community and diversity", **Frontiers in Microbiology**, v. 6, n. JUN, p. 1–15, 2015. DOI: 10.3389/fmicb.2015.00714.

WOJTASIEWICZ, B., STOŃ-EGIERT, J. "Bio-optical characterization of selected cyanobacteria strains present in marine and freshwater ecosystems", **Journal of Applied Phycology**, v. 28, n. 4, p. 2299–2314, 2016. DOI: 10.1007/s10811-015-0774-3. .

YANG, W., TANG, Z., ZHOU, F., *et al.* "Toxicity studies of tetracycline on *Microcystis aeruginosa* and *Selenastrum capricornutum*", **Environmental Toxicology and Pharmacology**, v. 35, n. 2, p. 320–324, 2013. DOI: 10.1016/j.etap.2013.01.006. DOI: 10.1016/j.etap.2013.01.006.

ZAMYADI, A., MACLEOD, S. L., FAN, Y., *et al.* "Toxic cyanobacterial breakthrough and accumulation in a drinking water plant : A monitoring and treatment challenge", v. 6, 2011. DOI: 10.1016/j.watres.2011.11.012.

ZHOU, S., SHAO, Y., GAO, N., *et al.* "Removal of *Microcystis aeruginosa* by potassium ferrate (VI): Impacts on cells integrity, intracellular organic matter release and disinfection by-products formation", **Chemical Engineering Journal**, v. 251, p. 304–309, 2014. DOI: 10.1016/j.cej.2014.04.081.

CHAPTER II

Comparison of UV-A photolytic and UV/TiO_2 photocatalytic effects on *Microcystis aeruginosa* PCC7813 and four microcystin analogues: a pilot scale study

In preparation for submission to Journal of Environmental Management (Qualis Capes A1)

Comparison of UV-A photolytic and UV/TiO_2 photocatalytic effects on *Microcystis aeruginosa* PCC7813 and four microcystin analogues: a pilot scale study

Arthours: Indira de Menezes Castro; José Capelo Neto; Carlos João Pestana; Allan Clemente; Jianing Hui; John Irvin; Nimal Gunaratne; Peter Robertson; Christine Edwards; Linda Lawton

ABSTRACT

To date, the high cost of supplying UV irradiation has prevented the widespread application of UV photolysis and titanium dioxide based photocatalysis in the water treatment sector. To overcome this problem, photolysis and heterogeneous photocatalysis applying TiO_2 coated glass beads under UV-LED illumination (365 nm) in a pilot scale reactor was developed to eliminate *Microcystis aeruginosa* PCC7813 and four microcystin analogues (MC-LR, -LY, -LW, -LF) with a view to deployment in drinking water reservoirs. UV-A (365 nm) photolysis was shown to be more effective than the UV/TiO_2 photocatalytic system for removal of *Microcystis aeruginosa* cells and microcystins. During photolysis, cell density significantly decreased over 5 days from an initial concentration of 5.8 x 10^6 cells mL^{-1} until few cells were left. Both intra- and extracellular microcystin concentration were significantly reduced by 100 and 92%, respectively, by day 5 of the UV treatment for all microcystin analogues. During UV/TiO_2 treatment, there was a great variability between replicates, making prediction of cyanobacterial cell and toxin behavior difficult. Further, the cell death during UV-A photolysis was shown to have long-term effects on *M. aeruginosa* PCC7813 cells, inhibiting regrowth for at least six days.

Key words: blue-green algae; photolysis; photocatalysis; cyanotoxins; reservoir treatment

Highlights

- UV-A photolysis most efficient elimination of cyanobacteria and toxins
- Complete inhibition of *M. aeruginosa* PCC7813 by UV-A photolysis
- 92% removal of four microcystins after UV-A photolysis (intra- and extracellular)

Graphical abstract

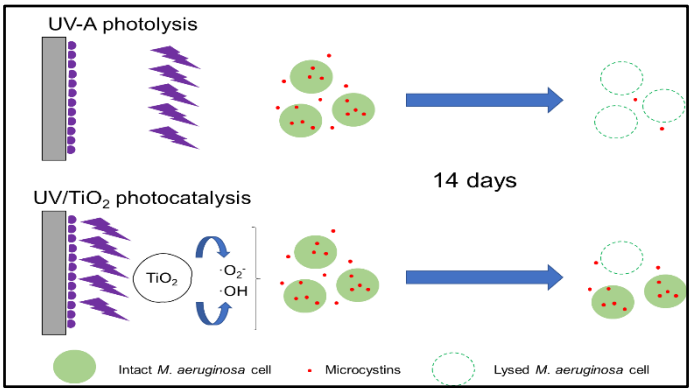

6 INTRODUCTION

Cyanobacterial blooms in freshwater reservoirs represent a threat to human and animal health because of the potential release of a wide variety of harmful metabolites, known collectively as cyanotoxins (Carmichael *et al*., 2001; Falconer *et al*., 1983; Jochimsen *et al*., 1998). Microcystins (MCs) are one of the most commonly reported cyanotoxins with over 247 analogues to date (Spoof and Catherine, 2017). Conventional water treatment (i.e., coagulation, flocculation, sedimentation or flotation and filtration) is used worldwide, however, these processes can promote cell rupture and consequently cyanotoxin release into the environment (Chang *et al*., 2018; Pestana *et al*., 2019). Further, conventional treatment methods are designed for the removal of suspended or colloidal particles and are not fit to remove dissolved contaminants including dissolved cyanotoxins (Chae *et al*., 2019; Vilela *et al*., 2012). In order to mitigate the effect of dissolved cyanobacterial toxins entering water treatment plants, advanced oxidation processes (AOPs) such as photocatalysis and photolysis can be used for the control of cyanobacterial cells and toxic metabolites within reservoirs (Fan *et al*., 2019; Matthijs *et al*., 2012; Ou *et al*., 2011a).

UV photolysis is an AOP that has been widely applied for the inactivation of pathogenic microbes in water treatment and other applications and can be used as a strategy for removing cyanobacteria and their toxins. A few studies have evaluated the effects of mainly UV-C (usually 254 nm) and UV-B (usually 312 nm) on microcystin degradation and *Microcystis aeruginosa* removal (Liu *et al*., 2010; Moon *et al*., 2017; Tao *et al*., 2018). This, however, is the first time that the degradation of *M. aeruginosa* PCC7813 and four microcystin analogues (MC-LR, MC-LW, MC-LY, MC-LF) under UV-A (365 nm) irradiation was investigated.

UV-irradiation-driven titanium dioxide (TiO_2) photocatalysis is another AOP that can be used to control cyanobacteria and their toxins. The TiO_2 photocatalytic effect is limited under visible light, which limits its application in drinking water treatment (Jin *et al*., 2019). TiO_2 activation needs to occur under UV light irradiation (< 387 nm) (Chang *et al*., 2018; Hu *et al*., 2017; Zhao *et al*., 2014) due to the energy required to overcome the band gap (3.2 eV and 3.0 eV for the anatase and rutile forms of TiO_2 respectively) between the valence and conduction bands (Chen *et al*., 2015; Hu *et al*., 2017; Pinho *et al*., 2015). The need for UV irradiation (below 387 nm) is a hurdle in the practical application of photolysis and photocatalysis (Chae *et al*., 2019). To overcome this, and to make the systems practical for application in reservoirs used for drinking water, the system investigated here employs UV (365 nm) light emitting

diodes (LEDs), which are low-cost (ca. USD 0.78 per LED), long life (approximately 100,000 working hours; Heering, 2004), low energy and are capable of activating TiO_2. In the current study, UV-LED-driven photolysis and heterogeneous TiO_2 photocatalysis was evaluated over 14 days for the elimination of *M. aeruginosa* PCC7813 as well as for the destruction of four microcystin analogues (MC-LR, MC-LW, MC-LY, MC-LF).

7 METHODS

7.1 Reagents

The chemicals for artificial fresh water (AFW) and BG-11 culture medium (Stanier *et al*., 1971) preparation were of reagent grade (Fisher Scientific, UK). AFW was prepared according to Akkanen and Kukkonen (2003) by dissolving $CaCl_2$ (11.8 mg L^{-1}), $MgSO_4$ (4.9 mg L^{-1}), $NaHCO_3$ (2.6 mg L^{-1}) and KCl (0.2 mg L^{-1}) in ultrapure water. For AFW, pH was adjusted to 7 with 1 M hydrochloric acid or 1 M sodium hydroxide if required. Acetonitrile, methanol, and trifluoroacetic acid used for high performance liquid chromatography analysis of microcystins were of HPLC grade (Fisher Scientific, UK). Diuron (3-(3,4-dichlorophenyl)-1,1-dimethylurea) (Sigma-Aldrich, UK) was used for photosynthetic activity assays. Isoton II Diluent obtained from Beckman Coulter (USA) was used for cyanobacterial cell density determination. All solutions were prepared using ultrapure water (18.2 MΩ) provided by an ELGA PURELAB system (Veolia, UK).

7.2 Cyanobacterial cultivation

The cyanobacterium *M. aeruginosa* PCC7813 (Pasteur Culture Collection) was grown in BG-11 medium at 21±1 °C with constant cool white fluorescent illumination with an average light intensity of 10.5 µmol photons m^{-2} s^{-1} and constant sparging with sterile air. This strain does not have gas vesicles and produces four main microcystin analogues (MC-LR, MC-LY, MC-LW and MC-LF).

7.3 Reactor setup of *M. aeruginosa* PCC7813 and microcystins treatment

A cell suspension of a 27 days-old culture of *M. aeruginosa* PCC7813 (5 x 10^6 cells mL^{-}

[1]) in AFW was prepared and sampled prior to addition to the reactors (C_0). The reactors (1000 x 90 mm) were made of a stainless-steel mesh with an aperture of 1.2 x 1.2 mm and 0.4 mm wire strength. Each reactor was placed inside an acrylic cylinder (1100 x 95 mm) that could be filled with 6.5 liters of *M. aeruginosa* suspension. The acrylic cylinders were sparged from the bases through a multi-porous air-stone with sterile air with the aid of a pump for continuous gentle air flow (1 L min^{-1} per reactor; Figure 1). The top of the acrylic cylinders was covered with a bung to avoid external contamination and to allow air exchanges. Also, an overhead low light intensity from the ambient light (2.5 µmol photons m^{-2} s^{-1}) was used. Triplicate reactors were prepared for each of the tested systems (UV-only, TiO_2-only and UV/TiO_2).

Figure 1 – Schematic representation of the experimental reactors design for (A) UV photolysis, (B) TiO_2-only and (C) UV/TiO_2 photocatalysis. 1 – acrylic cylinders containing the stainless-steel reactors, 2 – stainless-steel pods containing TiO_2 coated beads, 3 – empty stainless-steel pods, 4 – aeration pump for continuous gentle air flow, 5 – air flow distributor to achieve equal air pressure across all samples, 6 – silicone tubes connecting the air flow distribution and the reactors, 7 – UV light from UV-LED strip, 8 – power source connection.

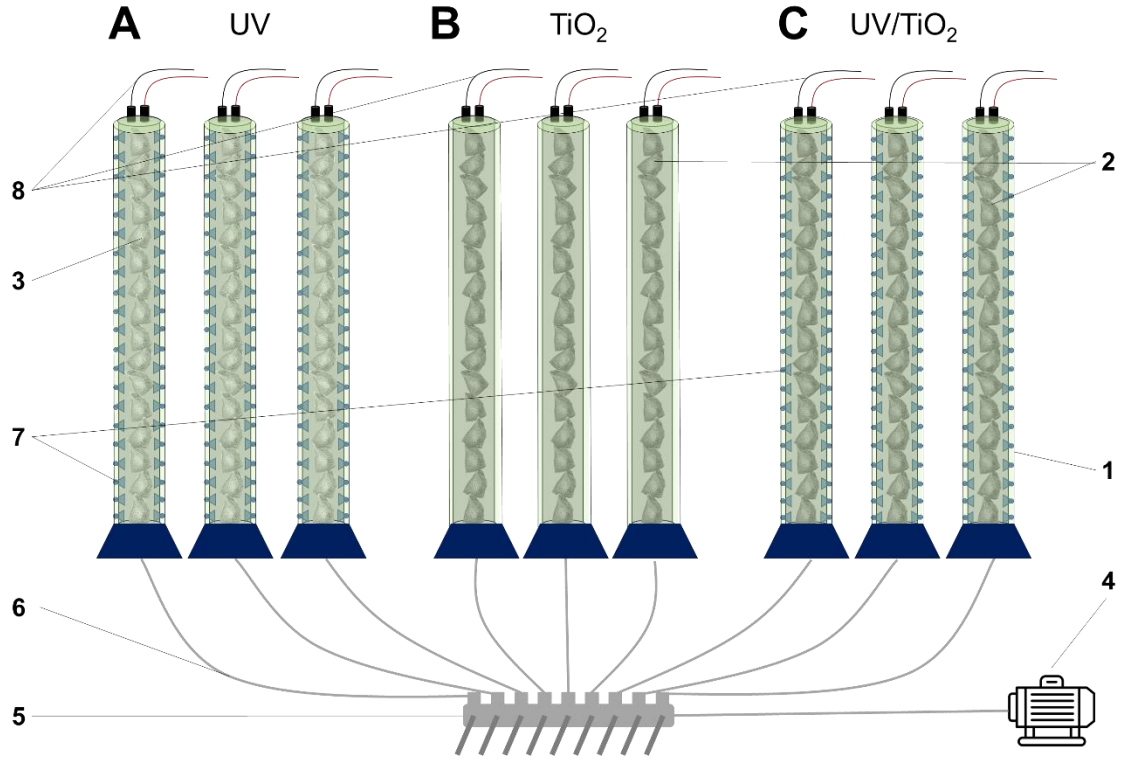

One set of three reactors for the UV-A treatment (photolysis) was prepared (Figure 1A) which consisted of reactors with 5 UV-LED strips (1 meter), each with 120 individual UV-LEDs (λ=365 nm and light intensity of 5 W m^{-2}), attached to the external surface of the acrylic cylinders and 6.5 L of the cyanobacterial cell suspension added. In the UV-A treatment, empty

stainless-steel wire mesh pods (aperture 1.2 x 1.2 mm, wire strength 0.4 mm) were placed inside the reactors without TiO_2 coated glass beads to allow observation of the effects of only UV-A light on *M. aeruginosa* PCC7813 and its four microcystin analogues. To determine if the TiO_2 coated beads influence the cells and toxins in the absence of UV light, a second set of triplicate reactors was prepared (Figure 1B), consisting of 6.5 L of the *M. aeruginosa* PCC7813 suspension and TiO_2 coated glass beads (3.2 g) inside tetrahedral stainless-steel pods (Figure S1). The TiO_2 coated beads were made from recycled glass that were prepared as per Pestana *et al*. (2020) and Hui *et al*. (2021) containing approximately 12% (w/w) TiO_2. In the TiO_2-only samples, no UV illumination was used, however, an overhead low light intensity (2.5 µmol photons m^{-2} s^{-1}) was used, since photosynthetic organisms, like cyanobacteria, require light to survive. Finally, a third set to test the efficacy of TiO_2 photocatalysis was prepared. The UV/TiO_2 treatment consisted of reactors with TiO_2 coated glass beads inside of the stainless-steel pods (Figure S1), 5 UV-LED strips and 6.5 liters of *M. aeruginosa* cell suspension (Figure 1C).

Samples were collected at the same time every day over 14 days. A total of 4 mL was removed at each sampling point, of which 1.5 mL was used for cell enumeration, 1.5 mL was used for intra/extracellular microcystin analysis and 1 mL was used for photosynthetic activity measurements. All aliquots were used immediately except for the aliquots for toxin determination, which were centrifuged for 10 minutes at 13000 G and the supernatant and cell pellets were stored separately at -20 °C until further processing and analysis.

7.4 *M. aeruginosa* PCC7813 regrowth experiment

To assess the regrowth of *M. aeruginosa* PCC7813 after 14 days of treatment, samples (50 mL) were removed from each reactor and mixed with an equal volume of BG-11 medium. Aliquots of this mixture (3 mL) were transferred to 28 sterile glass vials (4 mL volume) to allow for sacrificial sampling over seven days with four replicate samples. All four samples for one sampling point were placed in a sterile glass beaker (150 mL) and covered with a sterile petri dish lid (Figure S2). Immediately, one set of samples was removed and cell density was analyzed (C_0 sample), the remaining beakers were incubated at 21±1 °C on a 12/12 hours light/dark cycle illuminated by cool white fluorescent lights with an average light intensity of 10.5 µmol photons m^{-2} s^{-1} without agitation for the following 6 days and sampled at the same time every day.

7.5 Analysis

7.5.1 M. aeruginosa *PCC7813 cell density determination*

M. aeruginosa PCC7813 cell density was measured with a Multisizer 3 (Beckman Coulter, USA). A 50 µm aperture tube was used to detect particle sizes from 1 to 7 µm for both reactor treatments and regrowth experiments. Samples were diluted 200 to 1500-fold in Isoton II Diluent (Beckman Coulter, USA), depending on the sample cell density.

7.5.2 M. aeruginosa *PCC7813 photosynthetic activity evaluation*

A Mini-PAM system (Walz, Germany) was used for cyanobacterial photosynthetic activity analysis according to Menezes *et al*. (2020). In short, the minimal fluorescence F_0 was measured by adding 400 µL of sample into a cuvette under agitation followed by diuron (0.5 M) addition (20 µL) and the true maximal fluorescence measurement (F_M') by a saturating pulse under actinic light. The cyanobacterial photosynthetic activity can be determined by the maximal values of quantum yield of photosystem (PS) II calculated by F_V/F_M', where F_V is the difference between F_M' and F_0 (Stirbet *et al*., 2018).

7.5.3 *Intra- and extracellular microcystin determination by high-performance liquid chromatography (HPLC)*

After sampling, the liquid and solid portions of the sample were separated in a centrifuge for 10 minutes at 13000 G. The supernatant, representing the extracellular toxin component, was evaporated to dryness in an EZ-II evaporator (Genevac, UK). Dried samples were resuspended in 80% aqueous methanol (150 µL) and stored at -20 °C until analysis. Cell pellets, representing the intracellular toxin component, were resuspended in 80% aqueous methanol (150 µL), agitated in a dispersive extractor for 5 minutes at 2500 rpm and centrifuged for 10 minutes at 13000 G to remove cell debris. The resultant supernatant, representing the liberated intracellular content was stored at -20 °C until analysis. The concentrations of four microcystin analogues (MC-LR, MC-LY, MC-LW and MC-LF) were quantified by HPLC (Table 1).

Table 1 – Analytical conditions of HPLC for intra- and extracellular microcystins determination.

Parameters	Conditions
HPLC	2965 separation module and a 2996 photodiode array (PDA) detector (Waters, United States)
Column	Symmetry C18 column, 2.1 mm x 150 mm, 5 μm particle size (Waters, United States)
Mobile phase	A: 0.05% trifluoroacetic acid in ultrapure water (18.2 MΩ) B: 0.05% trifluoroacetic acid in acetonitrile
Gradient	Time (min) 0 25 26 29 35 Solvent A (%) 80 30 0 80 80
Flow rate	0.3 mL min^{-1}
Injection volume	35 μL
Column temperature	40 ºC
PDA scan range	200-400 nm

All chromatograms were extracted at 238 nm and quantified using standards (as per Enzo Life Sciences) for calibration between 0.001 and 5 μg mL^{-1} in the Empower software. The limit of quantification was 0.01 μg mL^{-1} for MC-LF and 0.005 μg mL^{-1} for the other microcystin analogues.

7.7 Statistical data analyses

All statistical analyses were performed using RStudio with a significance level of 5%. In order to verify if the TiO_2-only samples, UV and UV/TiO_2 treatments influenced cell numbers or toxin removal it is necessary to identify a significant reduction of cell density during treatment and intra- and extracellular microcystin concentration (dependent variables) over 14 days (independent variable). The results were pre-analyzed using different statistical models, i.e., linear, piecewise, linear-plato, exponential and logarithmic regression. The models were selected and adjusted using the linear or piecewise regression techniques using the mean of triplicates from each treatment group. The linear or piecewise regression techniques were selected because they were the models that presented the best fit with the data. The mean was selected to create each model because the mean values presented normal distribution according to Shapiro-Wilk Normality Test (data not shown). The linear regression consists in a linear relation between dependent (cell density and microcystins concentration) and independent

(time) variables. The piecewise regression consists in multiple linear models to the data for different ranges of the independent variable, which means that the tendency/inclination of the curve of the dependent variable will change over the independent variable. A detailed description of the data analysis and the model selection can be found in the supplementary material (S3).

8 RESULTS AND DISCUSSION

8.1 Treatment effects on *Microcystis aeruginosa* PCC7813 cell density and photosynthetic activity

The removal of *M. aeruginosa* PCC7813 in a photocatalytic and a photolytic reactor using UV-LEDs and TiO_2 coated beads was investigated. The effect of the UV-A treatment presented a piecewise regression tendency (Figure S3) with a cell density decrease from 5.4 x 10^6 cells mL^{-1} over 5 days until there were only 1.8 x 10^4 cells mL^{-1} left (significant tendency rate of 1.12 x 10^6 cells mL^{-1} day^{-1} until 5 days, $p<0.01$; Figure 2A).

Figure 2 – Effects of (A) UV-LED irradiation (365 nm), (B) TiO_2 coated glass beads under ambient light (13.7 µmol photons m^{-2} s^{-1}) and (C) photocatalytic treatment on *Microcystis aeruginosa* PCC7813 cell density using TiO_2 coated glass beads under UV-LED illumination (365 nm) over 14 days under sparging with sterile air. Data points represent individual replicates for each treatment.

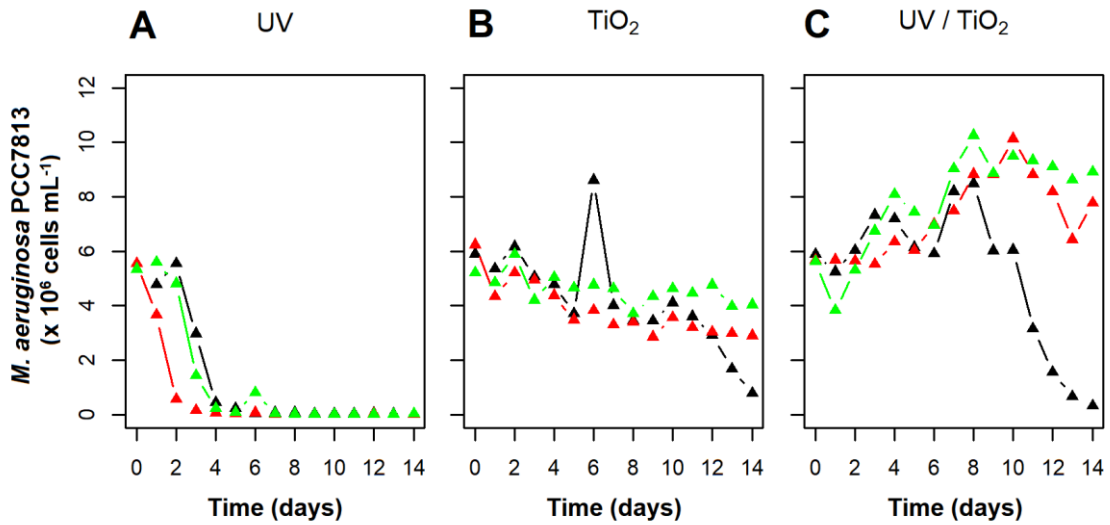

Biological replicates can commonly present different behaviors even when exposed to very similar conditions. *M. aeruginosa* PCC7813 cell numbers showed slightly different trends

during TiO_2-only treatment with variability increasing as the investigation progressed, particularly after day 10. The outlier observed in day 6 probably occurred due to lack of mixing during mixings, since samples were consistent until day 10. *M. aeruginosa* PCC7813 cell numbers decreased on average from to 5.8 x 10^6 to 2.6 x 10^6 cells mL^{-1} with a significant rate of 0.19 x 10^6 cells mL^{-1} day^{-1} (p<0.01) over 14 days (Figure 2B) represented by a linear regression (Figure S4). The variability that increased over time might have occurred due to adsorption of cells onto the surface of the TiO_2 layer on the beads and to adhesion of cells onto the inside walls of the reactor.

An inhibition in cell numbers was expected to be observed in the UV/TiO_2 treatment on the *M. aeruginosa* PCC7813 cell density based on previous bench-scale studies (Chang *et al*., 2018; Song *et al*., 2018; Wang *et al*., 2018, 2017; Pinho *et al*., 2012). However, the *M. aeruginosa* cell density could best be represented by a piecewise regression tendency (Figure S5) and significantly rose in the UV/TiO_2 treatment over eight days with a tendency of 0.46 x 10^6 cells mL^{-1} day^{-1} (p<0.01), and then decreased after day 8 with a tendency of 1 x 10^6 cells mL^{-1} day^{-1} (p<0.01; Figure 2C). The fact that the visible light available for cyanobacterial growth was probably insufficient (2.5 µmol photons m^{-2} s^{-1}) indicates that the coated glass beads might have converted some of the UV emitted by the LEDs into visible light, as previously observed (Li *et al*., 2016). Photoluminescence measurements of the TiO_2 coated glass beads show that the beads generate additional visible light, albeit with low efficiency. The spectrum presented an overlap with the blue absorption peak of chlorophyll *a* which, in addition to the nutrients available from the AFW, might have contributed to growth of the cyanobacteria (supplementary material S4). Mathew *et al*. (2012) also observed emission of new wavelengths in the range of visible light (387, 421, 485, 530 and 574 nm) from TiO_2 colloidal nanoparticles after the excitation wavelength of 274 nm.

Again, the sample behavior after day 8 is not a true reflection of the individual replicates. Replicate 1 (Figure 2C – black) showed degradation after 8 days (cell density decreased from 5.8 x 10^6 to 3.1 x 10^5 cells mL^{-1}), while the two other replicates (Figure 2C – red and green) did not, with a cell density increasing from 5.6 x 10^6 to 7.7 x 10^6 cells mL^{-1} for one of these replicates (red) and from 5.6 x 10^6 to 8.9 x 10^6 cells mL^{-1} in the other (green). Cyanobacterial growth probably stopped once nutrients were depleted which supported gradual cell death. In addition, the effects of the UV/TiO_2 photocatalytic treatment were probably inhibited by some other factors.

In order for the UV illumination to target a specific organism or to activate a catalyst, it

must be able to first transmit through the water (Summerfelt, 2003). The lack of photocatalytic removal in two out of to three samples during the UV/TiO_2 treatment could be explained by the interaction of the air flow with other components of the set-up. In the UV/TiO_2 photocatalytic treatment, coated beads inside of the pods might have dispersed the rising air flow into smaller air bubbles, therefore, the sparging might have attenuated the light to the point where an insufficient number of photons reached the TiO_2 to overcome the band gap and produce radicals that would be responsible for *M. aeruginosa* PCC7813 removal. The sparging might have stopped or slowed down in the reactor where photocatalytic removal of *M. aeruginosa* PCC7813 was observed, allowing the activation of TiO_2 coated beads by UV illumination and subsequent radical production. Also, the difference in the behavior of samples from the UV treatment (Figure 2A) and the black set during the UV/TiO_2 treatment (Figure 2C) might have occurred due to the presence of beads inside the pods in the UV/TiO_2 treatment that would have caused a shading effect that prevented photolysis in the UV/TiO_2 samples.

Direct photolysis and the indirect oxidation by extracellular ROS initially cause cellular stress and then damage to the cell membrane, without promoting the complete destruction of the cell (Ou *et al*. 2011a, 2011b). Photosynthetic activity as expressed as the F_V/F_M' ratio is a rapid method that can represent the level of stress and/or damage in cyanobacterial cells (Stirbet *et al*., 2018; Yang *et al*., 2013). Cyanobacterial photoinhibition causes a decline in the F_V/F_M' ratio, which means that the lower the F_V/F_M' ratio (photosynthetic activity) the more damage or stress there is to the cyanobacteria. During the UV treatment, cyanobacterial cells suffered an inhibition of photosynthetic activity especially at the beginning of the experiment from days 1 to 4 (Figure 3A). The photosynthetic activity decrease observed during photolysis corresponds to the decrease in the cell number observed until day 4 (Figure 2A). As previously reported by Menezes *et al*. (2020), photosynthetic activity measurements showed a faster response to cell damage than cell density measurements, indicating that cell stress occurred as early as 24 hours before cell density changes could be observed by cell density measurements. The large variability of samples in the current study is most likely a result of the very low cell density from day 4 (10^4 cells mL^{-1}), which were lower than the minimum concentration of cells required for cell stress determination, making reliable measurements of photosynthetic activity more difficult. Similarly, Noyma *et al*. (2015) reported damage to the photosynthetic structure (i.e., thylakoids, phycobilisomes and polyphosphate granules) of *Cylindrospermopsis raciborskii* (CYRF-01) after 6 hours UV-A illumination.

Photosynthetic activity remained steady for samples for the first 6 days of TiO_2-only

samples (Figure 3B), remaining at the same level for two out of three sets of replicates until the end of 14 days (Figure 3B – red and green). These results support the hypothesis from cell density observations (Figure 2B) that cells were not inhibited or damaged but were removed from suspension and thus not detected by the cell enumeration. Before carrying out the study, UV/TiO_2 treatment was expected to be the most effective treatment and cause damage to the photosynthetic system of *M. aeruginosa* PCC7813. However, relatively little effect was observed in this treatment over the first 8 days with only one of the replicates showing a decline in photosynthetic activity from day 7 onwards (Figure 3C – black) which also corresponds to the cell density decrease in one replicate during UV/TiO_2 treatment (Figure 2C – black).

Figure 3 – Effects of (A) UV-LED irradiation (365 nm), (B) TiO_2 coated glass beads under ambient light (13.7 µmol photons m^{-2} s^{-1}) and (C) photocatalytic treatment on *Microcystis aeruginosa* PCC7813 photosynthetic activity using TiO_2 coated glass beads under UV-LED illumination (365 nm) over 14 days under sparging with sterile air. Data points represent replicates from each treatment.

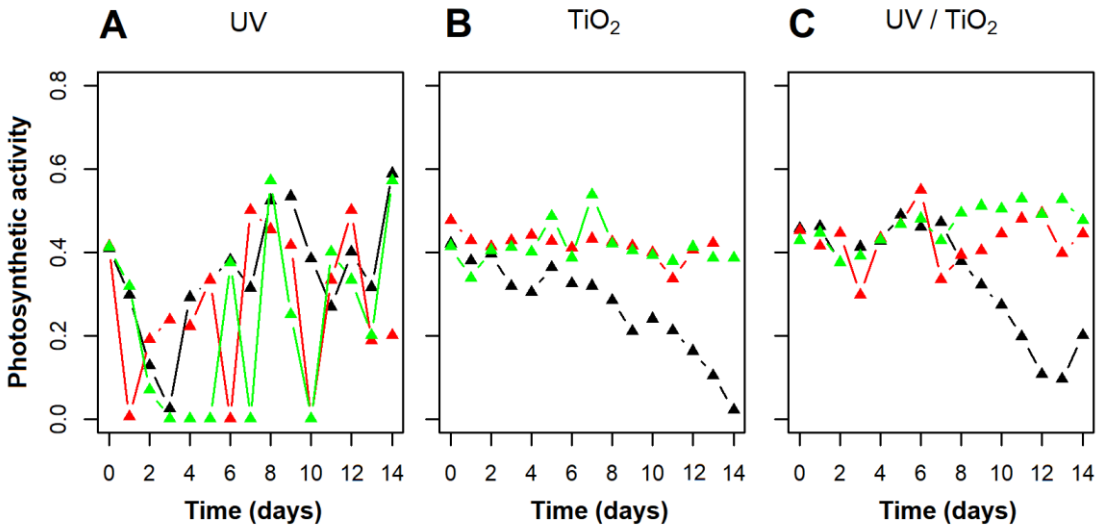

An initial significant decrease of *M. aeruginosa* PCC7813 cell density at the beginning of the experiment was expected which was what had been observed previously by other studies that evaluated *M. aeruginosa* cell density after TiO_2 photocatalytic treatment (Pestana *et al*., 2020; Chang *et al*., 2018; Song *et al*., 2018; Wang *et al*., 2018, 2017; Pinho *et al*., 2012). The study that presented most similarities to the current study was Pestana *et al*. (2020), which had quite similar experimental design albeit in a smaller scale. The differences in results between the two studies could be due to light attenuation of the bubbles being dispersed by the TiO_2

coated beads.

Photolysis by UV illumination (365 nm) was observed to be the most effective treatment for *M. aeruginosa* PCC7813 cell destruction in the current study. The reduction in the *M. aeruginosa* PCC7813 cell density (Figure 2A) might be explained by the fact that cyanobacteria do not produce sufficient ROS-scavenging enzymes (e.g., ROS produced by UV treatment; Sinha *et al*., 2018). ROS oxidize lipids and proteins inside the cyanobacterial cells, resulting in cell wall damage, followed by inactivation of enzymes and ultimately cell death (Sinha *et al*., 2018). Further, the effect of the UV treatment on *M. aeruginosa* PCC7813 cells might have been caused by indirect oxidation due to intracellular ROS (Ou *et al*. 2011a, 2011b). Intracellular ROS generation may have been enhanced by the presence of intracellular phycocyanin which is a natural cyanobacterial pigment (Robertson *et al*., 1999). Robertson *et al*. (1999) suggested that cell destruction can occur from the inside-out rather than the outside-in due to the production of both singlet oxygen and hydroperoxide radical facilitated by the intracellular phycocyanin upon UV-irradiation. After this, the intracellular ROS effects on cells were enhanced by phycocyanin, causing complete degradation of cells. Under UV illumination alone, phycocyanin can contribute to the degradation of cells by two mechanisms: firstly, during the electron transfer process, the photoexcited phycocyanin transfers an electron to oxygen, producing the superoxide radical that then becomes a hydroperoxide radical by protonation. Secondly, during the energy transfer process, phycocyanin and oxygen interact to produce singlet oxygen (Robertson *et al*., 1999). Both types of ROS then attack the cell structures from within.

Further, cyanobacteria release oxygen during photosynthesis which can interact to UV light and other organic compounds to produce ROS (Pattanaik et al., 2007). The ROS produced by UV-A illumination in the present might have also be responsible for damaging and removing *M. aeruginosa* PCC7813 cells.

UV-C (254 nm) has been widely applied as a germicide for inactivation of bacteria and viruses by denaturing the DNA of microorganisms and causing death or function loss (Boyd *et al*., 2020; Summerfelt, 2003). However, it is likely that the UV-A illumination (365 nm) used in the present study was able to destroy *M. aeruginosa* PCC7813 cells due to the generation of ROS and the presence of phycocyanin inside of the cyanobacterial cells. Therefore, UV-A illumination might be specific to cyanobacterial control and it would not affect other phytoplankton such as diatoms or green algae.

Ou et al. (2011a, 2011b) pointed out that the UV-C-induced damage occurs via either

direct photolysis or indirect oxidation by intra- and/or extracellular ROS. The UV irradiation causes damage to the photosynthesis system, including PS I, PS II and phycobilisome which interrupts the electron transport chain and retards the critical reactions during photosynthesis, followed by the decomposition of cytoplasmic inclusions (e.g., pigments and nutrients) and finally cell destruction and release of intracellular organic matter. The same mechanisms might have occurred during the present UV-A photolysis where the photosynthetic system of *M. aeruginosa* PCC7813 was affected (Figure 3A) and cellular destruction occurred due to intracellular ROS (Figure 2A).

Yang et al. (2015) evaluated the effects of high-energy UV-B illumination (280–320 nm) on a toxic (FACHB 915) and a non-toxic (FACHB 469) strain of *M. aeruginosa* photosynthetic activity. The UV-B irradiation resulted in an inhibition of the photosynthetic activity of both toxic and non-toxic strains over 3 days of exposure due to damage to photosystem II (Yang *et al*., 2015). However, both *M. aeruginosa* strains used by Yang et al. (2015) showed signs of photosynthetic activity recovery at the end of the experiment. This could not be observed in the current study due to the complete destruction of *M. aeruginosa* PCC7813 cells that culminated in the large variability of results.

8.2 Intra- and extracellular microcystin removal

The intracellular microcystin concentration for all analogues diminished significantly in a piecewise regression tendency (Figure S6 – S9) over the first 5 days of the UV treatment (Figure 4A) with the complete removal of all microcystin analogues by this time (approximate rate of 40, 22, 15 and 2.6 ng mL^{-1} day^{-1} of intracellular MC-LR, MC-LF, MC-LW and MC-LY, respectively, $p<0.01$ for all samples). The decrease of all four analogues of intracellular microcystins during UV treatment (Figure 4A) corresponds to the reduction of *M. aeruginosa* cell density (Figure 2A). For the TiO_2-only samples (Figure 4B), the mean values suggest a removal of 20, 43, 42 and 42% of intracellular MC-LR, MC-LF, MC-LW and MC-LY, respectively, or a significant decrease in a linear regression rate (Figure S10 – S13) of 3.7, 2.8, 2.9 and 0.3 ng mL^{-1} day^{-1} (for all samples $p<0.05$) over 14 days. Samples remained consistent over the first 11 days, however, it was possible to observe divergence in the results in the later stages. During UV/TiO_2 treatment, intracellular microcystins samples presented high variability over 14 days (Figure 4C) and while one replicate (Figure 4B – black) showed complete removal of all microcystins at the end of the experiment, another replicate (Figure 4B – green)

demonstrated microcystins concentration of 157, 74, 59 and 11 ng mL^{-1} for MC-LR, MC-LF, MC-LW and MC-LY respectively). It is noteworthy that across all the treatments all trends observed for any of the analogues is mirrored by the other analogues (Figure 4), for example, one replicate during the UV treatment (Figure 4A – red) decreased on day 2 for all analogues, followed by the other two replicates on day 4 (Figure 4A – green and black). These results suggest that other factors, such as cell clumping, light shading or reduced mixing may have influenced the sampling.

Figure 4 – Intracellular microcystin concentrations produced by *Microcystis aeruginosa* PCC7813 during (A) UV, (B) TiO_2 under ambient light (13.7 µmol photons m^{-2} s^{-1}) and (C) UV/TiO_2 treatment over 14 days under constant agitation. Data points represent replicates from each treatment.

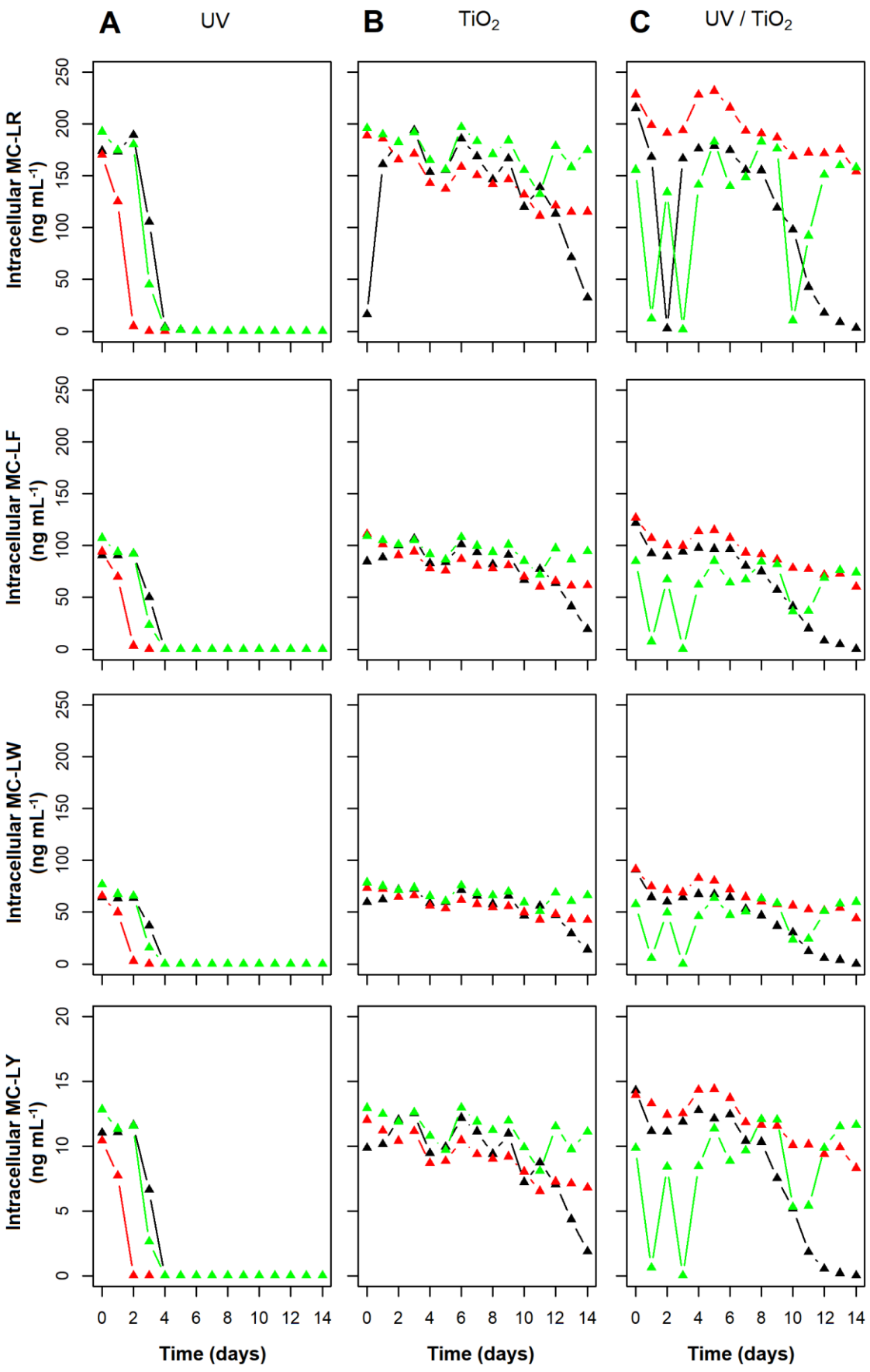
A
UV
B
TiO2
C
UV / TiO2
Intracellular MC-LR (ng mL-1)
Intracellular MC-LF (ng mL-1)
Intracellular MC-LW (ng mL-1)
Intracellular MC-LY (ng mL-1)
Time (days)
Time (days)
Time (days)

Figure 5 – Intracellular microcystin analogues ratio (toxin cell^{-1}) in *Microcystis aeruginosa* PCC7813 over 14 days of (A) UV, (B) TiO_2 under ambient light (13.7 µmol photons m^{-2} s^{-1}) and (C) UV/TiO_2 treatment under constant agitation. Data points represent replicates from each treatment.

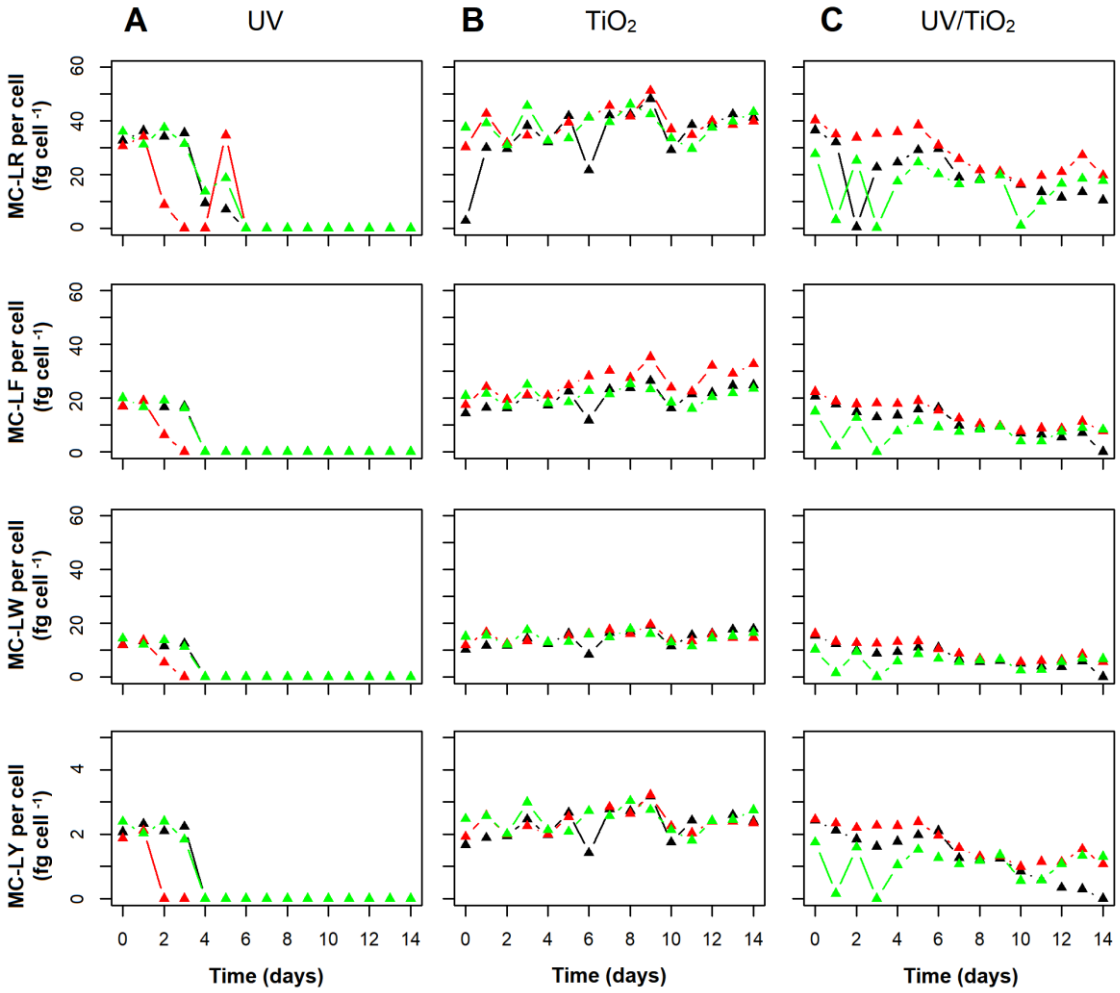

The toxin per cell of all microcystin analogues was completely removed during 14 days of UV treatment (figure 5A). The complete destruction of cells during photolysis (Figure 2A) could be confirmed by this corresponding decrease in the toxin ratio (i.e., toxin concentration per cell number). For TiO_2-only samples, the toxin concentration per cell increased (Figure 5B). Despite the slight decrease in cell number of TiO_2-only samples, no cell stress was detected when analyzing both photosynthetic activity (Figure 3B) and intracellular toxin (Figure 4B), indicating that cells were not actually damaged and/or dead but there was physical cell removal of intact healthy cells by adsorption of cells onto the surface of the TiO_2 beads and onto the surface of the reactors.

The amount of toxin per cell over 14 days in the UV/TiO_2 treatment diminished by 54, 64, 70 and 72% for MC-LR, -LY, -LW and -LF, respectively (Figure 5C). One reason for the

reduction in the toxin concentration per cell could be that some of the *M. aeruginosa* PCC7813 cells were detected and counted as living organisms, however, some of the cells were probably fragmented and inactive. Another reason for the decrease in toxin concentration could be microcystins binding to intracellular proteins which *M. aeruginosa* is known to do as demonstrated by Zilliges *et al*. (2011). Pestana *et al*. (2020) also observed a reduction in the toxin per cell ratio of the same intracellular microcystin analogues used in the present study (MC-LR, -LY, -LW and -LF) from the beginning to the end of a photocatalytic experiment using the same TiO_2 coated glass beads under UV/LED illumination (365 nm, 2.1 mW s^{-1}), which they ascribed to microcystins binding to intracellular proteins.

Microcystins are commonly released into the surrounding water after cell rupture by water treatment processes. Therefore, it is necessary that other water treatment technologies are applied to remove toxins that are released into the water since conventional treatments cannot remove dissolved components (Chow *et al*., 1999). After the liberation of intracellular microcystins during the UV treatment, samples could be best represented by a piecewise regression (Figure S18 – S21) with removal for all extracellular microcystins amounting to 92% for MC-LR and a complete removal of the other three analogues over the first 5 days (Figure 6A). The reduction in *M. aeruginosa* PCC7813 cell number (Figure 2A) is the most likely reason for the decrease of intracellular microcystins during the UV treatment (Figure 4A) due to cell lysis and release of the intracellular content to the surrounding water followed by the immediate removal of the extracellular microcystins by direct photolysis and indirect oxidation of ROS (Figure 6A). No significant change (p>0.05) in the extracellular concentration of any of the microcystin analogues was observed over 14 days in the TiO_2-only samples (Figure 6B), indicating that there was no microcystins release from the cells. This finding also corroborates the theory that cells were not actually destroyed in TiO_2-only samples but were adsorbed onto the reactor components. During UV/TiO_2 treatment, there was no increase in the extracellular microcystin concentrations for most samples over 14 days (Figure 6C – red and green). However, the cell reduction observed for one of the replicates (Figure 3C – black) and the complete decline of intracellular microcystins (Figure 4C – black) of one replicate in the UV/TiO_2 treatment may have promoted the subsequent increase of extracellular microcystins (Figure 6C – black). The toxin concentration released in this replicate (Figure 6C – black) corresponds to the concentration increase of the extracellular microcystins.

Figure 6 – Extracellular microcystin analogue concentrations produced by *Microcystis aeruginosa* PCC7813 during (A) UV, (B) TiO_2 under ambient light (13.7 µmol photons m^{-2} s^{-1}) and (C) UV/TiO_2 treatment over 14 days

under constant agitation. Data points represent replicates from each treatment.

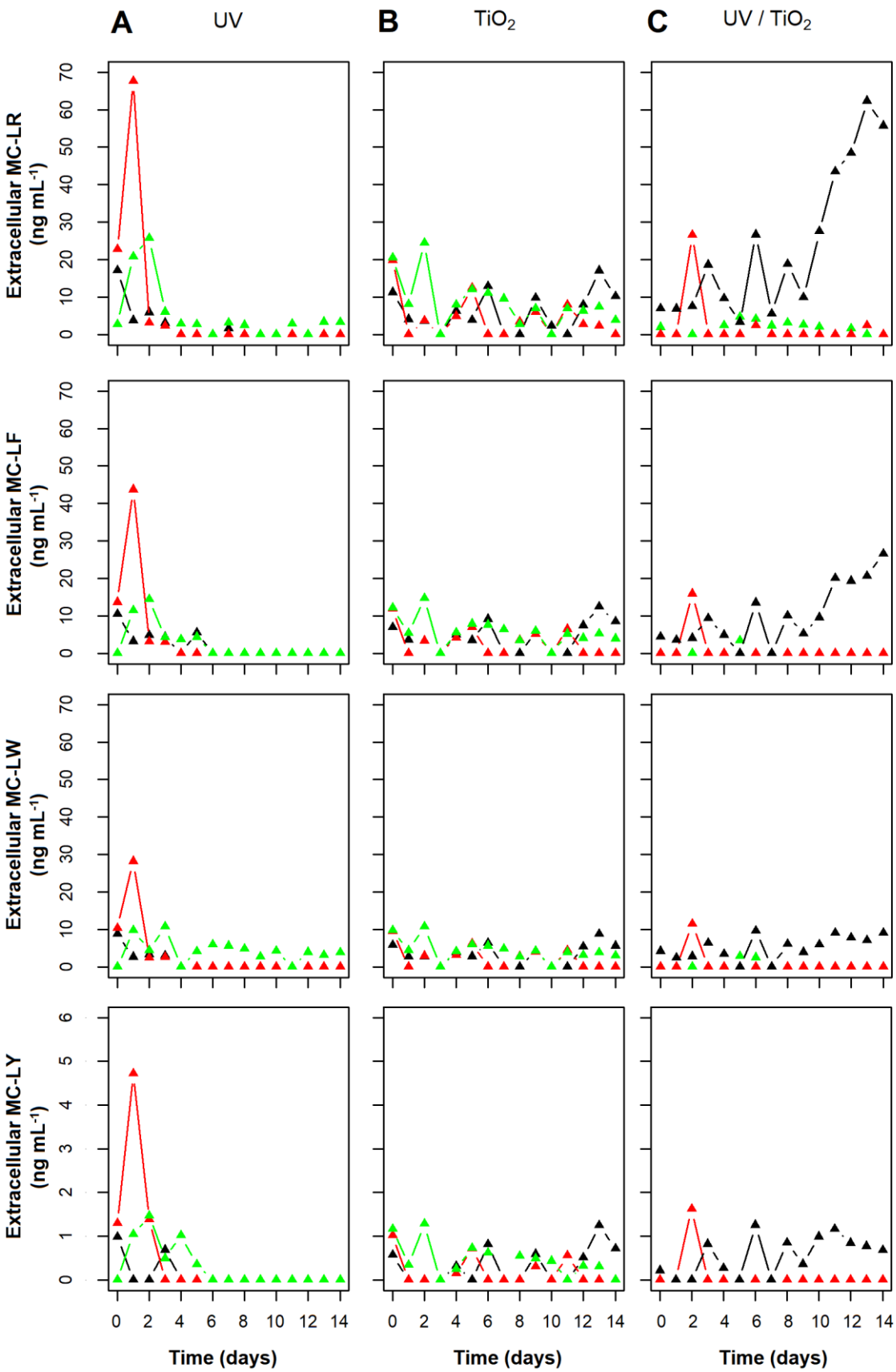

A study by Robertson *et al*. (1999) evaluated the destruction of MC-LR under UV/TiO_2 photocatalysis and photolysis in the presence of phycocyanin. The authors also observed a decline of MC-LR concentration when the sample was treated with only UV-A light in the presence of phycocyanin, corroborating the results of the current study. However, when no phycocyanin was present, the UV light had no effect on the toxin degradation, showing that phycocyanin acts as a photocatalyst for microcystin destruction under UV illumination until the pigment was completely bleached (Robertson *et al*., 1999).

Triantis *et al*. (2012) observed the effects of UV-A photolysis on the removal of MC-LR using four F15W/T8 black light tubes (maximum emission 365 nm and 717 W m^{-2}), but there was only a small decrease in MC-LR concentration (around 5%) after 30 minutes of photolysis. Despite the higher light energy used in the Triantis et al. (2012) study when compared to the current study (5 W m^{-2}), the small reduction in the MC-LR concentration might have occurred due to the fact that the present study analyzed biological samples. This means that cells contained phycocyanin, which must have enhanced the microcystins degradation, while Triantis et al. (2012) used a MC-LR standard and no phycocyanin.

Pestana *et al*. (2020) studied the destruction of the same microcystin analogues (MC-LR, -LY, -LF and -LW) under UV/TiO_2 photocatalysis with the same TiO_2 coated beads in a 7-day experiment. Intracellular microcystin analogues were removed by 49% and extracellular microcystins that were release after cell lysis were completely removed by UV/TiO_2 photocatalysis. Similar results were expected in the current study since the same TiO_2 coated beads under UV illumination, *M. aeruginosa* strain (PCC7813) and microcystin analogues were used. However, UV photolysis was more efficient for the removal of microcystins than the UV/TiO_2 photocatalytic treatment used in the present study. The difference in the results might have occurred due to the larger scale and lower initial cell concentration (6.5 L and 5 x 10^6 cells mL^{-1} in the current study compared to 30 mL and 15 x 10^6 cells mL^{-1} used in Pestana *et al*. (2020) study). Further, in the current study, growth in the three replicates of the UV/TiO_2 treatment occurred over the first 8 days (Figure 2C). Additionally, stronger mixing caused by the multi-porous air-stone in the base in the current study combined with a dispersion of the larger air bubbles by the TiO_2-coated glass bead that potentially attenuated the effects of the UV irradiation, rendering the UV/TiO_2 treatment less effective. Whereas, in the Pestana *et al*. (2020) study, only very gentle single point sparging was used from the top of the vials. Finally, the shadowing effect caused by the coated glass beads and the stainless-steel pods inside the reactors (which were not used in the Pestana *et al*. (2020) study) may have interfered in the

efficiency of the photocatalytic removal of the microcystins.

8.3 *Microcystis aeruginosa* PCC7813 regrowth post UV and UV/TiO_2 treatment

It is important to evaluate cyanobacterial recovery after treatment by analyzing the regrowth potential in order to understand the frequency at which each treatment should be applied, and whether the treatment remains effective in the long term.

UV-A treated samples showed limited regrowth (from 10^4 to 10^5 cells mL^{-1}), but the difference observed in cell concentration between the beginning of the regrowth experiment and day 6 was not significant (p=0.08) due to the fact that only few cells remained viable after UV treatment that were not inhibited/damaged (Figure 7A). The remaining *M. aeruginosa* PCC7813 cells presented a doubling rate of 1.9 days over 6 days of regrowth (Figure 7A). When analyzing mean cell regrowth in TiO_2-only samples, a great variability between replicates was, with one of the replicates (Figure 7B – black) presenting the lowest cell density after 14 days of exposure to TiO_2-only and no regrowth was detected. This replicate (Figure 7B – black) actually showed a decreased in cell density from 4.1 x 10^5 to 2.5 x 10^5 cells mL^{-1} over 6 days, while the other two replicates (Figure 7B – red and green) presented a doubling rate of 2.9 and 3.8 days, respectively. The same sample variability was observed in regrowth samples from the UV/TiO_2 treatment (Figure 7C). While cell concentrations in two replicates (Figure 7C – black and green) doubled at a rate of 4.2 and 4.7 days respectively, the third replicates (Figure 7C – red) presented a decrease in cell density from 4.1 x 10^6 to 1.4 x 10^5 cells mL^{-1} over 6 days.

Wilson *et al*. (2006) stated an average doubling rate for 32 strains of *Microcystis* cultured in BG-11 medium as 2.8 days. As expected, some UV treatment samples from the current study presented a faster doubling rate of 1.9 days and some UV/TiO_2 treatment samples showed a slower doubling rate of 4.2 and 4.7 days, while some of the TiO_2-only samples presented a more similar doubling rate as the Wilson *et al*. (2006) study of 2.9 and 3.8 days.

Despite the lower cell density after 6 days of regrowth in UV treatment due to the initial low inoculation cell density (Figure 7A), the cells in UV treatment showed the fastest doubling rate (1.9 days) when compared to cells from TiO_2-only samples and UV/TiO_2 treatment (Figures 7B and C), as previously observed by Dunn and Manoylov (2016). In the UV treatment, the low cell density numbers mean low competition for resources, hence this is often when growth is fastest. Similar observations were made in the Pestana *et al*. (2020) photocatalytic study, where the average doubling rate of *M. aeruginosa* PCC7813 in the TiO_2-only samples was

approximately seven days. The slowest doubling time in Pestana *et al*. (2020) study might have occurred due to the high initial inoculation cell density of 15 × 10^6 cells mL^{-1} in 30 mL.

Figure 7 – Effects of (A) UV-LED irradiation (365 nm), (B) TiO_2 coated glass beads under ambient light (13.7 µmol photons m^{-2} s^{-1}) and (C) photocatalytic treatment on *Microcystis aeruginosa* PCC7813 regrowth using TiO_2 coated glass beads under UV-LED illumination (365 nm) over seven days under cool white fluorescent lights of 10.5 µmol photons m^{-2} s^{-1}. Data points represent replicates from each treatment (n = 4).

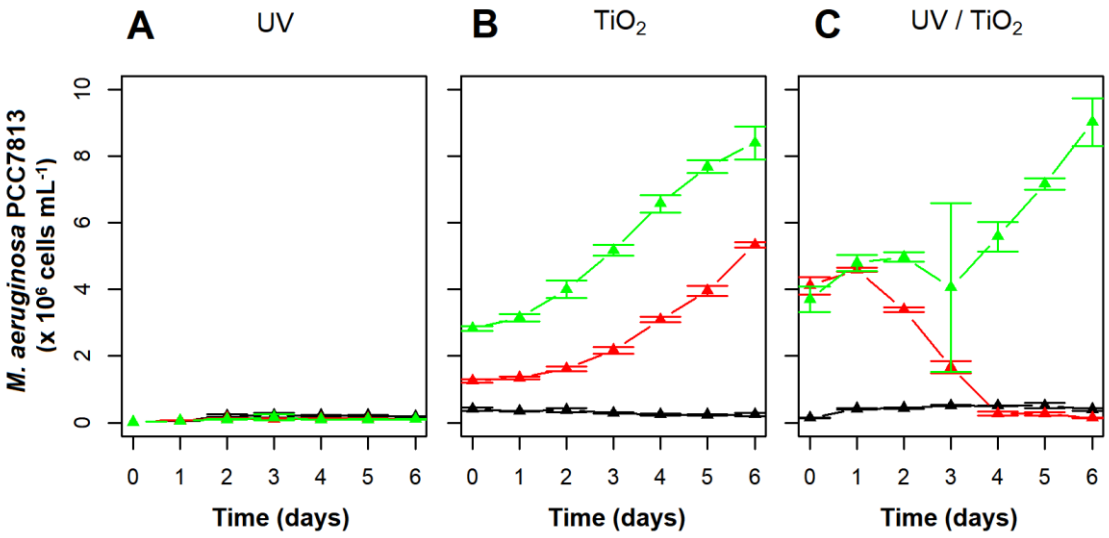

Ou *et al*. (2012) studied the effects of different UV-C dosages (140-4200 mJ cm^{-2}) on *M. aeruginosa* FACHB-912 recovery over 7 days. There was significant reduction in the photosynthetic parameter analyzed and proxy-measurement for viability or cell counts (e.g., quantum yield and chlorophyll *a* concentration) for samples irradiated at 350, 700, 1400 and 4200 mJ cm^{-2}, showing the irreversible inhibition of the photosynthetic system in the *M. aeruginosa* cells FACHB-912 after UV-C irradiation which then inhibited the reproduction and recovery of *M. aeruginosa* cells (Ou *et al*., 2012).

A study by Huang *et al*. (2011) evaluated the regrowth potential of *M. aeruginosa* after 24 hours of ZnO/γ-Al_2O_3 photocatalytic treatment under solar light. Photocatalyzed samples were maintained at 25°C in the incubation chamber under a fluorescent lamp with a 12/12 hours light/dark cycle over 12 days. By the end of the regrowth experiment, the cell density of treated samples was less than 85% of that of the control, highlighting the long-lasting effect of photocatalysis on *M. aeruginosa* cells even though a different type of photocatalyst and

irradiation was applied (Huang *et al*., 2011).

9 CONCLUSION

The current study investigated the effects of UV-A photolysis and a UV/TiO_2 photocatalytic system using TiO_2 coated glass beads on *M. aeruginosa* PCC7813 cells and the four main microcystin analogues (MC-LR, -LY, -LW and -LF) this strain produces. Both systems had energy-efficient UV illumination supplied by UV-LEDs for cyanobacteria and cyanotoxin control. The UV photolysis was able to consistently remove cyanobacterial cells and toxins and therefore was shown to be more effective than the UV/TiO_2 photocatalytic system which only presented a delayed removal of cells and concerningly actually promoted growth in the first 8 days. All the data analysis (cell density, photosynthetic activity, toxin per cell, intra- and extracellular toxin) indicate that UV photolysis was capable of not only inhibiting/damaging *M. aeruginosa* PCC7813 cells, but it completely destroyed them. The complete cell death of *M. aeruginosa* PCC7813 cells made subsequent regrowth impossible. It was demonstrated that larger scale UV-LED-driven reactors are as effective as bench-scale set-ups, indicating that use *in-situ* would be possible. Further, it is likely that UV-A illumination might be specific to cyanobacterial control due to the presence of phycocyanin inside of the cyanobacterial cells, making *in-situ* application of this treatment safe for other phytoplankton (e.g., diatoms and green algae). To confirm this, the effects of UV photolysis on other cyanobacteria species should be investigated, especially because the strain used (PCC7813) does not contain aerotopes which have been shown to enhance the effects of UV illumination.

In practice, many aspects of the reactor design need to be optimized and field-tested to allow *in-situ* application inside reservoirs: vertical or horizontal orientation of reactors, optimization of the active surface area and contact time, incorporation of waterproof UV-LEDs, and powering the units *in-situ*. The current study has successfully demonstrated that UV-LED-based advanced oxidation techniques could be operated at a larger-than-bench scale and control cyanobacteria and their toxins.

REFERENCES

AKKANEN, J., KUKKONEN, J.V.K., 2003. Measuring the bioavailability of two hydrophobic organic compounds in the presence of dissolved organic matter. Environ. Toxicol. Chem. 22, 518–524.

BOYD, B., SUSLOV, S.A., BECKER, S., GREENTREE, A.D., MAKSYMOV, I.S., 2020. Beamed UV sonoluminescence by aspherical air bubble collapse near liquid-metal microparticles. Sci. Rep. 10, 1–8. https://doi.org/10.1038/s41598-020-58185-2

CARMICHAEL, W.W., AZEVEDO, S.M.F.O., AN, J.S., MOLICA, R.J.R., JOCHIMSEN, E.M., LAU, S., RINEHART, K.L., SHAW, G.R., EAGLESHAM, G.K., 2001. Human fatalities form cyanobacteria: Chemical and biological evidence for cyanotoxins. Environ. Health Perspect. 109, 663–668. https://doi.org/10.1289/ehp.01109663

CHAE, S., NOEIAGHAEI, T., OH, Y., KIM, I.S., PARK, J.S., 2019. Effective removal of emerging dissolved cyanotoxins from water using hybrid photocatalytic composites. Water Res. 149, 421–431. https://doi.org/10.1016/j.watres.2018.11.016

CHANG, C.W., HUO, X., LIN, T.F., 2018. Exposure of *Microcystis aeruginosa* to hydrogen peroxide and titanium dioxide under visible light conditions: Modeling the impact of hydrogen peroxide and hydroxyl radical on cell rupture and microcystin degradation. Water Res. 141, 217–226. https://doi.org/10.1016/j.watres.2018.05.023

CHEN, L., ZHAO, C., DIONYSIOU, D.D., O'SHEA, K.E., 2015. TiO_2 photocatalytic degradation and detoxification of cylindrospermopsin. J. Photochem. Photobiol. A Chem. 307–308, 115–122. https://doi.org/10.1016/j.jphotochem.2015.03.013

CHOW, C.W.K., DRIKAS, M., HOUSE, J., BURCH, M.D., VELZEBOER, R.M.A., 1999. The impact of conventional water treatment processes on cells of the cyanobacterium *Microcystis aeruginosa*. Water Res. 33, 3253–3262. https://doi.org/10.1016/S0043-1354(99)00051-2

DUNN, R.M., MANOYLOV, K.M., 2016. The Effects of Initial Cell Density on the Growth and Proliferation of the Potentially Toxic Cyanobacterium *Microcystis aeruginosa*. J. Environ. Prot. (Irvine,. Calif). 07, 1210–1220. https://doi.org/10.4236/jep.2016.79108

FALCONER, I.R., BERESFORD, A.M., RUNNEGAR, M.T.C., 1983. Evidence of liver damage by toxin from a bloom of the blue-green alga, *Microcystis aeruginosa*. Med. J. Aust. 1, 511–514. https://doi.org/10.5694/j.1326-5377.1983.tb136192.x

FAN, F., SHI, X., ZHANG, M., LIU, C., CHEN, K., 2019. Comparison of algal harvest and hydrogen peroxide treatment in mitigating cyanobacterial blooms via an *in situ* mesocosm experiment. Sci. Total Environ. 694, 133721. https://doi.org/10.1016/j.scitotenv.2019.133721
HEERING, W., 2004. UV-sources - Basics, Properties and Applications. Int. Ultrav. Assoc. 6, 7–13.

HU, XI, HU, XINJIANG, TANG, C., WEN, S., WU, X., LONG, J., YANG, X., WANG, H., ZHOU, L., 2017. Mechanisms underlying degradation pathways of microcystin-LR with

doped TiO_2 photocatalysis. Chem. Eng. J. 330, 355–371. https://doi.org/10.1016/j.cej.2017.07.161

HUANG, W.J., LIN, T.P., CHEN, J.S., SHIH, F.H., 2011. Photocatalytic inactivation of cyanobacteria with ZnO/γ-Al_2O_3 composite under solar light. J. Environ. Biol. 32, 301–307.

HUI, J., PESTANA, C.J., CAUX, M., GUNARATNE, H.Q.N., EDWARDS, C., ROBERTSON, P.K.J., LAWTON, L.A., IRVINE, J.T.S., 2021. Graphitic-C_3N_4 coated floating glass beads for photocatalytic destruction of synthetic and natural organic compounds in water under UV light. J. Photochem. Photobiol. A Chem. 405, 112935. https://doi.org/10.1016/j.jphotochem.2020.112935

JIN, Y., ZHANG, S., XU, H., MA, C., SUN, J., LI, H., 2019. Application of N-TiO_2 for visible-light photocatalytic degradation of *Cylindrospermopsis raciborskii*. More difficult than that for photodegradation of *Microcystis aeruginosa*? *. Environ. Pollut. 245, 642–650. https://doi.org/10.1016/j.envpol.2018.11.056

JOCHIMSEN, E.., CARMICHAEL, W.W., An, J., Cardo, D.M., Cookson, S.T.; Holmes, C.E.M.; Antunes, B.C.; Melo Filho, D.A.; Lyra, T.M.; Barreto, V.S.T; Azevedo, S.M.F.O. & Jarvis, W.., 1998. Liver failure and death after exposure to microcystins. N. Engl. J. Med. 338, 873–878. https://doi.org/10.1080/13504509.2013.856048 M4 - Citavi

LI, L., SAHI, S.K., PENG, M., LEE, E.B., MA, L., WOJTOWICZ, J.L., MALIN, J.H., CHEN, W., 2016. Luminescence-and nanoparticle-mediated increase of light absorption by photoreceptor cells: Converting UV light to visible light. Sci. Rep. 6. https://doi.org/10.1038/srep20821

LIU, X., CHEN, Z., ZHOU, N., SHEN, J., YE, M., 2010. Degradation and detoxification of microcystin-LR in drinking water by sequential use of UV and ozone. J. Environ. Sci. 22, 1897–1902. https://doi.org/10.1016/S1001-0742(09)60336-3

MATHEW, S., KUMAR PRASAD, A., BENOY, T., RAKESH, P.P., HARI, M., LIBISH, T.M., RADHAKRISHNAN, P., NAMPOORI, V.P.N., VALLABHAN, C.P.G., 2012. UV-visible photoluminescence of TiO_2 nanoparticles prepared by hydrothermal method. J. Fluoresc. 22, 1563–1569. https://doi.org/10.1007/s10895-012-1096-3

MATTHIJS, H.C.P., VISSER, P.M., REEZE, B., MEEUSE, J., SLOT, P.C., WIJN, G., TALENS, R., HUISMAN, J., 2012. Selective suppression of harmful cyanobacteria in an entire lake with hydrogen peroxide. Water Res. 46, 1460–1472. https://doi.org/10.1016/j.watres.2011.11.016

MENEZES, I., MAXWELL-MCQUEENEY, D., PESTANA, C.J., EDWARDS, C., LAWTON, L.A., 2020. Chemosphere Oxidative stress in the cyanobacterium *Microcystis aeruginosa* PCC 7813 : Comparison of different analytical cell stress detection assays. https://doi.org/10.1016/j.chemosphere.2020.128766

MOON, B.R., KIM, T.K., KIM, M.K., CHOI, J., ZOH, K.D., 2017. Degradation mechanisms of Microcystin-LR during UV-B photolysis and UV/H_2O_2 processes: Byproducts and pathways. Chemosphere 185, 1039–1047. https://doi.org/10.1016/j.chemosphere.2017.07.104

NOYMA, N.P., SILVA, T.P., CHIARINI-GARCIA, H., AMADO, A.M., ROLAND, F., MELO, R.C.N., 2015. Potential effects of UV radiation on photosynthetic structures of the bloom-forming cyanobacterium *Cylindrospermopsis raciborskii* CYRF-01. Front. Microbiol. 6, 1–13. https://doi.org/10.3389/fmicb.2015.01202

OU, H., GAO, N., DENG, Y., QIAO, J., WANG, H., 2012. Immediate and long-term impacts of UV-C irradiation on photosynthetic capacity, survival and microcystin-LR release risk of *Microcystis aeruginosa*. Water Res. 46, 1241–1250. https://doi.org/10.1016/j.watres.2011.12.025

OU, H., GAO, N., DENG, Y., QIAO, J., ZHANG, K., LI, T., DONG, L., 2011a. Mechanistic studies of *Microcystic aeruginosa* inactivation and degradation by UV-C irradiation and chlorination with poly-synchronous analyses. DES 272, 107–119. https://doi.org/10.1016/j.desal.2011.01.014

OU, H., GAO, N., DENG, Y., WANG, H., ZHANG, H., 2011b. Inactivation and degradation of *Microcystis aeruginosa* by UV-C irradiation. Chemosphere 85, 1192–1198. https://doi.org/10.1016/j.chemosphere.2011.07.062

PATTANAIK, B., SCHUMANN, R., KARSTEN, U., 2007. Effects of Ultraviolet Radiation on Cyanobacteria and Their Protective Mechanisms. Limnology 29–45.

PESTANA, C.J., CAPELO-NETO, J., LAWTON, L., OLIVEIRA, S., CARLOTO, I., LINHARES, H.P., 2019. The effect of water treatment unit processes on cyanobacterial trichome integrity. Sci. Total Environ. 659, 1403–1414. https://doi.org/10.1016/j.scitotenv.2018.12.337

PESTANA, C.J., PORTELA NORONHA, J., HUI, J., EDWARDS, C., GUNARATNE, H.Q.N., IRVINE, J.T.S., ROBERTSON, P.K.J., CAPELO-NETO, J., LAWTON, L.A., 2020. Photocatalytic removal of the cyanobacterium *Microcystis aeruginosa* PCC7813 and four microcystins by TiO_2 coated porous glass beads with UV-LED irradiation. Sci. Total Environ. 745, 141154. https://doi.org/10.1016/j.scitotenv.2020.141154

PINHO, L.X., AZEVEDO, J., MIRANDA, S.M., ÂNGELO, J., MENDES, A., VILAR, V.J.P., VASCONCELOS, V., BOAVENTURA, R.A.R., 2015. Oxidation of microcystin-LR and cylindrospermopsin by heterogeneous photocatalysis using a tubular photoreactor packed with different TiO_2 coated supports. Chem. Eng. J. 266, 100–111. https://doi.org/10.1016/j.cej.2014.12.023

PINHO, L.X., AZEVEDO, J., VASCONCELOS, V.M., VILAR, V.J.P., BOAVENTURA, R.A.R., 2012. Decomposition of *Microcystis aeruginosa* and microcystin-LR by TiO_2 oxidation using artificial UV light or natural sunlight. J. Adv. Oxid. Technol. 15, 98–106. https://doi.org/10.1515/jaots-2012-0111

ROBERTSON, P.K.J., LAWTON, L.A., CORNISH, B.J.P.A., 1999. The Involvement of Phycocyanin Pigment in the Photodecomposition of the Cyanobacterial Toxin, Microcystin-LR. J. Porphyr. Phthalocyanines 3, 544–551. https://doi.org/10.1002/(sici)1099-1409(199908/10)3:6/7<544::aid-jpp173>3.0.co;2-7

SINHA, A.K., EGGLETON, M.A., LOCHMANN, R.T., 2018. An environmentally friendly approach for mitigating cyanobacterial bloom and their toxins in hypereutrophic ponds: Potentiality of a newly developed granular hydrogen peroxide-based compound. Sci. Total Environ. 637–638, 524–537. https://doi.org/10.1016/j.scitotenv.2018.05.023

SONG, J., WANG, XUEJIANG, MA, J., WANG, XIN, WANG, J., XIA, S., ZHAO, J., 2018. Removal of *Microcystis aeruginosa* and Microcystin-LR using a graphitic-C_3N_4/TiO_2 floating photocatalyst under visible light irradiation. Chem. Eng. J. 348, 380–388. https://doi.org/10.1016/j.cej.2018.04.182

SPOOF, L., CATHERINE, A., 2017. Cyanobacteria samples: preservation, abundance and biovolume measurements, in: Meriluoto, J., Spoof, L., A. Codd, G. (Eds.), Handbook of Cyanobacterial Monitoring and Cyanotoxin Analysis. John Wiley & Sons, Chichester, UK, pp. 526–537. https://doi.org/10.1002/9781119068761

STANIER, R.Y., KUNISAWA, R., MANDEL, M., COHEN-BAZIRE, G., 1971. Purification and properties of unicellular blue-green algae (order *Chroococcales*). Bacteriol. Rev. 35, 171–205. https://doi.org/10.1128/mmbr.35.2.171-205.1971

STIRBET, A., LAZÁR, D., PAPAGEORGIOU, G.C., GOVINDJEE, 2018. Chlorophyll *a* Fluorescence in Cyanobacteria: Relation to Photosynthesis, Cyanobacteria: From Basic Science to Applications. https://doi.org/10.1016/B978-0-12-814667-5.00005-2

SUMMERFELT, S.T., 2003. Ozonation and UV irradiation - An introduction and examples of current applications. Aquac. Eng. 28, 21–36. https://doi.org/10.1016/S0144-8609(02)00069-9

TAO, Y., HOU, D., ZHOU, T., CAO, H., ZHANG, W., WANG, X., 2018. UV-C suppression on hazardous metabolites in *Microcystis aeruginosa*: Unsynchronized production of microcystins and odorous compounds at population and single-cell level. J. Hazard. Mater. 359, 281–289. https://doi.org/10.1016/j.jhazmat.2018.07.052

TRIANTIS, T.M., FOTIOU, T., KALOUDIS, T., KONTOS, A.G., FALARAS, P., DIONYSIOU, D.D., PELAEZ, M., HISKIA, A., 2012. Photocatalytic degradation and mineralization of microcystin-LR under UV-A, solar and visible light using nanostructured nitrogen doped TiO_2. J. Hazard. Mater. 211–212, 196–202. https://doi.org/10.1016/j.jhazmat.2011.11.042

VILELA, W.F.D., MINILLO, A., ROCHA, O., VIEIRA, E.M., AZEVEDO, E.B., 2012. Degradation of [D-Leu]-Microcystin-LR by solar heterogeneous photocatalysis (TiO_2). Sol. Energy 86, 2746–2752. https://doi.org/10.1016/j.solener.2012.06.012

WANG, XIN, WANG, XUEJIANG, ZHAO, J., SONG, J., SU, C., WANG, Z., 2018. Surface modified TiO_2 floating photocatalyst with PDDA for efficient adsorption and photocatalytic inactivation of *Microcystis aeruginosa*. Water Res. 131, 320–333. https://doi.org/10.1016/j.watres.2017.12.062

WANG, XIN, WANG, XUEJIANG, ZHAO, J., SONG, J., WANG, J., MA, R., MA, J., 2017. Solar light-driven photocatalytic destruction of cyanobacteria by F-Ce-TiO_2/expanded perlite floating composites. Chem. Eng. J. 320, 253–263. https://doi.org/10.1016/j.cej.2017.03.062

WILSON, A.E., WILSON, W.A., HAY, M.E., 2006. Intraspecific variation in growth and morphology of the bloom-forming cyanobacterium *Microcystis aeruginosa*. Appl. Environ. Microbiol. 72, 7386–7389. https://doi.org/10.1128/AEM.00834-06

YANG, W., TANG, Z., ZHOU, F., ZHANG, W., SONG, L., 2013. Toxicity studies of tetracycline on *Microcystis aeruginosa* and *Selenastrum capricornutum*. Environ. Toxicol. Pharmacol. 35, 320–324. https://doi.org/10.1016/j.etap.2013.01.006

YANG, Z., KONG, F., SHI, X., YU, Y., ZHANG, M., 2015. Effects of UV-B radiation on microcystin production of a toxic strain of *Microcystis aeruginosa* and its competitiveness against a non-toxic strain. J. Hazard. Mater. 283, 447–453. https://doi.org/10.1016/j.jhazmat.2014.09.053

ZHAO, C., PELAEZ, M., DIONYSIOU, D.D., PILLAI, S.C., BYRNE, J.A., O'SHEA, K.E., 2014. UV and visible light activated TiO_2 photocatalysis of 6-hydroxymethyl uracil, a model compound for the potent cyanotoxin cylindrospermopsin. Catal. Today 224, 70–76. https://doi.org/10.1016/j.cattod.2013.09.042

ZILLIGES, Y., KEHR, J.C., MEISSNER, S., ISHIDA, K., MIKKAT, S., HAGEMANN, M., KAPLAN, A., BÖRNER, T., DITTMANN, E., 2011. The cyanobacterial hepatotoxin microcystin binds to proteins and increases the fitness of *Microcystis* under oxidative stress conditions. PLoS One 6. https://doi.org/10.1371/journal.pone.0017615

10 SUPPLEMENTARY MATERIALS

S1 Tetrahedral pods

Titanium dioxide porous glass beads were placed inside of tetrahedral pods manufactured from a stainless-steel mesh with aperture of 1.2 x 1.2 mm and wire strength of 0.4 mm. Stainless-steel sheets were cut (15 x 13 cm) and then folded into the final tetrahedral form of pods (Figure S1). Empty pods were also used during UV photolysis evaluation. The tetrahedral pods were placed inside of the reactors.

Figure S1 – Stainless-steal tetrahedral pod containing TiO_2 coated porous recycled glass beads used during *Microcystis aeruginosa* PCC7813 and microcystins photocatalytic treatment under UV/LED irradiation containing titanium dioxide coated porous glass beads.

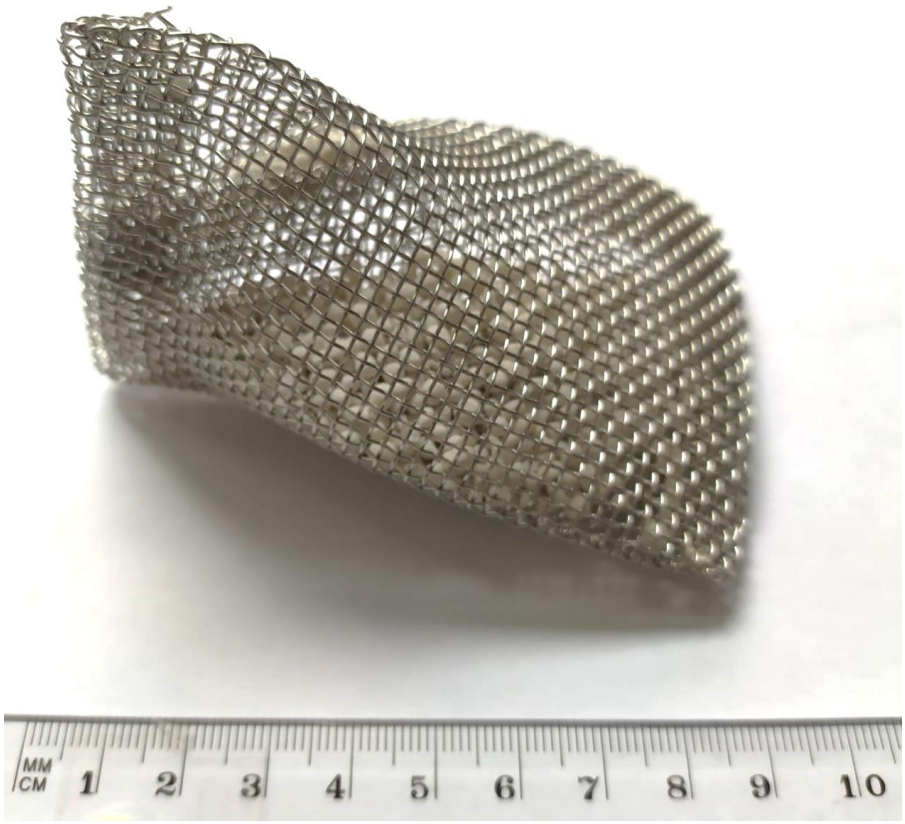

S2 *Microcystis aeruginosa* PCC7813 regrowth experimental design

Microcystis aeruginosa PCC7813 cellular regrowth was evaluated using a regrowth set up (Figure S2) over 7 days to evaluate the potential cyanobacterial recovery under optimal conditions after UV/TiO_2 photocatalytic treatment. After the treatment, aliquots containing *Microcystis aeruginosa* PCC7813 (1.5 mL) were added to 1.5 mL BG-11 medium inside four 4 mL glass vials that were in a 150 mL beaker.

Figure S2 – (A) Top view and (B) side view representation of 150 mL beaker and 4 mL vials used in the *Microcystis aeruginosa* PCC7813 regrowth experiment stored at 21±1 °C on a 12/12 hours light/dark cycle illuminated by cool white fluorescent lights with an average light intensity of 10.5 µmol photons m^{-2} s^{-1} without agitation.

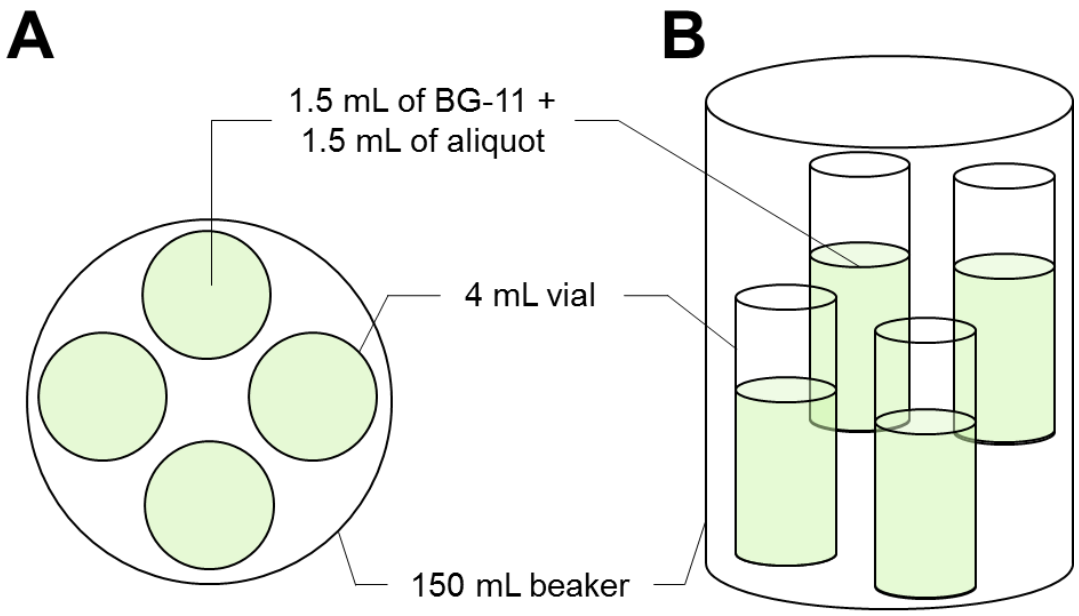

S3 Statistical data analysis

The type of statistical model (linear, piecewise, linear-plato, exponential and logarithmic regression) was selected for each dependent variable for each type of treatment according to the values of R^2, adjusted R^2, Akaike information criteria (AIC) and Bayesian information criteria (BIC). The models that presented the highest R^2 and adjusted R^2 and the lowest AIC and BIC were chosen (Table S1).

The graphic data analysis for each type of treatment (i.e., UV/TiO_2, TiO_2-only and UV) showed that the results can be interpreted using two classes of statistical models: linear, which shows a linear relation between dependent and independent variables, (Equation S1) and piecewise regression, which consists in multiple linear models for different ranges of the independent variable (Equation S2).

$$Y = \beta_0 + \beta_1 X \qquad \text{Equation S1}$$

$$Y = \begin{cases} \beta_0 + \beta_1 X, & X \leq \theta \\ \beta_0 + \beta_2 X + \theta(\beta_1 - \beta_2), & X > \theta \end{cases} \qquad \text{Equation S2}$$

Where Y is the dependent variable (cell density during the treatment and intra- and extracellular microcystins), β_0 is the intercept, β_1 and β_2 are the coefficients of the independent variable of each model, X is the independent variable (time) and θ is the breakpoint that determines the change in the behavior of the dependent variables for the piecewise regression model. The breakpoint is also where the inclination of the linear function changes. Each dependent variable demonstrated a different breakpoint θ.

Each model was considered adjusted when the requirements simultaneously fit:

- Independent variable (day) coefficients significant (p<0.05) by t-test.
- Obtained model shows significant F-statistics (p<0.05).
- Confidence interval of independent variable (day) coefficients estimated by 95% do not contain the value 0.
- Graphic analysis of residues, i.e., residuals vs fitted (homoscedasticity) and Q-Q plot – normality (Figure S3 – S29). For the graphic analysis of homoscedasticity and residuals vs leverage, all the points must be randomly distributed around 0, while the Q-Q plot – normality graph must show all the points distributed around a straight line and the scale-

location.

Table S1 – Values of R^2, adjusted R^2, Akaike information criteria (AIC) and Bayesian information criteria (BIC) for selection of model (linear or piecewise regression) for the dependent variable cell density during UV/TiO_2 treatment.

Treatment	**Analysis**	**R^2**	**Adjusted R^2**	**AIC**	**BIC**	**Model chosen**
UV	Cell density	0.97	0.97	15.41	18.25	Piecewise regression
TiO_2	Cell density	0.73	0.71	28.01	30.14	Linear regression
UV/TiO_2	Cell density	0.79	0.75	33.41	36.24	Piecewise regression
UV	Intracellular MC-LR	0.97	0.96	-84.67	-81.84	Piecewise regression
TiO_2	Intracellular MC-LR	0.46	0.42	-72.92	-70.79	Linear regression
UV/TiO_2	Intracellular MC-LR	0.34	0.23	-54.92	-52.09	Piecewise regression
UV	Intracellular MC-LY	0.97	0.96	-166.83	-164	Piecewise regression
TiO_2	Intracellular MC-LY	0.72	0.7	-161.41	-159.29	Linear regression
UV/TiO_2	Intracellular MC-LY	0.54	0.46	-142.69	-139.86	Piecewise regression
UV	Intracellular MC-LW	0.97	0.96	-113.53	-110.7	Piecewise regression
TiO_2	Intracellular MC-LW	0.86	0.85	-110.23	-108.1	Linear regression
UV/TiO_2	Intracellular MC-LW	0.58	0.51	-90.07	-87.24	Piecewise regression
UV	Intracellular MC-LF	0.97	0.96	-102.99	-100.16	Piecewise regression
TiO_2	Intracellular MC-LF	0.77	0.76	-102.62	-100.5	Linear regression
UV/TiO_2	Intracellular MC-LF	0.62	0.56	-81.07	-78.24	Linear regression
UV	Extracellular MC-LR	0.72	0.68	-113	-110.17	Piecewise regression

TiO_2	Extracellular MC-LR	0.11	0.04	-117.25	-115.13	Linear regression
UV/TiO_2	Extracellular MC-LR	0.57	0.54	-116.74	-114.62	Linear regression
UV	Extracellular MC-LY	0.74	0.69	-196.05	-193.21	Piecewise regression
TiO_2	Extracellular MC-LY	0.04	-0.04	-203.01	-200.88	Linear regression
UV/TiO_2	Extracellular MC-LY	0.37	0..06	-0.01	-214.37	Linear regression
UV	Extracellular MC-LW	0.44	0.34	-130.17	-127.34	Piecewise regression
TiO_2	Extracellular MC-LW	0.11	0.04	-138.57	-136.45	Linear regression
UV/TiO_2	Extracellular MC-LW	0.03	-0.04	-153.27	-151.15	Linear regression
UV	Extracellular MC-LF	0.70	0.66	-125.67	-122.84	Piecewise regression
TiO_2	Extracellular MC-LF	0.07	0	-131.08	-128.96	Linear regression
UV/TiO_2	Extracellular MC-LF	0.37	0.33	-136.83	-134.7	Linear regression

Figure S3 – Graphic analysis of residuals according to criteria A) homoscedasticity and B) Q-Q plot – normality for the dependent variable cell density during UV treatment.

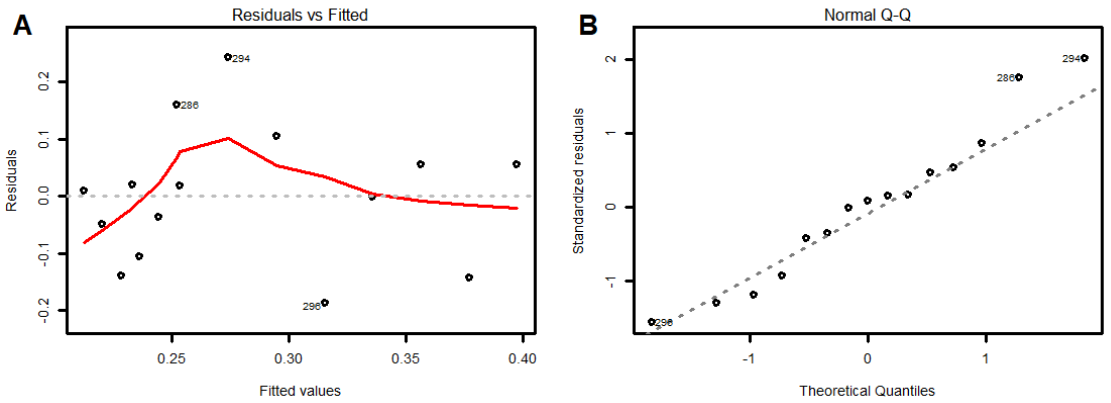

Figure S4 – Graphic analysis of residuals according to criteria A) homoscedasticity and B) -Q plot – normality for the dependent variable cell density during TiO_2 treatment.

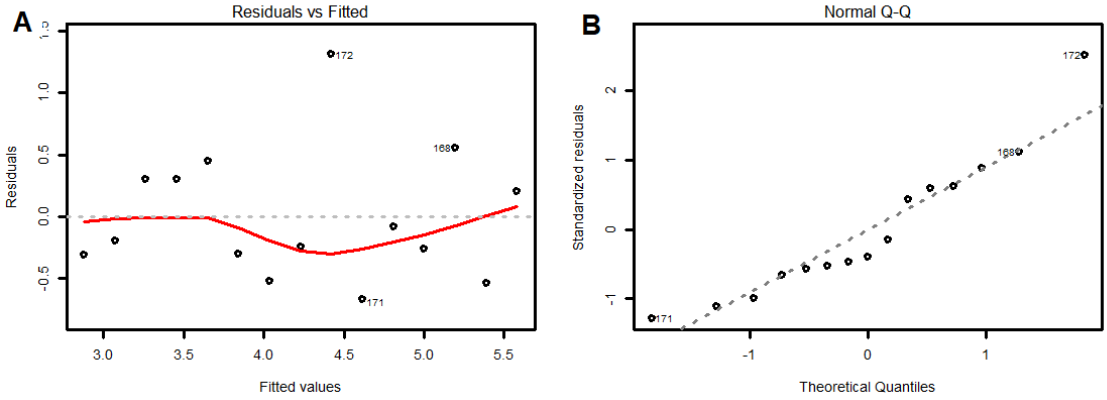

Figure S5 – Graphic analysis of residuals according to criteria A) homoscedasticity and B) Q-Q plot – normality for the dependent variable cell density during UV/TiO_2 treatment.

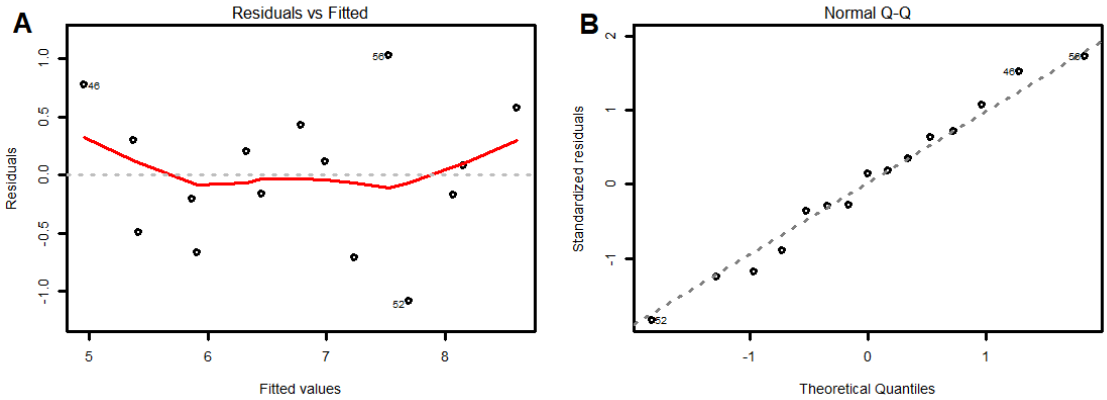

Figure S6 – Graphic analysis of residuals according to criteria A) homoscedasticity and B) Q-Q plot – normality for the dependent variable intracellular microcystin-LR during UV treatment.

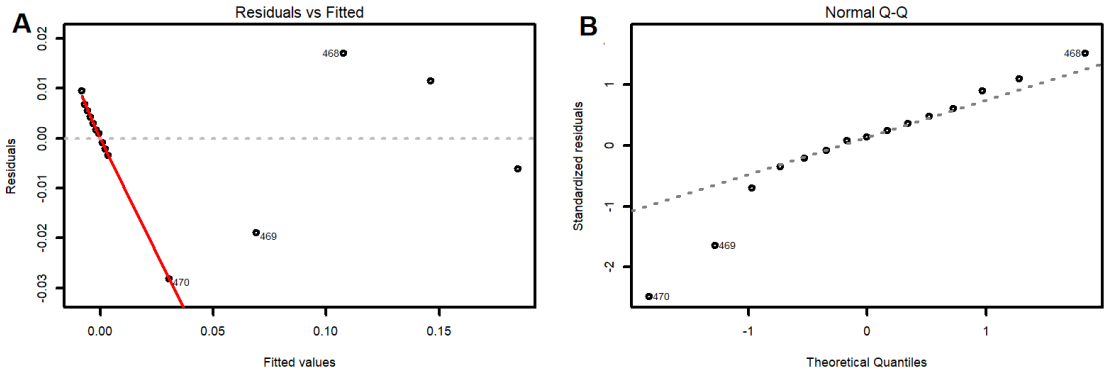

Figure S7 – Graphic analysis of residuals according to criteria A) homoscedasticity and B) Q-Q plot – normality for the dependent variable intracellular microcystin-LY during UV treatment.

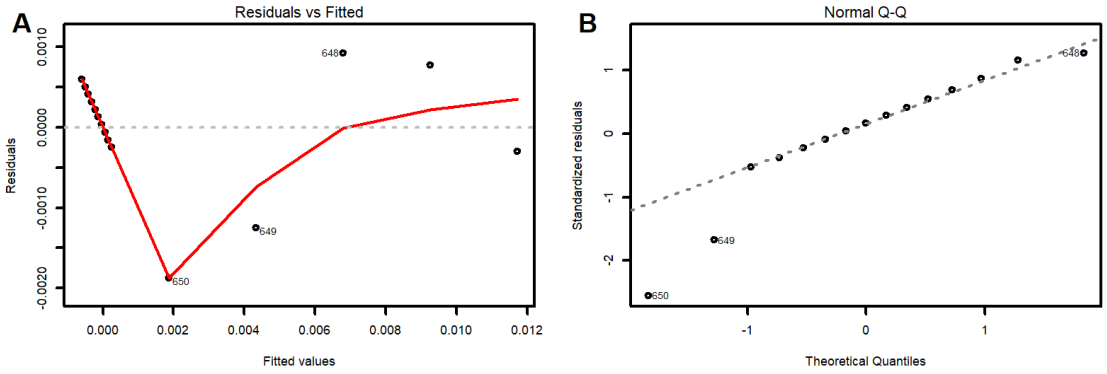

Figure S8 – Graphic analysis of residuals according to criteria A) homoscedasticity and B) Q-Q plot – normality for the dependent variable intracellular microcystin-LW during UV treatment.

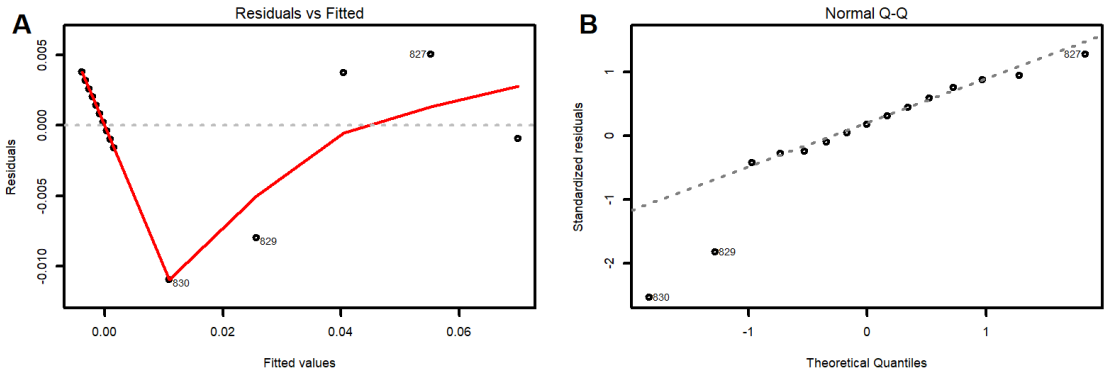

Figure S9 – Graphic analysis of residuals according to criteria A) homoscedasticity and B) Q-Q plot – normality for the dependent variable intracellular microcystin-LF during UV treatment.

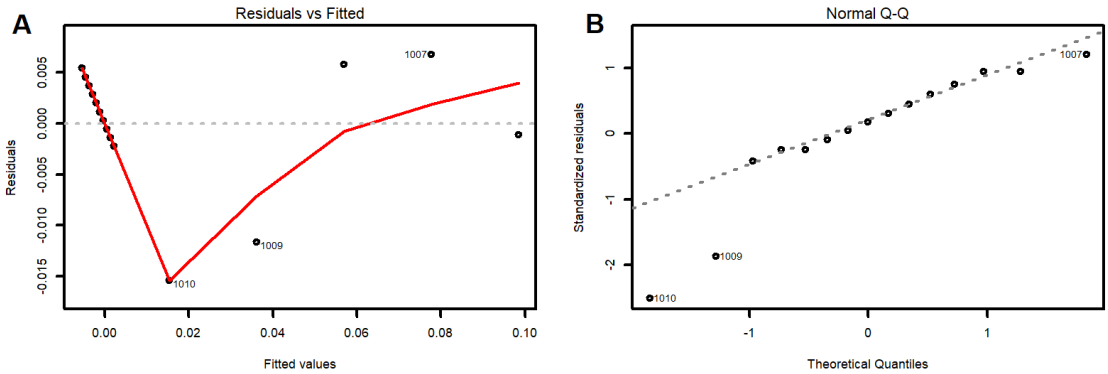

Figure S10 – Graphic analysis of residuals according to criteria A) homoscedasticity and B) Q-Q plot – normality for the dependent variable intracellular microcystin-LR during TiO_2 treatment.

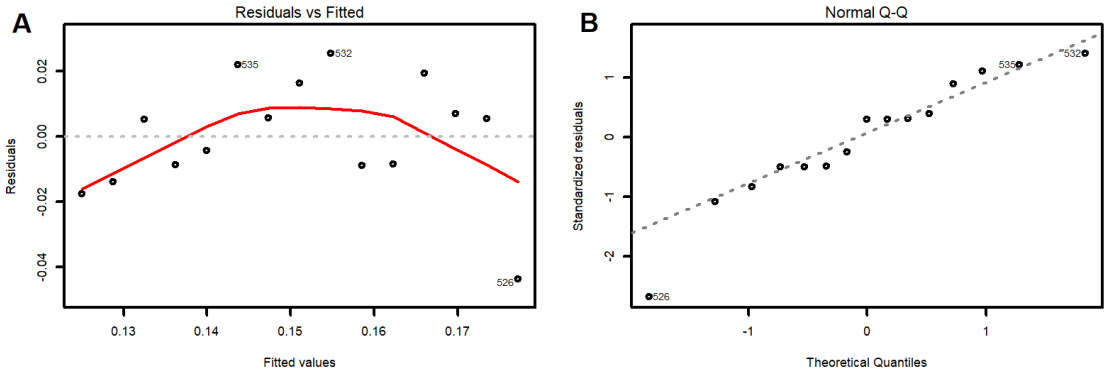

Figure S11 – Graphic analysis of residuals according to criteria A) homoscedasticity and B) Q-Q plot – normality for the dependent variable intracellular microcystin-LY during TiO_2 treatment.

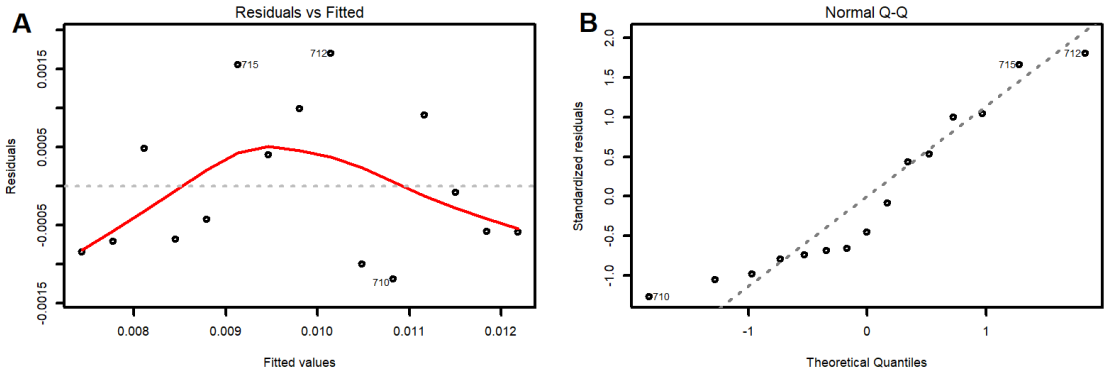

Figure S12 – Graphic analysis of residuals according to criteria A) homoscedasticity and B) Q-Q plot – normality for the dependent variable intracellular microcystin-LW during TiO_2 treatment.

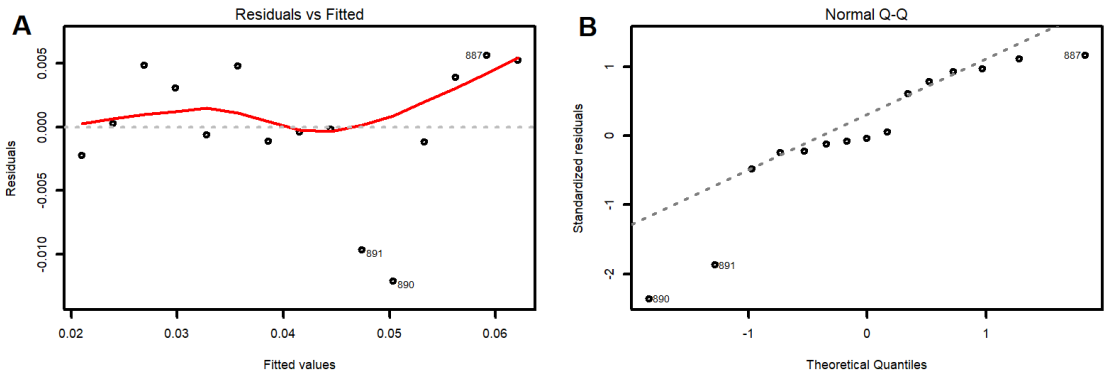

Figure S13 – Graphic analysis of residuals according to criteria A) homoscedasticity and B) Q-Q plot – normality for the dependent variable intracellular microcystin-LF during TiO_2 treatment.

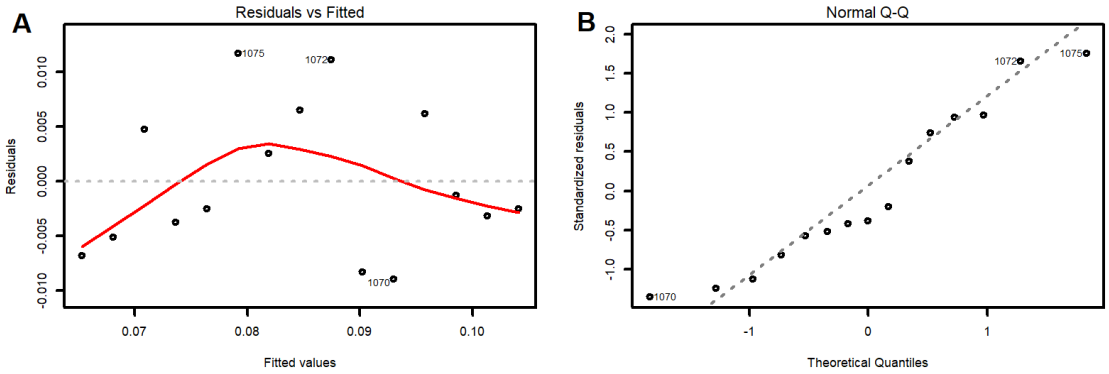

Figure S14 – Graphic analysis of residuals according to criteria A) homoscedasticity and B) Q-Q plot – normality for the dependent variable intracellular microcystin-LR during UV/TiO_2 treatment

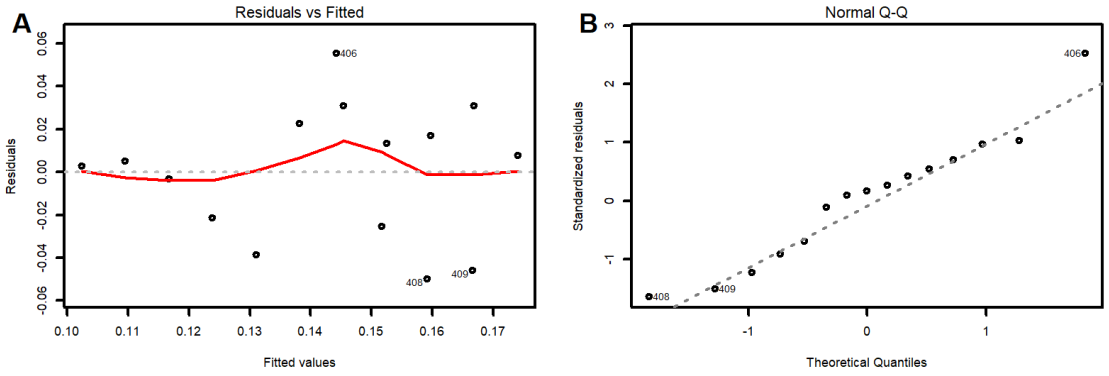

Figure S15 – Graphic analysis of residuals according to criteria A) homoscedasticity and B) Q-Q plot – normality for the dependent variable intracellular microcystin-LY during UV/TiO_2 treatment.

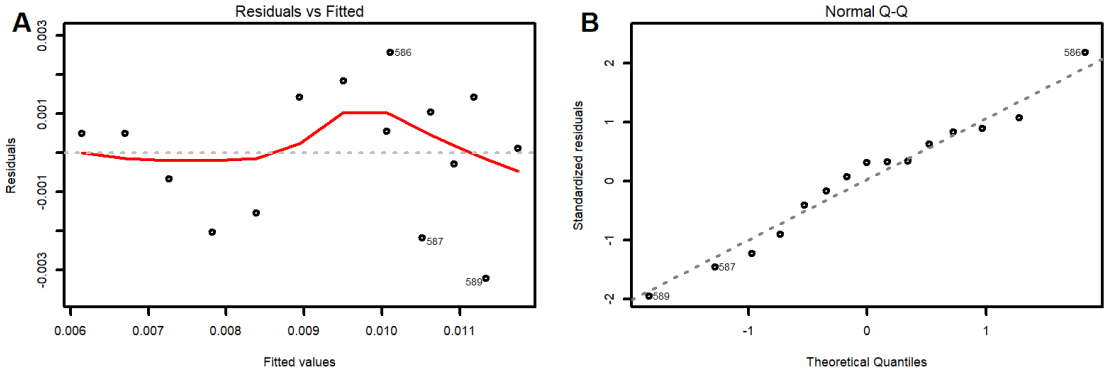

Figure S16 – Graphic analysis of residuals according to criteria A) homoscedasticity and B) Q-Q plot – normality for the dependent variable intracellular microcystin-LW during UV/TiO_2 treatment.

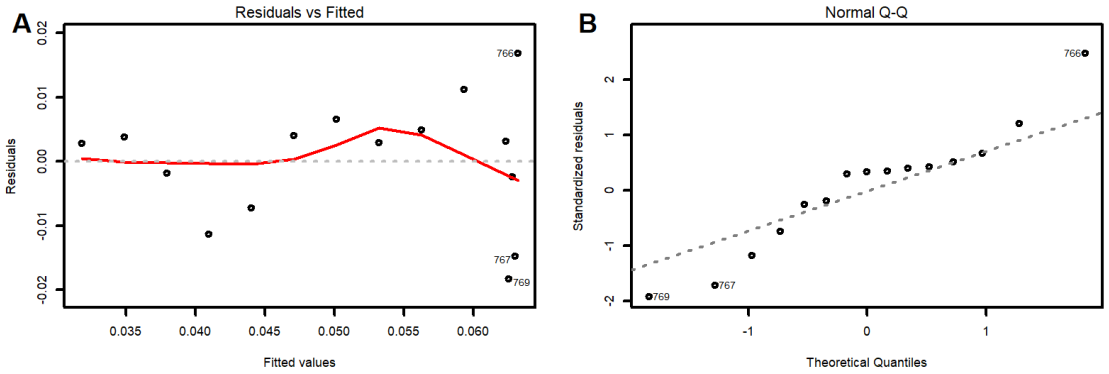

Figure S17 – Graphic analysis of residuals according to criteria A) homoscedasticity and B) Q-Q plot – normality for the dependent variable intracellular microcystin-LF during UV/TiO_2 treatment.

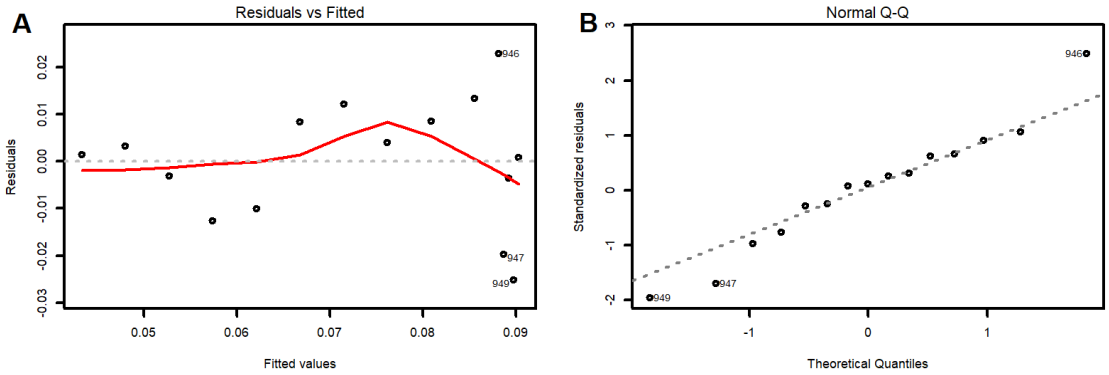

Figure S18 – Graphic analysis of residuals according to criteria A) homoscedasticity and B) Q-Q plot – normality for the dependent variable extracellular microcystin-LR during UV treatment.

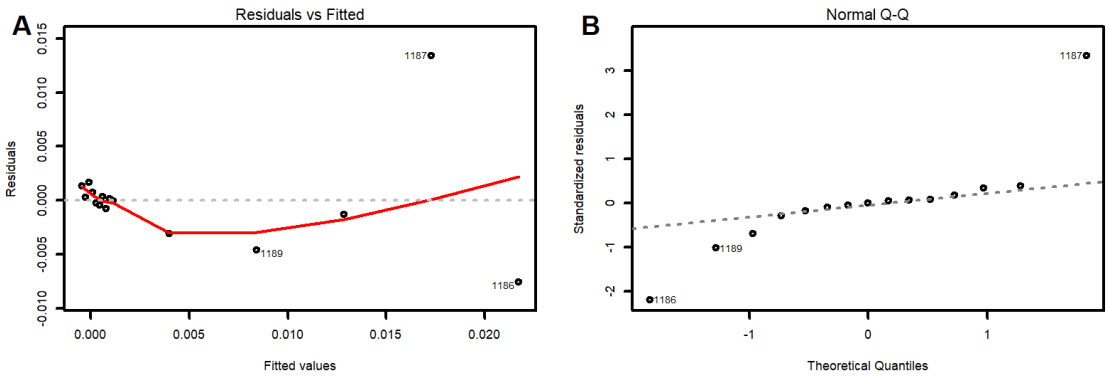

Figure S19 – Graphic analysis of residuals according to criteria A) homoscedasticity and B) Q-Q plot – normality for the dependent variable extracellular microcystin-LY during UV treatment.

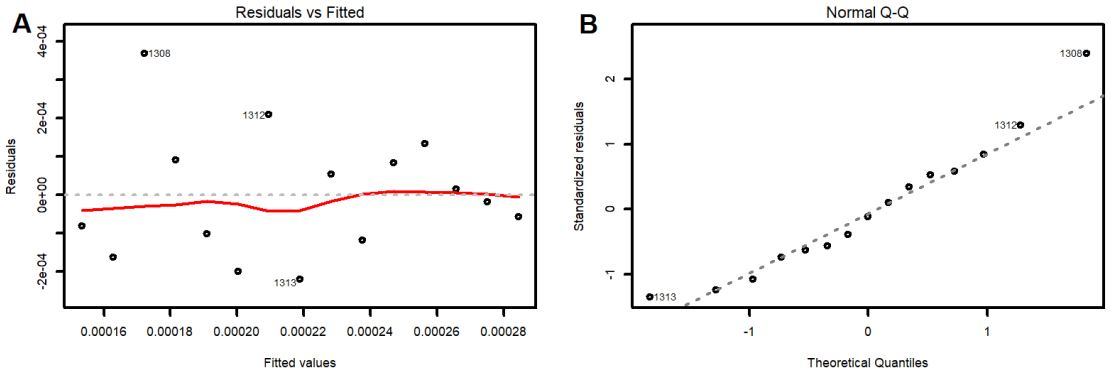

Figure S20 – Graphic analysis of residuals according to criteria A) homoscedasticity and B) Q-Q plot – normality for the dependent variable extracellular microcystin-LW during UV treatment.

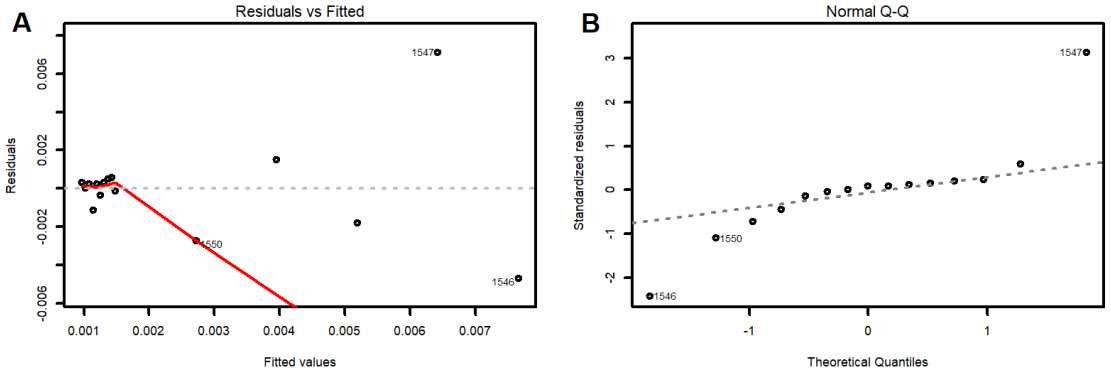

Figure S21 – Graphic analysis of residuals according to criteria A) homoscedasticity B) Q-Q plot – normality for the dependent variable extracellular microcystin-LF during UV treatment.

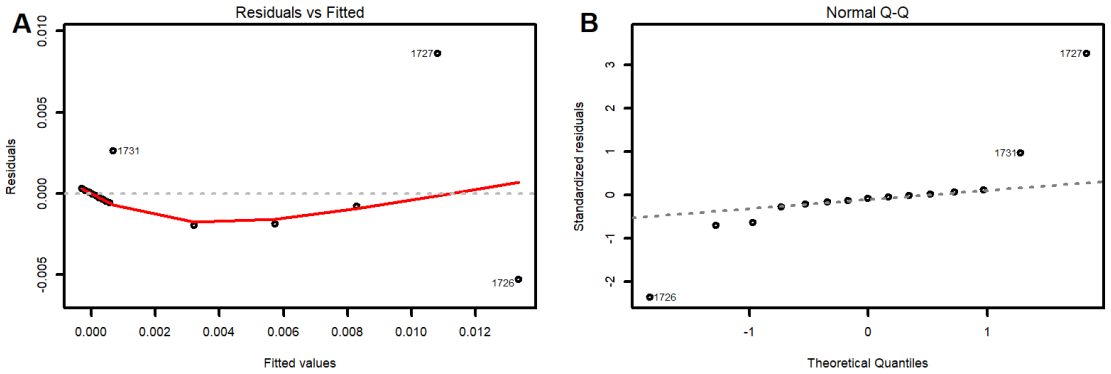

Figure S22 – Graphic analysis of residuals according to criteria A) homoscedasticity and B) Q-Q plot – normality for the dependent variable extracellular microcystin-LR during TiO_2 treatment.

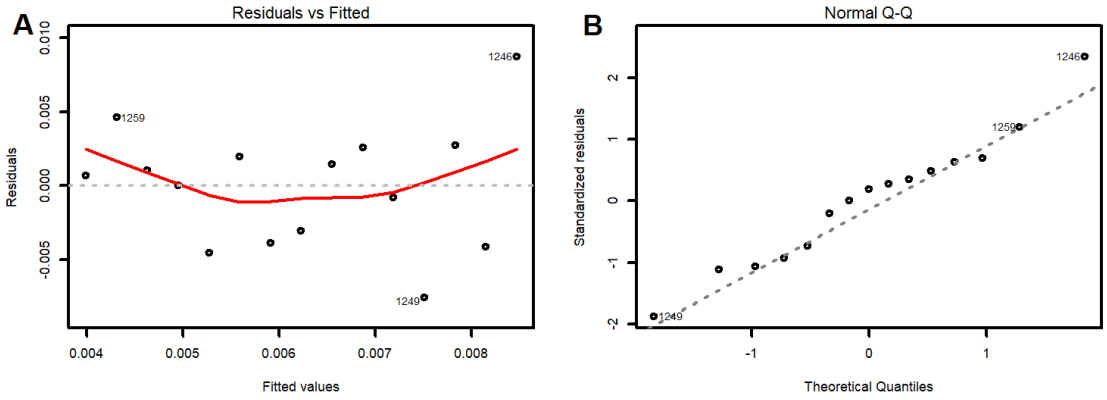

Figure S23 – Graphic analysis of residuals according to criteria A) homoscedasticity and B) Q-Q plot – normality for the dependent variable extracellular microcystin-LY during TiO_2 treatment.

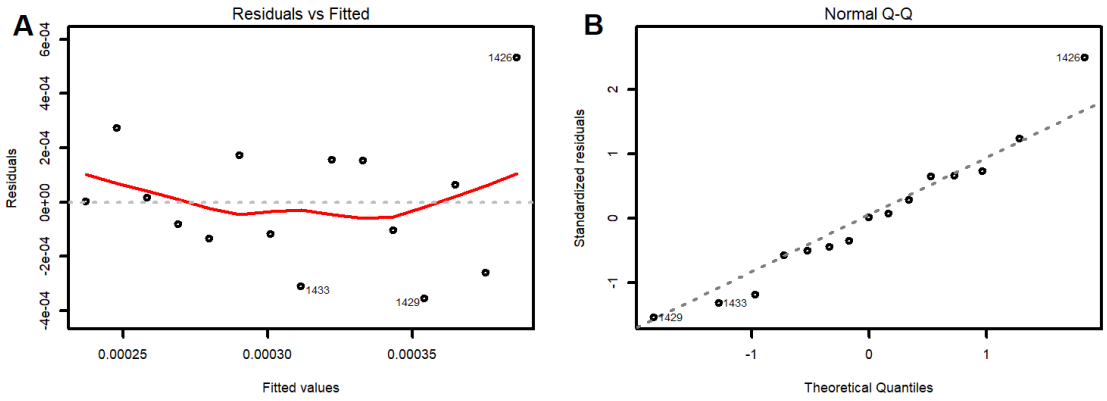

Figure S24 – Graphic analysis of residuals according to criteria A) homoscedasticity and B) Q-Q plot – normality for the dependent variable extracellular microcystin-LW during TiO_2 treatment.

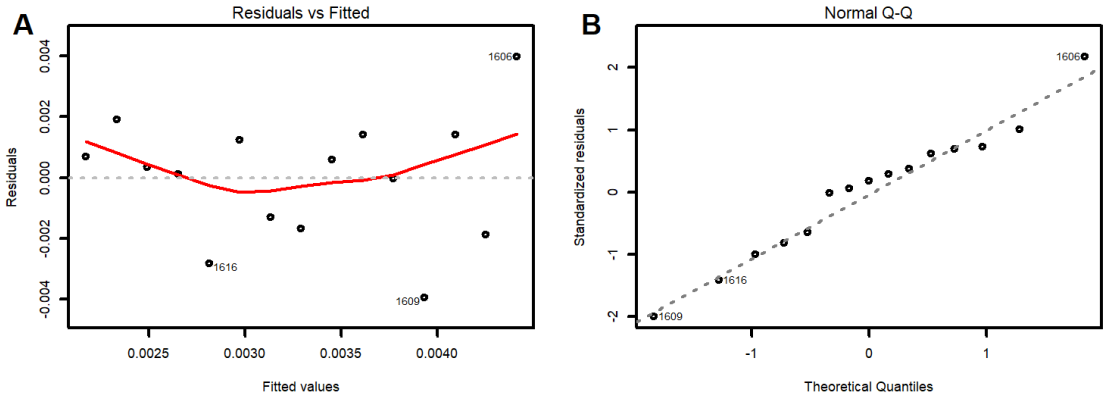

Figure S25 – Graphic analysis of residuals according to criteria A) homoscedasticity and B) Q-Q plot – normality for the dependent variable extracellular microcystin-LF during TiO_2 treatment.

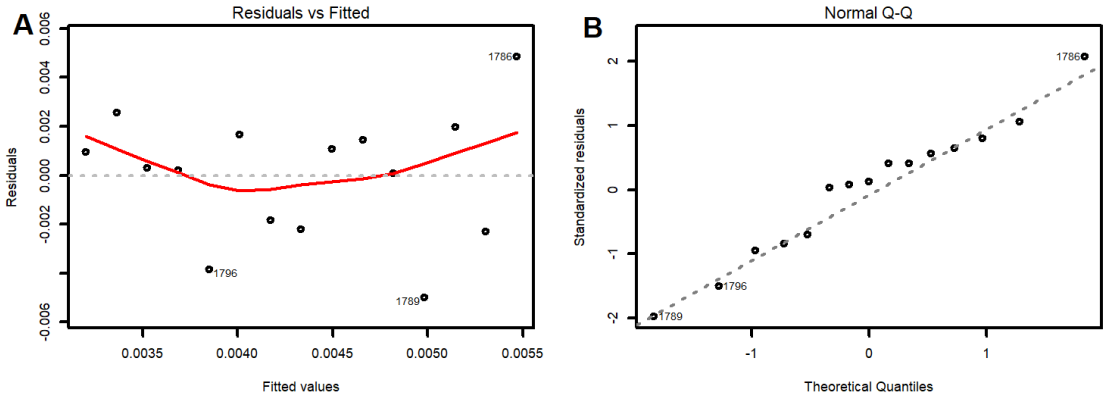

Figure S26 – Graphic analysis of residuals according to criteria A) homoscedasticity and B) Q-Q plot – normality for the dependent variable extracellular microcystin-LR during UV/TiO_2 treatment.

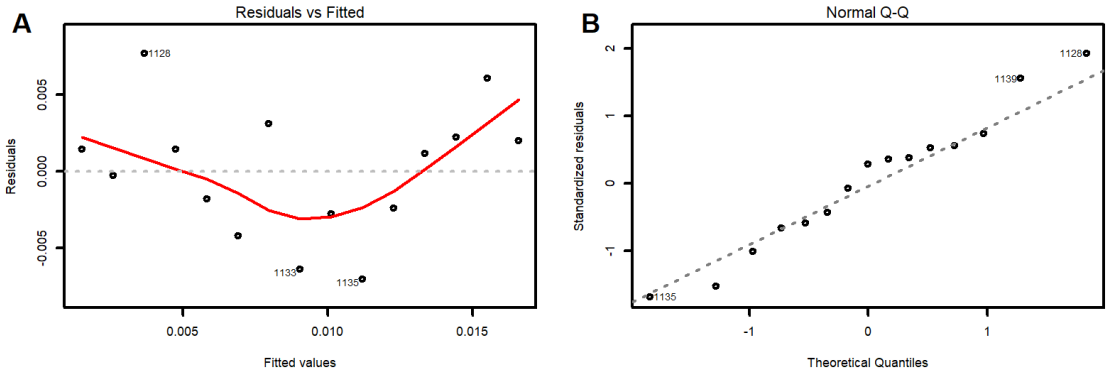

Figure S27 – Graphic analysis of residuals according to criteria A) homoscedasticity and B) Q-Q plot – normality for the dependent variable extracellular microcystin-LY during UV/TiO_2 treatment.

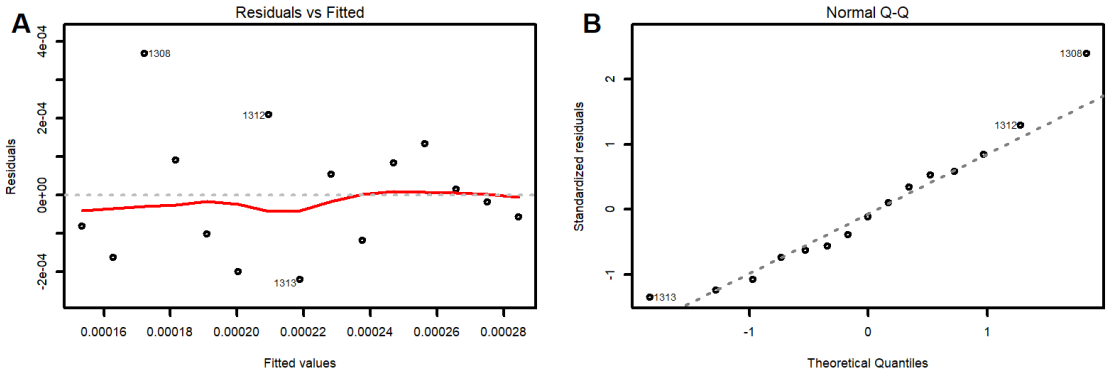

Figure S28 – Graphic analysis of residuals according to criteria A) homoscedasticity and B) Q-Q plot – normality for the dependent variable extracellular microcystin-LW during UV/TiO_2 treatment.

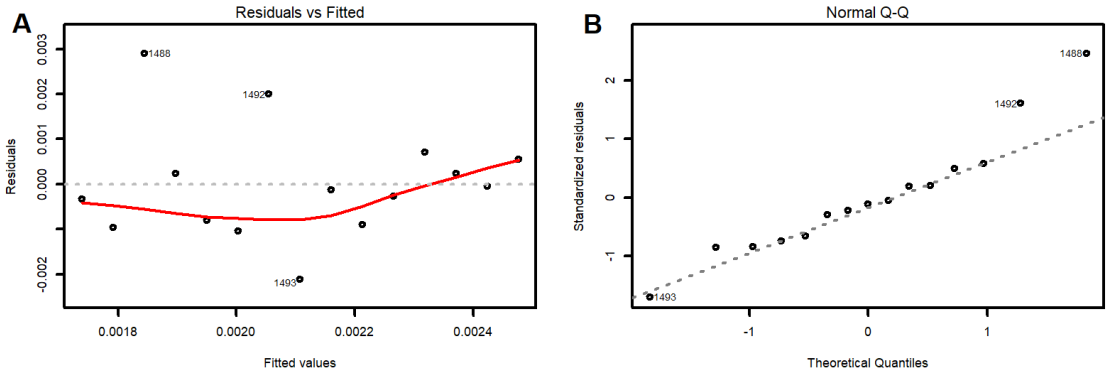

Figure S29 – Graphic analysis of residuals according to criteria A) homoscedasticity and B) Q-Q plot – normality for the dependent variable extracellular microcystin-LF during UV/TiO_2 treatment.

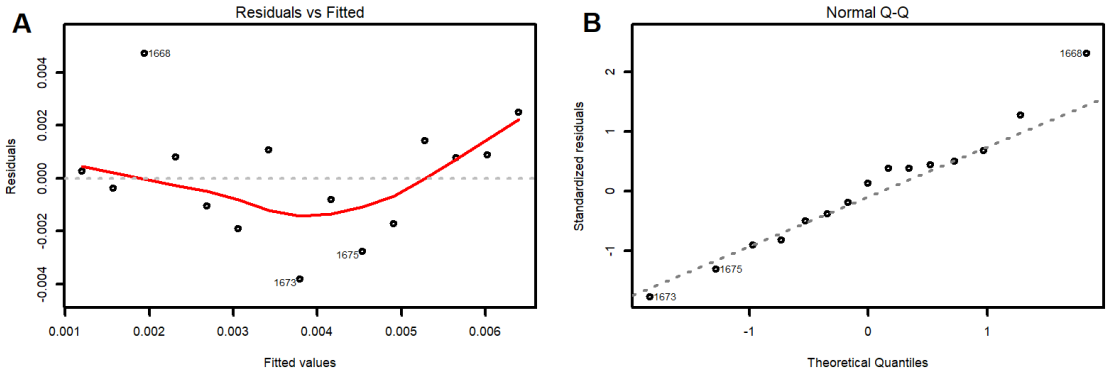

S4 Photoluminescence measurements of TiO_2 coated glass beads

Photoluminescence measurements of both uncoated and TiO_2 coated beads were performed to verify if any UV illumination was converted into visible light during treatment. For the photoluminescence quantum yield (PLQY) under 365 nm illumination, the beads were loaded into a UV-transparent cuvette in air and the absolute photoluminescence quantum efficiency was measured using Hamamastu PLQY instrument.

Both uncoated and TiO_2 coated beads presented deep-blue photoluminescence (Figure S30), with a low quantum efficiency of 4% (uncoated sample) and 7% (TiO_2 coated sample). The data show that the beads do generate additional visible light, albeit with low efficiency. The spectrum has good overlap with the blue absorption peak of chlorophyll a, and so may contribute to growth of the cyanobacteria. Due to this, during the UV/TiO2 treatment, *M. aeruginosa* PCC7813 cells were receiving sufficient light to grow in earlier stages, but also UV illumination and/or hydroxyl radicals generated during treatment which inhibit growth.

Figure S30 – Fluorescence spectra of uncoated glass beads (black line) and TiO_2 coated glass beads (red line) with an excitation wavelength of 365 nm.

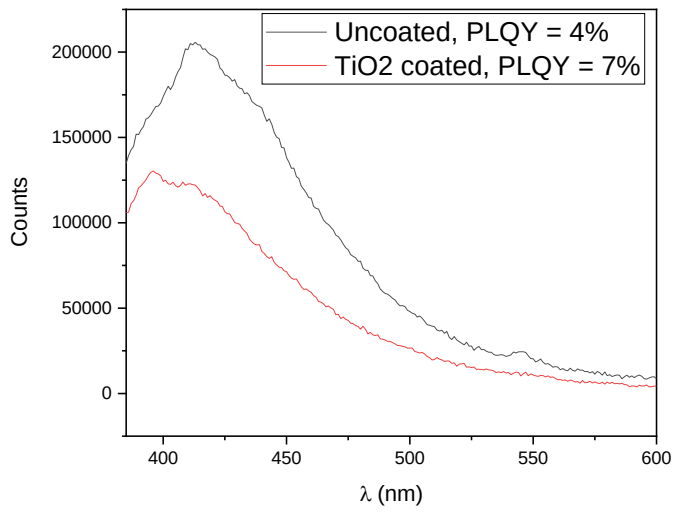

11 GENERAL CONCLUSIONS

Due to the inefficiency of conventional water treatment for the removal of cyanobacteria and their toxins, it is necessary to apply complementary technologies based on the production of ROS that can be applied in freshwater reservoirs. It is important to study and understand these applications for cyanobacterial treatment.

The first study demonstrated the successful reduction of cyanobacterial cell numbers, viability and microcystin contents by hydrogen peroxide. Also, from the five methods investigated for cell stress determination (cell density, photosynthetic activity, chlorophyll content, intra- and extracellular microcystin), the Mini-PAM fluorometer measuring photosynthetic activity was the most rapid analysis and presented the fastest response time (6 hours). Chlorophyll concentration decreased by 10% after 48 hours and cell density was reduced by 97% after 24 hours in samples treated with 20 mg L^{-1} H_2O_2. Intracellular microcystins analogues reduced by at least 96% after 24 hours of H_2O_2 treatment. No increase in extracellular microcystin concentration was detected, which suggests that the intracellular microcystins released into the surrounding water were completely removed.

In the second study, a photolytic system an energy efficient low-level UV illumination supplied by UV-LEDs (365 nm) was able to significantly reduce *M. aeruginosa* PCC7813 cell density from 5.8 x 10^6 cells mL^{-1} until few cells were left and to remove intra- and extracellular microcystins by 100 and 92%, respectively. The photocatalytic system using TiO_2 coated glass beads and UV-LED illumination showed a great variability between replicates, making prediction of cyanobacterial cell and toxin behavior difficult. The reactors were design for in reservoir application in order to ease the burden of water treatment plants for the removal of cyanobacteria and cyanotoxins. The reactor's system design is completely modular allowing for vertical or horizontal orientation. Optimization of photocatalytical active surface area and contact time can be achieved by the addition of more reactor units. Electrical power can be supplied by mains power or through renewable energy with a rechargeable battery system. The flexibility in the photoreactor design also allows other *in-situ* applications.

GENERAL REFERENCES

BARROIN, G., FEUILLADE, M., 1986. "Hydrogen peroxide as a potential algicide for *Oscillatoria Rubescens* D.C.", **Water Res.**, v. 20, n. 5, p. 619–623, 1986.

BARROS, M. U. G. **Prospecção de *Cylindrospermopsis raciborskii* em reservatórios no Ceará e efeitos da depleção de nutrientes na sua concentração celular.** 2013. 100 f. Dissertação (Mestrado em Engenharia Civil) - Centro de Tecnologia, Universidade Federal do Ceará, Fortaleza, 2013.

CHANG, C. W., HUO, X., LIN, T. F. "Exposure of *Microcystis aeruginosa* to hydrogen peroxide and titanium dioxide under visible light conditions: Modeling the impact of hydrogen peroxide and hydroxyl radical on cell rupture and microcystin degradation", **Water Research**, v. 141, p. 217–226, 2018. DOI: 10.1016/j.watres.2018.05.023.

ELLIOTT, J. A. Is the future blue-green? A review of the current model predictions of how climate change could affect pelagic freshwater cyanobacteria. **Water Research**. v. 46, n. 5, p. 1364-1371, 2012.

FAGAN, R., MCCORMACK, D. E., DIONYSIOU, D. D., *et al.* "A review of solar and visible light active TiO_2 photocatalysis for treating bacteria, cyanotoxins and contaminants of emerging concern", **Materials Science in Semiconductor Processing**, v. 42, p. 2–14, 2016. DOI: 10.1016/j.mssp.2015.07.052.

FALCONER, I. R., BERESFORD, A. M., RUNNEGAR, M. T. Evidence of liver damage by toxin from a bloom of the blue-green alga *Microcystis aeruginosa*. **Med. J. Aust**. v. 1, p. 511–4, 1983. DOI: 10.5694/j.1326-5377.1983.tb136192.x

FAN, F., SHI, X., ZHANG, M., *et al.* "Comparison of algal harvest and hydrogen peroxide treatment in mitigating cyanobacterial blooms via an in situ mesocosm experiment", **Science of The Total Environment**, v. 694, p. 133721, 2019. DOI: 10.1016/j.scitotenv.2019.133721.

FAN, J., DALY, R., HOBSON, P., HO, L., BROOKES, J. Impact of potassium permanganate on cyanobacterial cell integrity and toxin release and degradation. **Chemosphere**. v. 92, p. 529–534, 2013a. DOI: 10.1016/j.chemosphere.2013.03.022

FAN, J., HO, L., HOBSON, P., BROOKES, J., 2013b. Evaluating the effectiveness of copper sulphate, chlorine, potassium permanganate, hydrogen peroxide and ozone on cyanobacterial cell integrity. **Water Res**. v. 47, p. 5153–5164, 2013b. DOI: 10.1016/j.watres.2013.05.057.

FIOREZE, M., SANTOS, E., P., SCHMACHTENBERG, N. “Advanced oxidative processes: fundamentals and environmental application”, **Revista Eletrônica em Gestão, Educação e Tecnologia Ambiental**, v. 18, n. 1, p. 79-91, 2014.

LOPES, I. K. C. **Identificação de cianobactérias produtoras de saxitoxinas em reservatório de usos múltiplos no seminário cearense.** 2013. 74 f. Dissertação (Mestrado em Engenharia Civil: Saneamento Ambiental) – Centro de Tecnologia, Universidade Federal do Ceará, Fortaleza, 2013.

PAERL, H. W.; PAUL V. J. Climate change: links to global expansion of harmful cyanobacteria. **Water Research**. v. 46, n. 5, p. 1349-1363, 2012.

JOCHIMSEN, E. M., CARMICHAEL, W. W. AN, J. S., CARDO, D. M., COOKSON, S. T., HOLMES, C. E. M., ANTUNES, M. B. D., DEMELO, D. A., LYRA, T. M., BARRETO, V. S. T., AZEVEDO, S. M. F. O., JARVIS, W. R.. Liver failure and death after exposure to microcystins at a hemodialysis center in Brazil. **The New England Journal of Medicine.** v. 338, p. 873–878, 1998. DOI: 10.1056/nejm199803263381304

PESTANA, C. J., EDWARDS, C., PRABHU, R., *et al.* "Photocatalytic degradation of eleven microcystin variants and nodularin by TiO_2 coated glass microspheres", **Journal of Hazardous Materials**, v. 300, p. 347–353, 2015. DOI: 10.1016/j.jhazmat.2015.07.016.

PIGNATELLO, J. J., OLIVEROS, E., MACKAY, A. A. “Advanced oxidation processes for organic contaminant destruction based on fenton reaction and related chemistry”, **Critical Reviews in Environmental Science and Technology**, v. 36, n. 1, p. 1-84, 2006.

PINHO, L.X., AZEVEDO, J., MIRANDA, S.M., ÂNGELO, J., MENDES, A., VILAR, V.J.P., VASCONCELOS, V., BOAVENTURA, R.A.R., 2015. Oxidation of microcystin-LR and cylindrospermopsin by heterogeneous photocatalysis using a tubular photoreactor packed with different TiO_2 coated supports. **Chem. Eng. J**. v. 266, p. 100–111, 2015. DOI: 10.1016/j.cej.2014.12.023.

PRAETORIUS, A., ARVIDSSON, R., MOLANDER, S., *et al.* "Facing complexity through informed simplifications: A research agenda for aquatic exposure assessment of nanoparticles", **Environmental Sciences: Processes and Impacts**, v. 15, n. 1, p. 161–168, 2013. DOI: 10.1039/c2em30677h.

SCHAUMANN, G. E., PHILIPPE, A., BUNDSCHUH, M., *et al.* "Understanding the fate and biological effects of Ag- and TiO_2-nanoparticles in the environment: The quest for advanced analytics and interdisciplinary concepts", **Science of the Total Environment**, v. 535, p. 3–19, 2015. DOI: 10.1016/j.scitotenv.2014.10.035.

SPOOF, L., CATHERINE, A., "Cyanobacteria samples: preservation, abundance and biovolume measurements". In: MERILUOTO, J., SPOOF, L., A. CODD, G. (Org.), **Handbook of Cyanobacterial Monitoring and Cyanotoxin Analysis**, Chichester, UK, John Wiley & Sons, 2017. p. 526–537. DOI: 10.1002/9781119068761.

TSAI, K. "Ecotoxicology and Environmental Safety Effects of two copper compounds on *Microcystis aeruginosa* cell density, membrane integrity, and microcystin release", **Ecotoxicology and Environmental Safety**, v. 120, p. 428–435, 2015. DOI: 10.1016/j.ecoenv.2015.06.024.

ZAMYADI, A., MACLEOD, S. L., FAN, Y., *et al.* "Toxic cyanobacterial breakthrough and accumulation in a drinking water plant : A monitoring and treatment challenge", v. 6, 2011. DOI: 10.1016/j.watres.2011.11.012.

ZHAO, C., PELAEZ, M., DIONYSIOU, D. D., *et al.* "UV and visible light activated TiO_2 photocatalysis of 6-hydroxymethyl uracil, a model compound for the potent cyanotoxin

cylindrospermopsin", **Catalysis Today**, v. 224, p. 70–76, 2014. DOI: 10.1016/j.cattod.2013.09.042.

ZHU, X., CHANG, Y., CHEN, Y. "Toxicity and bioaccumulation of TiO_2 nanoparticle aggregates in *Daphnia magna*", **Chemosphere**, v. 78, n. 3, p. 209–215, 2010. DOI: 10.1016/j.chemosphere.2009.11.013.